Cross–linked 'Silicone Oil'/Water Emulsions

By

Declan O.H. Teare

A thesis submitted to the University of Bristol in accordance with the requirements for the Degree of Doctor of Philosophy in the Faculty of Science.

Department of Physical Chemistry

September 1997

Abstract

In order for stable emulsions of two, mutually insoluble liquids to be formed, an emulsifying agent and some form of energy input are usually required. This energy is provided in many instances by a mechanical shearing action (comminution mechanism). The resulting droplet dispersion often has a very broad size distribution.

Stable, monodisperse emulsions of polydimethylsiloxane (PDMS) can be produced. No surfactant or mechanical comminution is required as emulsification occurs following a simple polymerisation reaction of silane monomers in an aqueous alkaline medium.

The physical characteristics of the PDMS droplets can be closely controlled by addition of cross–linking monomer to the initial reaction mixture. Depending on the cross–linker concentration droplets, microgel–like or solid particles, of a particular size, viscosity and density can be formed.

The stability of PDMS emulsion droplets in water, with varying concentrations of cross–linker, has been studied by following changes in the droplet size distribution. The effect of electrolyte, pH and osmotic pressure on the stability has been followed. The presence of cross–linker does not significantly alter the colloidal stability of the PDMS dispersions.

Measurements of the electrophoretic mobility of cross–linked emulsions have been made to calculate the zeta–potential of the droplets. Using a simple DLVO calculation, with van der Waals and electrostatic forces only it was found that a large barrier to coalescence existed at the critical coagulation concentration. This deviation from theory may be attributed to droplet deformation and/or hydrophobic interactions.

Cross–linked PDMS emulsions osmotically swell with good solvents and reach an equilibrium size depending on the polymer volume fraction. Only above a threshold cross–linker concentration is existence of a gel–type structure shown.

Publication

"Inorganic 'Silicone Oil' Microgels"

Michael I. Goller, Timothy M. Obey, Declan O.H. Teare, Brian Vincent and Matthias R. Wegener.

Colloids and Surfaces A: Physicochemical and Engineering Aspects 123–124 (1997) pp 183–193.

Presentations

"Monodisperse 'Silicone Oil' in Water Emulsions"

3rd UK Colloid & Surface Science Student Meeting, University of Hull (1995).

"Liquid Latex Particles with Controlled Properties"

69th Colloid & Surface Symposium, University of Utah, Salt Lake City (1995).

"Novel Monodisperse 'Silicone Oil' in Water Emulsions"

5th European Student Conference, Ven, Sweden (1995).

"Liquid Polymer Latex Particles with Controlled Properties"

5th Family Meeting of the MACRO Group–Aspects of Polymer Chemistry, Loughborough University of Technology (1995).

Memorandum

This thesis is based upon work carried out between October 1993 and January 1997, under the supervision of Professor Brian Vincent in the Department of Physical Chemistry, University of Bristol. Except where acknowledged by reference the work is original and has not been submitted for any other degree.

September 1997

Acknowledgements

My first mention must go to Professor Brian Vincent, without whom none of this work would have been possible and who provided insight and suggestions throughout the work. An extra mention must go to Dr. Tim Obey who has maintained a level of interest in this work despite being 'transferred' to another position.

The faces which have passed through the BV lab at Bristol are too many to name but special mention must go to Andy 'the curse' Loxley, Andy Cox (Romàrio), Pete 'I'm curing AIDS and cancer' Dowding, Jennie and Brian Saunders, James Weeks, Nigel Wright, Helen Crowther, Nick Marston, 'Chopper' Goller, 'Mad' Matt, 'Keefy' Bean, Stu Bradbrook, Gavin Markham, Paul Jenkins, Greg Alan, Pauline Elks, Sylvie Neyret and Gayle Morris. Apologies to anyone who has been accidentally omitted! My exploits on the BV 5–a–side football team are well known and I would like to thank the TC group as a whole for providing such welcome losing opposition over the last three years.

I would also like to acknowledge my housemates and many friends I have made in Bristol over the last 6 years.

I would like to dedicate this thesis in memory of Nigel Thurman, the most genuine person I have ever known and to Sally, who has been a calming influence and a constant source of hope and encouragement throughout the latter part of my Ph.D.

Contents

	Page
Chapter 1: Introduction	**1**
1.1 Definition	1
1.2 Emulsion Formation	2
1.2.1 Preparation of monodisperse emulsions by porous membrane emulsification	4
1.2.2 Preparation of monodisperse emulsions by fractionated crystallisation	5
1.2.3 Preparation of monodisperse emulsions by aerosol mechanisms	6
1.3 Emulsification by Nucleation and Growth	7
1.4 Apparent Spontaneous Emulsification	8
1.5 Applications of Emulsions	10
1.6 PDMS Emulsions	11
1.7 Objectives	12
1.8 References	13
Chapter 2: Emulsions	**17**
2.1 Introduction	17
2.2 Emulsion Stability	18
2.2.1 Emulsion creaming or sedimentation	19
2.2.2 Ostwald ripening	21
2.3 Interdroplet Interactions: Droplet Coagulation	23
2.3.1 Electrical double–layer interactions	23
2.3.2 London–van der Waals interactions	25
2.3.3 Steric interactions	27
2.3.4 Total potential energy of interaction	27
2.4 Thin Film Thinning: Droplet Coalescence	29

2.4.1 Introduction 29
2.4.2 Thermodynamics of film thinning 31
2.4.3 Forces acting across a thin film: disjoining pressure 31
2.4.4 Hydrodynamics of film thinning 33
2.4.5 Film rupture 34
2.5 Surfactant Stabilised Emulsions 35
2.6 References 36

Chapter 3: Polydimethylsiloxane Emulsions 38
3.1 Silicones 38
3.1.1 Introduction 38
3.1.2 Synthesis of silicones 39
3.1.3 Properties of silicones 41
3.1.4 Applications of silicones 42
3.2 PDMS (Silicone oil) in Water Emulsions: Experimental 44
3.2.1 Materials 44
3.2.2 Preparation of PDMS emulsions 44
3.2.3 Isolation of the PDMS phase 47
3.2.4 Physical properties of the PDMS phase 48
3.2.5 Determination of PDMS volume fraction in the emulsion 49
3.3 Measurement of Droplet Size by PCS 51
3.3.1 Introduction 51
3.3.2 Theory 52
3.3.3 Analysis of droplet size 53
3.4 PDMS (Silicone Oil) in Water Emulsions: Results and Discussion 55
3.4.1 Emulsion preparation 55
3.4.2 PDMS characterisation 60
3.5 References 66

Chapter 4: Physical Properties of PDMS Emulsions 68

4.1 Experimental Methods 68

4.1.1 PDMS droplet stability to coagulation 68

4.1.2 PDMS droplet stability to freeze–thawing 70

4.1.3 PDMS emulsion stability to increases in osmotic pressure 70

4.1.4 Surface charge measurements 73

4.2 Results 74

4.2.1 PDMS droplet stability to coagulation by electrolyte 74

4.2.2 PDMS droplet stability to coagulation by pH 79

4.2.3 PDMS droplet stability to osmotic pressure 82

4.3 Electrophoresis 83

4.3.1 Theory 83

4.3.2 Electrophoretic mobility measurements of PDMS emulsions 85

4.3.3 Mobility measurements 87

4.3.4 Calculation of zeta–potentials 92

4.4 DLVO Pair Potentials 94

4.4.1 Calculations from experimental data 94

4.4.2 Theoretical pair potential calculations 96

4.4.3 Possibilities for deviations from DLVO theory 98

4.5 References 99

Chapter 5: Swelling of Silicone Microgels by Solvents 101

5.1 Introduction 101

5.1.1 Osmotic Swelling of O/W Emulsions 103

5.1.2 Osmotic swelling of cross–linked PDMS droplets 105

5.2 Swelling of PDMS Emulsions By Solvent: Experimental 106

5.3 Swelling of PDMS Emulsions By Solvent: Results 107

5.3.1 Swelling by n-heptane 107

5.3.2 Swelling by other solvents 113

5.3.3 Discussion of swelling results 118
5.3.4 Electrophoretic mobility of swollen PDMS emulsions 119
5.4 Introduction of Organic Dye Molecules into PDMS Emulsions 121
5.5 References 123

Chapter 6: Conclusions and Further Work **124**
6.1 Conclusions 124
6.2 Suggestions For Further Work 127
6.2.1 Droplet coalescence at a planar oil/water interface 127
6.2.2 Analysis of the PDMS by DSC 128
6.2.3 Other possibilities for further work 128
6.3 References 129

List of Plates

		Page
3.1 (a)	0.01 v/v PDMS emulsion (diameter = 2220 ± 134 nm)	57
3.1 (b)	0.04 v/v PDMS emulsion (diameter = 1556 ± 272 nm)	57
5.1 (a)	0.01 v/v PDMS + n–heptane emulsion (diameter = 2220 ± 190 nm)	112
5.1 (b)	0.01 v/v PDMS + toluene emulsion (diameter = 2440 ± 580 nm)	112

List of Tables

		Page
3.1	Comparison of PDMS with other polymers	41
3.2	Experimental data of PDMS phases	65
4.1	Pair potential repulsive maxima	95
4.2	Experimental pair potentials for PDMS emulsions with pH	95

List of Figures

		Page
1.1	Schematic representation of surfactant stabilised emulsions	1
2.1	Schematic representation of emulsion creaming or sedimentation	19
2.2	Structure of the electrical double layer	23
2.3	Schematic of the potential energy curves for an emulsion droplet	28
2.4	Diagrammatic representation of the thin film and border regions between two PDMS droplets (from [19])	30
2.5	Schematic representation of the 'dimple' between two emulsion droplets	33

3.1	The basic structure of PDMS	38
3.2	General synthesis of silicones	39
3.3	The general structure of cyclic silicones	40
3.4	The chemical structure of the silane monomers used	45
3.5	Proposed reaction scheme for the formation of the PDMS	45
3.6	Typical PCS set–up	54
3.7	Variation of droplet size for PDMS emulsions with initial monomer concentration	55
3.8	Effect of cross–linking monomer on droplet size	58
3.9	Growth in size of undialysed emulsions with effect of cross–linker	59
3.10	The effect of cross–linker on the density of the PDMS phase	62
3.11	The effect of cross–linker on the viscosity of the PDMS phase	62
3.12	Effect of cross–linker on the surface and interfacial tension of the PDMS phase	63
3.13	Effect of cross–linker on the freezing and melting points of the PDMS phase	64
4.1	The 'Secondary Osmometer'	71
4.2	The osmotic pressure of dextran polymer solutions	72
4.3	Example of the linear $\log\tau$ / $\log\lambda$ for a PDMS emulsion	74
4.4	The effect of KCl on PDMS emulsion stability; $\delta(\log\tau)/\delta(\log\lambda)$ plot	75
4.5	The effect of KCl on PDMS emulsion stability; linearity plot	76
4.6	The CCC of a 0% MTES PDMS emulsion	77
4.7	The CCC of a 10% MTES PDMS emulsion	78
4.8	The CCC of a 20% MTES PDMS emulsion	78
4.9	The coalescence of a 0% MTES PDMS emulsion at low pH	79
4.10	The coalescence of a 10% MTES PDMS emulsion at low pH	80
4.11	The coalescence of a 20% MTES PDMS emulsion at low pH	80
4.12	The coalescence of PDMS emulsions at high osmotic pressure	82

4.13 PALS cell and electrode design 86
4.14 Effect of cross–linker on droplet electrophoretic mobility 88
4.15 The averaged size of the emulsion droplets for electrophoresis 89
4.16 The effect of KCl on the electrophoretic mobility of a PDMS emulsion 90
4.17 The effect of cross–linker on electrophoretic mobility with pH 91
4.18 Zeta–potentials of cross–linked PDMS droplets 92
4.19 The effect of electrolyte on the ζ–potential of a PDMS emulsion 93
4.20 The effect of pH on the ζ–potential of cross–linked PDMS emulsions 93
4.21 Theoretical pair potential curves for different ζ–potentials for PDMS droplets 96
4.22 Theoretical pair potential curves for different electrolyte concentrations for PDMS droplets of constant zeta–potential 97
5.1 Schematic representation of PDMS droplets swelling by hydrocarbon 101
5.2 The partial free molar energy of solvent in a swelling droplet 104
5.3 Size of PDMS emulsion droplets swollen by n–heptane as a function of swelling time for various concentrations of cross–linker 107
5.4 Increase in volume of n–heptane in swollen PDMS emulsion drops as a function of swelling time for various concentrations of cross–linker 108
5.5 Actual volume of n–heptane in swollen PDMS droplets as a function of swelling time for various concentrations of cross–linker 109
5.6 The volume fraction of PDMS in n–heptane swollen PDMS droplets as a function of swelling time for various concentrations of cross–linker 109

5.7 Size of PDMS droplets swollen by n–heptane as a function of swelling time by 'standing' diffusion 111
5.8 Size of PDMS droplets swollen by n–octane as a function of swelling time for various concentrations of cross–linker 114
5.9 Size of PDMS droplets swollen by cyclohexane as a function of swelling time for various concentrations of cross–linker 114
5.10 Size of PDMS droplets swollen by dimethyldiethoxysilane as a function of swelling time for various concentrations of cross–linker 115
5.11 Size of PDMS droplets swollen by styrene as a function of swelling time for various concentrations of cross–linker 115
5.12 Volume fraction of PDMS in n–octanol swollen droplets as a function of swelling time for various concentrations of cross–linker 116
5.13 Volume fraction of PDMS in n–octane swollen emulsion droplets as a function of swelling time for various concentrations of cross–linker 116
5.14 Zeta–potential of PDMS emulsion droplets swollen by n–heptane 120
5.15 Chemical structure of Sudan yellow dye 121

Chapter 1: Introduction

1.1 Definition

IUPAC (1992) define an emulsion as "a dispersion of droplets of one liquid in another one with which it is incompletely miscible. Emulsions of droplets of an organic liquid (an "oil") in an aqueous solution are indicated by the symbol O/W and emulsions of aqueous droplets in an organic liquid as W/O. With emulsions droplets can often exceed the usual limits for colloids in size. A microemulsion is defined as a thermodynamically stable emulsion."

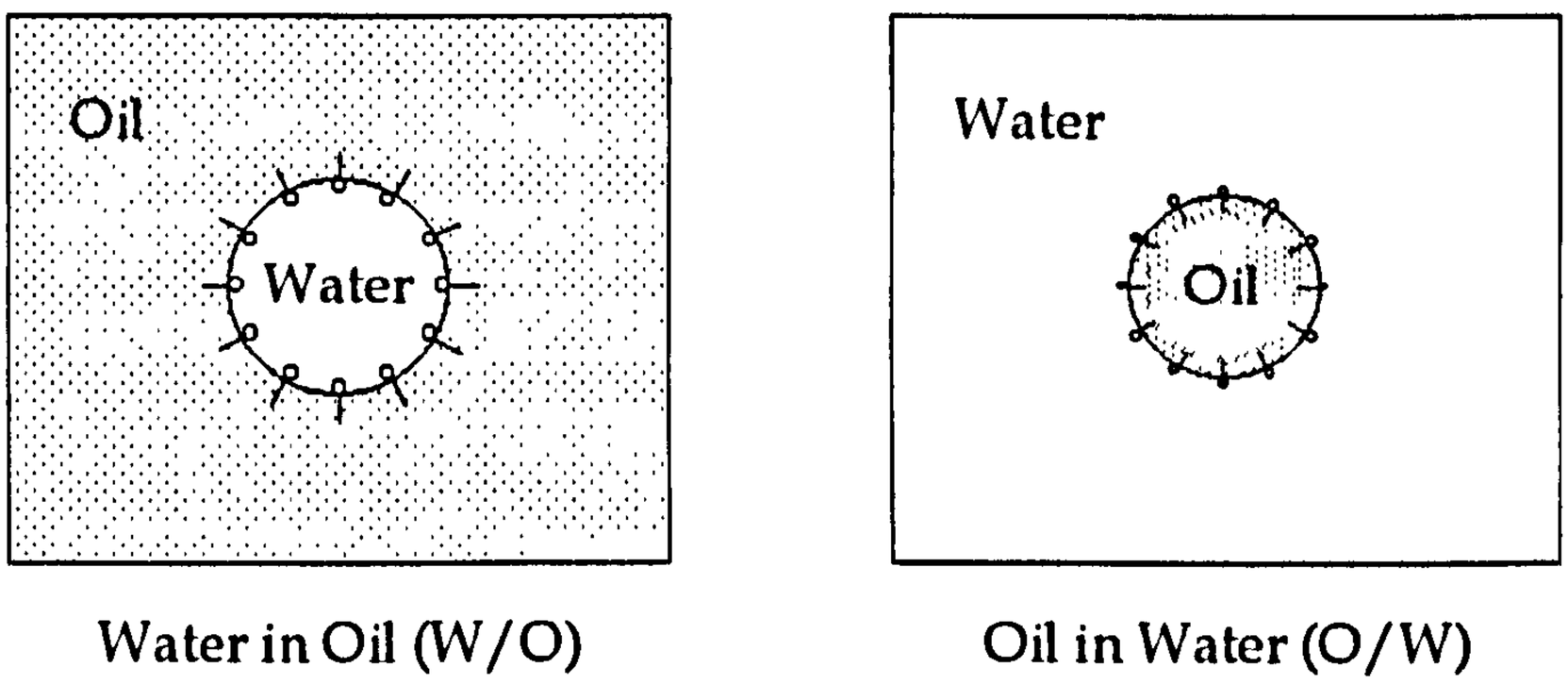

Figure 1.1: Schematic representation of surfactant stabilised emulsions

Figure 1.1 shows a generalised representation of the two major types of emulsion; oil in water (O/W) and water in oil (W/O) dispersions. In general the average droplet size in an emulsion tends to be greater than 100 nm in diameter. Emulsions generally will have an appearance ranging from a milky–white opaqueness to a grey translucence depending on the average droplet diameter. Microemulsions, which can be considered as a separate class of emulsion, typically have a diameter of 100 nm or less and appear transparent.

1.2 Emulsion Formation

The fundamental aspect of emulsions is that they are thermodynamically unstable species and will attempt to revert back to the most stable situation, namely the two distinct non–dispersed oil and water phases. As a result all emulsions need some form of stabilisation in order to retain their structure. This normally involves a third component known as an emulsifying agent to be present. These can be classified into three types:

(i) Surface–active materials

(ii) Naturally occurring materials

(iii) Finely divided solids

The process of dispersion of a liquid into another immiscible liquid is referred to as emulsification. The function of the emulsifier is therefore to facilitate emulsification and promote emulsion stability. The emulsifying agent forms an ordered structure around the oil–water interface of the droplet, which helps prevent coagulation and coalescence. It is very unusual to find a stable emulsion that can be formed without the addition of any emulsifier to the component oil and water phases.

All emulsions require an input of energy in order to become dispersed. This is normally provided either by an external source such as the mechanical energy in a comminution mechanism or the energy is associated with a phase change. The free energy of emulsion formation may be given by [1]:

$$\Delta G = \Delta A \gamma^{\alpha\beta} - T\Delta S_{disp} \qquad \textbf{1.1}$$

where ΔA is the increase in the interfacial area, $\gamma^{\alpha\beta}$ the interfacial tension between the two immiscible liquids α and β and $T\Delta S_{disp}$ is the entropy change associated with the dispersion of fine liquid droplets. In general the first term on the right hand side of equation 1.1 is the dominant term. ΔG is nearly always positive, so emulsification is usually a non–spontaneous process.

Conditions can occur when ΔG is negative and emulsification is spontaneous. In order for this to happen the value of $T\Delta S_{disp}$ must exceed $\Delta A\,\gamma^{\alpha\beta}$. This occurs in the case of microemulsions [2-5], where equilibrium values of $\gamma^{\alpha\beta}$ are low enough for this to be the case. The important criterion with microemulsions is that the *dynamic* value of $\gamma^{\alpha\beta}$ decreases transiently to very small values.

Most emulsions are formed using dispersion methods [6,7]. This usually involves mechanical agitation (comminution) to disperse the oil in the aqueous phase or vice versa. This can be achieved by mechanical shearing of large droplets by equipment such as the colloid mill, homogeniser, ultrasonic emulsifier or just simple agitation of two phases together with an emulsifier.

Emulsions can also be prepared by utilising the physicochemical properties of surfactants as emulsifiers, i.e. the phase inversion technique (PIT method) [8,9] or the surfactant–phase emulsification technique [10,11], etc.

The emulsions produced by these techniques tend to be polydisperse (i.e. they have a wide droplet size distribution). This is because the emulsification conditions cannot be precisely controlled. A 'monodisperse' emulsion is, by definition, strictly impossible. More realistically a 'monodisperse' emulsion will have a narrow droplet size distribution. It is rare for these 'monodisperse' emulsions to be produced.

The preparation of 'monodisperse' emulsions is an important, but as yet largely unachieved, objective for understanding the fundamental principles governing emulsion behaviour. Preparative techniques have been developed by which a 'monodisperse' emulsion can be formed. These include membrane emulsification, fractionated crystallisation and aerosol sprays. A brief outline of these techniques follows.

One possible method to form a 'monodisperse' emulsion is via a nucleation and growth mechanism from an initially homogeneous phase. Nucleation describes the spontaneous appearance of a new phase from a metastable solution of the material in question. This will be discussed in section 1.3.

1.2.1 Preparation of 'monodisperse' emulsions by porous membrane emulsification

There are two related mechanisms for producing 'monodisperse' W/O and O/W emulsions. One is known as Shirasu–porous–glass (SPG) filter emulsification [12,13] and the other, more recently developed technique, as cross–flow membrane emulsification [14]. The concept of both techniques is simple and involves the injection of one phase through a porous substrate (membrane) so those droplets formed at the ends of the pores at the membrane surface come into contact with the continuous phase.

SPG emulsification is carried out using a porous glass of $CaO–Al_2O_3–B_2O_3–SiO_2$ via a continuous or a batch process. The bigger the pore sizes the larger the droplets formed.

Cross–flow membrane emulsification is a development of the SPG technique. This involves passing the discontinuous phase through a porous medium and injecting the droplets so formed directly into a moving continuous phase.

By varying the trans–membrane pressure and the cross–flow velocity for particular pore sizes the droplet size distribution and production rate can be controlled. Of critical importance is the hydrophobicity of the pore channels and membrane surface. For instance the surfaces have to be rendered hydrophobic and hydrophilic for the production of W/O [15] and O/W [16] emulsions respectively.

1.2.2 Preparation of 'monodisperse' emulsions by fractionated crystallisation

Fractionated crystallisation is a technique that relies on depletion interactions for purifying an initially polydisperse emulsion to a 'monodisperse' system [17]. The method is based on the liquid–solid phase transition induced by the attractive depletion interaction, which can be produced by surfactant micelles [18-20]. As the depth of the depletion potential increases linearly with the droplet diameter (refer to equation 1.2), the liquid–solid transition may be used to fractionate in size spherical dispersions, following a fractionated crystallisation scheme. The phase transition occurs at higher surfactant concentrations (above the critical micelle concentration, CMC) as the droplet diameter decreases.

When two droplets come too close to each other, the interdroplet spacing becomes an excluded volume for the micelles formed by the excess surfactant. This depletion of micelles leads to a non–compensated pressure acting on the droplets. This attractive contact potential (U_c) is described by equation 1.2 [19].

$$U_c = \frac{3}{2} kT\phi_m \frac{\sigma}{\sigma_m} \qquad 1.2$$

Here k is the Boltzmann constant, T the absolute temperature, ϕ_m is the volume fraction of surfactant micelles, σ is the diameter of the emulsion droplets and σ_m is the diameter of the surfactant micelles. The interaction range is found to be equal to the small object diameter.

The addition of surfactant up to a concentration just above the CMC to an initially polydisperse emulsion results in a cream (or sediment) which is separated from the dilute phase. Additional surfactant is added to the dilute phase to further increase the concentration and the resultant concentrated layer is again separated and the same treatment repeated to the dilute phase. After progressive treatments a set of cream samples are obtained. These are

then diluted back to the original oil volume fraction and the preceding operations repeated with different suitable surfactant concentrations. This continues until a suitably narrow size distribution is achieved.

Since the liquid–solid phase transition induced by depletion forces is entropic, the precise nature of surfactant, dispersed and continuous phases is not of great importance. This method has been successfully used in a number of examples [21-25] where the desirability for 'monodisperse' emulsions has been significant in determining the experimental data.

1.2.3 Preparation of 'monodisperse' emulsions by aerosol mechanisms

Another method, which may in principle be used for forming 'monodisperse'd emulsions is the 'aerosol' route which involves forming a stream of droplets which is then directed into the second bulk phase [26]. Such a stream can be formed from a jet emerging from a capillary, or induced mechanically by a so–called 'chopper blade' technique or induced electrostatically to 'atomise' the jet.

Electrospray (ES) atomisation is the only process capable of dividing a liquid into uniform fragments with controllable dimensions from the micrometer, down to the nanometer, range. This method relies on the natural formation of a sharp liquid cone when the meniscus at the end of a capillary tube is charged to several kilovolts with respect to a neighbouring grounded electrode. The apex region of the cone is not static. In the 'cone–jet' mode the conical tip deforms continuously into a thin steady jet which breaks up into a stream of charged drops. This spray is referred to as an electrospray [27,28]. Similar methods, which tend to produce droplets at a slower rate (and are not as commonly used), include the 'dripping' method and the 'harmonic spraying' method as described by Cloupeau [29,30].

Aerosols generated by acoustic atomisation have been used to manufacture 'monodisperse' droplets, particularly for polymerisation. This technique relies on a piezoelectric transducer [31] or a piezoceramic oscillator [32] that vibrates and breaks up a liquid jet into droplets. The size of the droplets produced can be controlled by the size of the orifice they emerge from, the frequency of the oscillator and the liquid flow rate.

1.3 Emulsification by Nucleation and Growth

The PDMS emulsion used in this work is synthesised by a mechanism analogous to the base–catalysed hydrolysis and polymerisation of tetraethoxysilane (TEOS) to form colloidal silica particles [33]. The method of formation of the PDMS emulsions is discussed later (refer to section 3.2.2). It proceeds via a nucleation and growth mechanism without any added surfactant. This process is also found in many cases for the preparation of emulsifier–free or emulsifier–starved polymerisation reactions [34-36].

Nucleation involves the initial formation of small nuclei from a homogeneous phase. When the monomer has a high degree of solubility in water, initiation of polymerisation occurs in the aqueous phase. Intermediates (or radicals) generated in the aqueous phase add monomer units until they exceed their solubility and precipitate. The precipitated molecules form spherical droplets, which will absorb any emulsifier, if present, or surface–active oligomers formed in solution (which act as an *in–situ* surfactant in the case of the PDMS droplets described in this thesis) and monomer to form primary droplets.

These primary droplets thus formed, particularly in the situation of an expanding interface, are not stable in the colloidal sense. Stability is obtained when enough charged groups have formed at the interface to give the droplet an adequate electrostatic surface potential. Thus, primary droplets may either

persist or coagulate and coalesce with already existing droplets or other primary droplets. This will occur until the potential energy of electrostatic repulsion between the droplets is sufficient to ensure colloidal stability in the ionic environment in which the droplet is formed.

Droplet nucleation continues throughout polymerisation. The formation of new droplets is moderated by the capture and flocculation of precipitating oligomeric radicals and primary droplets by already existing mature droplets. A steady state is reached where the rate of nucleation of primary droplets and the rate of primary droplet capture is equal. Generally the quicker the polymerisation is to reach this steady state, the narrower the final size distribution will be. The longer the nucleation stage proceeds, the more coagulation occurs which leads to a broader distribution.

1.4 Apparent Spontaneous Emulsification

Apparent spontaneous emulsification [37] may occur under non–equilibrium conditions when two liquids are brought together. There are three mechanisms by which this can happen; the diffusion and stranding mechanism [38], interfacial turbulence and transient negative interfacial tension [39]. It is often difficult to determine which mechanism is occurring and to distinguish truly spontaneous emulsification from that which occurs with very slight mixing.

The diffusion and stranding mechanism involves nucleation and growth of droplets from localised super–saturation near an interface [37,40]. This happens when toluene, containing dissolved ethanol, is placed in contact with an aqueous phase. As the water–soluble alcohol diffuses ahead into the water it leaves the insoluble toluene behind. The interface becomes highly irregular in structure. This process is driven by the negative enthalpy of solution of ethanol in water.

The second mechanism involves break up of an interface between two liquids by capillary waves to form emulsion droplets. These thermal fluctuations, caused by diffusion of surface–active material to the interface, increase with temperature and change the interfacial tension. Flow of liquid parallel to the interface also assists emulsification and if interfacial tension gradients are present then droplets may become trapped between the two phases [41].

The third mechanism involves the apparent presence of 'negative' interfacial tensions. This occurs in oil–water systems with a third component in both phases. The interfacial tension is lowered where increasing amounts of surfactant and co–surfactant can apparently extrapolate the tension to negative values. What actually results (rather than a negative tension per se), is expansion of the interface and emulsification at the interface. Interfacial tensions remain low but positive due to the depletion of the monolayer during expansion [39].

This phenomenon can occur when a homogenous two component liquid mixture is cooled below its upper consolute temperature. A small temperature quench into a metastable region will result in droplets of the minority phase forming by nucleation of monodisperse droplets. Examples where this occurs includes mixtures of polyisoprene and polyethylene–propylene [42], isobutyric acid and water [43], and 2-6 lutidine and water [44].

Adjustment of the concentration of a component, or a chemical reaction can also produce a new phase. This last method is commonly used to form solid/liquid dispersions such as Ag sols and polystyrene latices.

1.5 Applications of Emulsions

Many differing classes of emulsions are used in both industrial and in many every day products and applications. Often it is a particular feature of that emulsions stability, concentration, droplet size, viscosity, emulsifier and rheological behaviour that determines the function [45,46].

Chappat [45] has listed several examples demonstrating the wide application of emulsions. These include the following:

(i) Emulsions in milk and dairy products

(ii) Emulsions in the food indusry

(iii) Emulsions in pharmacy

(iv) Cosmetic emulsions

(v) Agricultural emulsions

(vi) Bitumen emulsions in road construction

Emulsions can occur in other applications including paints, photographic films, coatings, lubrication, petroleum extraction etc.

The stability of the emulsions in all these applications is crucial. In milk and dairy products the emulsions are stabilised by natural phospholipids. Changing the O/W ratio results in cream, cheese and butter which is an inverse (W/O) emulsion. In foods the emulsions have to be stable over a wide temperature range for a long period of time. Consumer satisfaction with the product is also important.

Droplet size and toxicity are the critical requirements for pharmaceutical emulsions. The dispersions have to have long term stability (1–2 years). Multiple emulsions (i.e. W/O/W) and encapsulated emulsions are also employed, particularly for sustained release [47]. Similarly, cosmetic emulsions need to be non–toxic. Consistency of feel and application to the skin are relevant attributes in this area.

Agricultural emulsions have differing needs [48]. The emulsions are applied as formulations designed to get an active ingredient across a material barrier. As such wetting and spreading characteristics are important.

Bitumen emulsions require good stability to survive the process from manufacture to application as a fine film. The oil droplets need to adhere strongly onto the road surface and then the emulsion needs to be broken when put in contact with the surface. Thus a fine balance between stability and instability is required in this case.

Emulsions are useful in applications because they tend to be environmentally friendly, O/W emulsions in particular avoid using large amounts of solvents. Emulsions are fluid in nature and tend to spread easily. This homogeneity enables good, even distribution of an active agent. Storage of emulsions for long periods must be tightly controlled to maintain the nature of the dispersion, as must be the consistency for personal products. Certain emulsions need to be broken in order to achieve the desired effect, for example as mentioned for agricultural sprays and road emulsions. Average droplet sizes in most commercially and industrially encountered emulsions tend to be of the order of a few microns.

1.6 PDMS Emulsions

Obey [49] first described the synthesis of 'monodisperse' silicone oil/water emulsions. The droplet size and electrophoretic mobility of the emulsions were studied using dynamic light scattering and electrophoresis. The effect of ammonia and monomer concentration on the droplet size was investigated. The PDMS phase was characterised principally by ^{29}Si and ^{1}H NMR, mass spectrometry and gel–permeation chromatography. The results showed that the most abundant polymeric species is the cyclic tetramer octamethyltetrasiloxane (D_4). It was shown that the ratio of linear to cyclic

polymer in the PDMS phase may be altered by changing the amount of ethanol and/or monomer present in the initial reaction mixture.

Wegener [50] investigated the effect of adding cross–linking monomer to the initial reaction mixture together with ethanol. Results showed that at low cross–linker concentrations, emulsions are initially formed, whilst above a volume fraction of 0.4, particles were formed. Dilution with ethanol indicated that the particles were of a soft 'microgel type' nature. Analysis of the PDMS by NMR indicated the formation of cross–linked network structures.

Anderson [51] investigated the effect of the addition of surfactant on the eventual average emulsion droplet size and the molecular weight and chemical composition of the PDMS phase. The surfactants used were both ionic and non–ionic. The presence of surfactant indicated that the proportion of linear to cyclic PDMS was increased and the average droplet size decreased.

It should be pointed out here that the PDMS emulsion forms spontaneously via a nucleation and growth mechanism. However, mechanical energy is required initially to ensure dissolution of the starting monomer.

1.7 Objectives

As a 'monodisperse', surfactant–free emulsion, the PDMS emulsions described in this thesis provides an ideal system for studying the physical and colloidal properties of liquid/liquid dispersions. Since emulsions are extremely important in a number of industrial applications (refer to section 1.5), their stability is of critical importance. An understanding of the de–emulsification process is a subject of practical, as well as fundamental, interest. With the PDMS emulsion it should be possible to follow the

phenomena of coagulation and coalescence and to examine whether the emulsion behaves as predicted by theory.

Depending on the level of added cross–linking monomer in the reaction mixture (refer to section 1.6) either liquid droplets or microgel–type particles are formed. A microgel particle is a cross–linked particle that can be swollen in size by a good solvent. The study of microgel particles occupies a growing niche in the field of colloid science [52]. Cross–linked PDMS droplets/gels provide an opportunity to study the osmotic swelling of an inorganic micogel.

Cross–linking will also affect the nature of the PDMS phase. With the addition of cross–linker, it should be possible to change the characteristics of the silicone oil (density, viscosity, molecular weight etc.) and hence the emulsion droplets. The effects of the viscosity of the internal liquid phase can alter the motion of a liquid droplet, provided that the oil/water interface is fluid in nature. As the PDMS emulsion has no added emulsifier, the droplets present an ideal case for studying droplet motion, for example the movement in an electric field (electrophoresis).

1.8 References

1. Tadros, Th.F. and Vincent, B., *in* "Encyclopaedia of Emulsion Technology" (P. Beecher, Ed.), Vol. 1, Chap. 3. Marcel Dekker, New York, 1983.

2. Shinoda, K. and Friberg, S. *Advances in Colloid and Interface Science* **4**, 281 (1975).

3. Schulman, J.H. and Cockbain, E.G. *Transactions of the Faraday Society* **36**, 651 (1940).

4. Prince, L.M. *Journal of Colloid and Interface Science* **23**, 165 (1967).

5. Prince, L.M., "Microemulsions: Theory and Practice.", Academic Press, New York, 1977.

6. Walstra, P., *in* "Encyclopaedia of Emulsion Technology" (P. Beecher, Ed.), Vol. 1, Chap. 2. Marcel Dekker, New York, 1983.

7. Gopal, E.S.R., *in* "Emulsion Science" (P. Sherman, Ed.), Chap. 1. Academic Press, London, 1968.

8. Shinoda, K. *Journal of Colloid and Interface Science* **24**, 4 (1967).

9. Shinoda, K. and Saito, H. *Journal of Colloid and Interface Science* **30**, 258 (1969).

10. Albers, W. and Overbeek, J.Th.G. *Journal of Colloid and Interface Science* **14**, 501 (1959).

11. Boyd, J., Parkinson, C. and Sherman, P. *Journal of Colloid and Interface Science* **41**, 359 (1972).

12. Nakashima, T. and Shimizu, M. *Ceramics* **21**, 408 (1986).

13. Kandori, K., Kishi, K. and Ishikawa, T. *Colloids and Surfaces* **55**, 73 (1991).

14. Peng, S. and Williams, R.A., *From* "Control of Particulate Processes IV", Delft, Engineering Formulation, New York, 1997

15. Katoh, R., Asano, Y., Furuya, A., Sotoyama, K., Tomita, M. and Okonogi, S. *Journal of the Japanese Society For Food Science and Technology - Nippon Shokuhin Kagaku Kogaku Kaishi* **44**, 44 (1997).

16. Nakashima, T. and Shimizu, M. *Kagaku Kogaku Ronbunshu* **19**, 984 (1993).

17. Bibette, J. *Journal of Colloid and Interface Science* **147**, 474 (1991).

18. McClements, D.J. *Colloids and Surfaces a-Physicochemical and Engineering Aspects* **90**, 25 (1994).

19. Bibette, J., Roux, D. and Nallet, F. *Physical Review Letters* **65**, 2470 (1990).

20. Richetti, P. and Kekicheff, P. *Physical Review Letters* **68**, 1951 (1992).

21. Barchini, R. and Saville, D.A. *Langmuir* **12**, 1442 (1996).

22. Bibette, J., Morse, D.C., Witten, T.A. and Weitz, D.A. *Physical Review Letters* **69**, 2439 (1992).

23. Calderon, F.L., Biais, J. and Bibette, J. *Colloids and Surfaces a-Physicochemical and Engineering Aspects* **74**, 303 (1993).

24. Hemar, Y., Herrmann, N., Lemarechal, P., Hocquart, R. and Lequeux, F. *Journal De Physique II* **7**, 637 (1997).

25. Calderon, F.L., Stora, T., Monval, O.M., Poulin, P. and Bibette, J. *Physical Review Letters* **72**, 2959 (1994).

26. Hengelmolen, R., PhD. Thesis, University of Bristol (1994).

27. Tang, K.Q. and Gomez, A. *Journal of Colloid and Interface Science* **175**, 326 (1995).

28. Tang, K.Q. and Gomez, A. *Journal of Colloid and Interface Science* **184**, 500 (1996).

29. Cloupeau, M. and Prunetfoch, B. *Journal of Electrostatics* **25**, 165 (1990).

30. Cloupeau, M. and Prunetfoch, B. *Journal of Aerosol Science* **25**, 1021 (1994).

31. Panagiotou, T. and Levendis, T.A. *Journal of Applied Polymer Science* **43**, 1549 (1991).

32. Brenn, G., Helpio, T. and Durst, F. *Chemical Engineering Science* **52**, 237 (1997).

33. Stöber, W., Fink, A. and Bohn, E. *Journal of Colloid and Interface Science* **26**, 62 (1968).

34. Vanderhoff, J. *Journal of Polymer Science: Polymer Symposium* **72**, 161 (1985).

35. Goodwin, J.W., Hearn, J., Ho, C.C. and Ottewill, R.H. *Colloid and Polymer Science* **252**, 464 (1974).

36. Fitch, R.M. and Tsai, C.H., *in* "Polymer Colloids" (R. M. Fitch, Ed.), Vol. 1, Plenum Press, New York and London, 1971.

37. Davies, J.T. and Rideal, E.K., "Interfacial Phenomena." 2nd ed., Academic Press, New York, 1963.

38. Davies, J.T. and Haydon, D.A. *Procedures of the Second International Congress on Surface Activity* **1**, 417 (1957).

39. Vermeulen, M., Joos, P. and Ghosh, L. *Journal of Colloid and Interface Science* **140**, 41 (1990).

40. Miller, C.A. *Colloids and Surfaces* **29**, 89 (1988).

41. Kaminski, A. and McBain, J.W. *Procedures of the Royal Society (London) Series A* **198**, 447 (1949).

42. Cumming, A., Wiltzius, P. and Bates, F.S. *Physical Review Letters* **65**, 863 (1990).

43. Wong, N-C. and Knobler, C.M. *Physical Review A* **24**, 3205 (1981).

44. Krishnamurthy, S. and Goldburg, W.I *Physical Review A* **22**, 2147 (1980).

45. Chappat, M. *Colloids and Surfaces a-Physicochemical and Engineering Aspects* **91**, 57 (1994).

46. Israelachvili, J. *Colloids and Surfaces a-Physicochemical and Engineering Aspects* **91**, 1 (1994).

47. Davis, S.S., Hadgraft, J. and Palin, K., *in* "Encyclopaedia of Emulsion Technology" (P. Beecher, Ed.), Vol. 2, Chap. 3. Marcel Dekker, New York, 1985.

48. Becher, D.Z., *in* "Encyclopaedia of Emulsion Technology" (P. Beecher, Ed.), Vol. 2, Chap. 7. Marcel Dekker, New York, 1985.

49. Obey, T.M. and Vincent, B. *Journal of Colloid and Interface Science* **163**, 454 (1994).

50. Wegener, M., M.Sc. thesis, University of Bristol (1993).

51. Anderson, K.R., Obey, T.M. and Vincent, B. *Langmuir* **10**, 2493 (1994).

52. Saunders, B.R. and Vincent, B. *Colloid and Polymer Science* **275**, 9 (1997).

Chapter 2: Emulsions

2.1 Introduction

Most emulsions and microemulsions contain (at least) three components: an organic 'oil' phase, an aqueous phase and the emulsifier (usually a surfactant or polymer which adsorbs at the oil/water interface) [1]. It is unusual to find an emulsion with just oil and an aqueous phase present, with the emulsifier being effectively a functionalised part of the oil phase in a water continuous (O/W) emulsion; this is the case for the PDMS/water emulsions described in this thesis.

All emulsions (excepting microemulsions) are thermodynamically unstable and will try to revert back to a separate two-phase system by de-emulsification. The paths by which de-emulsification can take place are well defined. However, emulsions can appear to be stable over long periods of time. By stating that an emulsion is 'stable' it is implied that the size distribution of droplets does not significantly change with time. Such kinetically stable emulsions are described as being 'metastable'.

The emulsion stability needs to be controlled in order to avoid de-emulsification. The balance of interdroplet interactions (arising from attractive and repulsive forces) determines the colloidal stability of the emulsion. The understanding of these and other factors is essential in order to control the stability of emulsions. The intrinsic properties of the emulsion such as the polarisability and density of the dispersed phase determine the attractive forces. The properties of the interfacial region, for example the presence of an electric double layer or steric interactions, determine repulsive forces. Other phenomena related to the solubility and density of the dispersed phase also play a role, alongside interdroplet forces, in determining the emulsion stability.

2.2 Emulsion Stability

The most important property of an emulsion is its stability. An emulsion's stability concerns its ability to resist breakdown into two bulk phases. Emulsion breakdown mechanisms can be broadly categorised into the following processes; creaming (or sedimentation), Ostwald ripening, coagulation and coalescence. A further possible breakdown process is phase inversion, which is only relevant for surfactant–stabilised systems. This process is not relevant to this work and is not discussed in this thesis.

The most obvious form of breakdown involves droplet–droplet collisions that result in coagulation and/or coalescence to form larger droplets. Eventually complete phase separation occurs. This process may take seconds or years, depending on the kinetic stability of the emulsion. An emulsion prepared by simply homogenising two immiscible liquids will have a very short lifetime. In order to increase the life–span of an emulsion some form of emulsifier needs to be present. There are several classes of emulsifiers that can stabilise droplets by different mechanisms. However, in all cases the emulsifier stabilises the droplet by forming an adsorbed film on the surface at the interface between the oil and water phases.

There are several factors associated with emulsifiers that influence and favour emulsion stability. A lowered interfacial tension (as described in section 1.2, particularly in the formation of microemulsions) associated with surfactant adsorbed at the interface will help to facilitate the formation of the large interfacial area associated with emulsions. Film thinning and coalescence is reduced by the Gibbs–Marangoni effect caused by adsorbed emulsifiers (refer to section 2.4). Emulsifiers also create a tangential stress, which impedes or prevents internal circulation, thus giving the droplet rigidity.

The rate of creaming or sedimentation of an emulsion will be reduced if the continuous medium has a high viscosity. Smaller droplet sizes and density–matching of the oil and water phases also similarly increase the

stability by decreasing the creaming/sedimentation rate (refer to section 2.2.1).

Monodisperse emulsions are inherently more stable than polydisperse emulsions due to reduced effects of Ostwald ripening (refer to section 2.2.2).

The presence of an electrostatic charge at the interface, caused by ionic surfactants or adsorbed polyelectrolyte will aid emulsion life–time. This is due to the overlap of similarly charged electric double layers (refer to section 2.3).

Droplets with a mechanically strong and elastic interfacial film tend to be more stable. To this end adsorbed polymers, protein molecules and solid particles at the interface are particularly effective and these will also impart a steric stabilisation mechanism on the droplets (refer to section 2.3.3)

2.2.1 Emulsion creaming or sedimentation

This breakdown process occurs where there is a difference between the density of the dispersed phase and the continuous medium.

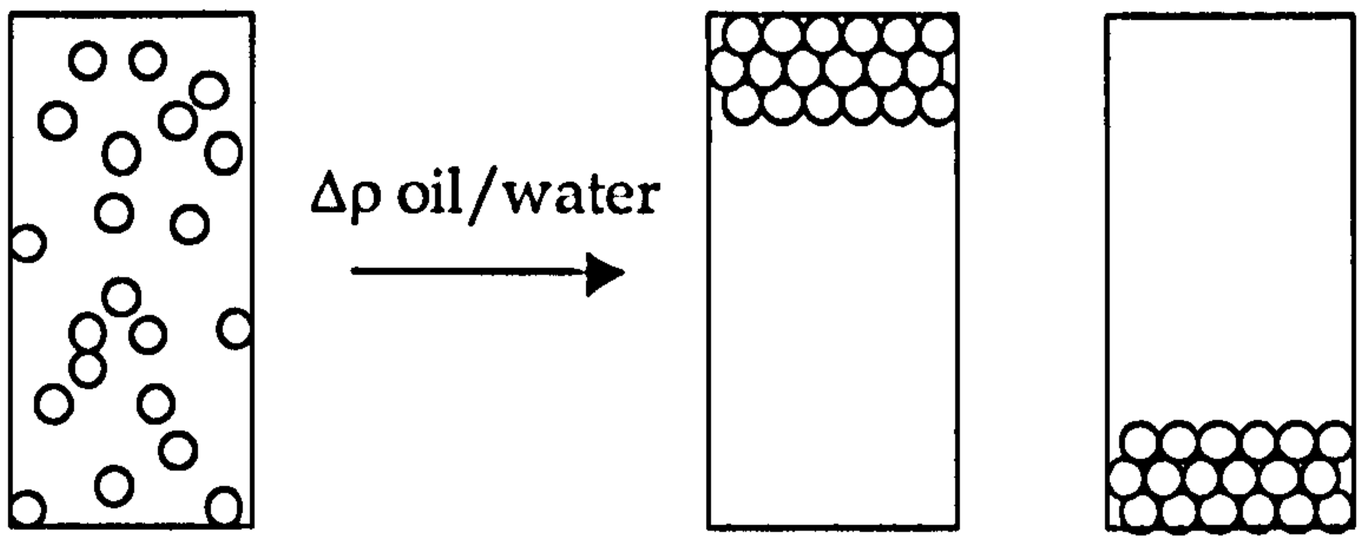

Figure 2.1: Schematic representation of emulsion creaming or sedimentation

Droplets acting under the force of gravity will either rise or fall depending on the density gradient (as in figure 2.1). The resulting cream or

sediment will consist of a concentrated dispersion of close–packed droplets. No change in the droplet size necessarily occurs as a consequence, but with droplets in such close proximity to each other the probability of droplet coalescence is increased.

Creaming rates are determined by the difference in density and also the average droplet size and droplet size distribution. If the droplets are small enough then the diffusional kinetic energy (i.e. the Brownian motion of the droplets) is sufficient to oppose the gravitational force. The velocity of a droplet can be determined by equating the hydrodynamic drag force (Stoke's law) with gravitational force:

$$\frac{4}{3}\pi r^3 \Delta\rho g = 6\pi\eta_o r v \qquad 2.1$$

Thus,

$$v = \frac{2\Delta\rho g r^2}{9\eta_o} \qquad 2.2$$

where v is the velocity of a droplet of radius r in a liquid of viscosity η_o, $\Delta\rho$ is the difference in density between phases and g the acceleration due to gravity. For example, a PDMS droplet of density 0.95 g cm^{-3}, diameter 1 μm and at a temperature of 25 °C in pure water will have a creaming rate of 0.1 μm $hour^{-1}$. For a droplet of diameter 2 μm the rate increases to 0.4 μm $hour^{-1}$. This is assuming that the droplets are undeformable, non–interacting spheres with smooth surfaces. For dilute, monodisperse emulsions equation 2.1 should be valid

With many emulsion systems it is desirable to decrease the rate of creaming or sedimentation. For instance a homogeneous dispersion is important in many pharmaceutical and industrial applications. This can be achieved most effectively by either decreasing $\Delta\rho$ or increasing η_0.

2.2.2 Ostwald ripening

Two liquids forming an emulsion often have finite mutual solubilities. If the emulsion is initially polydisperse, larger droplets will grow at the expense of the smaller droplets. The system will tend to a final equilibrium state in which there could be one, large droplet. This ageing process in emulsions (and other colloidal dispersions) is known as Ostwald ripening [2,3].

In an emulsion there is a dynamic equilibrium whereby the rates of dissolution and absorption of the dispersed phase balance in order that the saturation solubility of the dispersed phase in the dispersion medium can be maintained. In a polydisperse emulsion the smaller droplets will have a greater solubility than the larger droplets and so will tend to dissolve while the larger ones grow. The determining factor for the rate of this repartitioning is the solubility of the dispersed phase in its surrounding medium. If the dispersed phase is highly insoluble then the process is of little or no consequence. If the dispersed phase is fairly soluble, Ostwald ripening occurs to such an extent that the expected lifetime of such dispersions is reduced.

A pressure difference exists across any curved interface. For a spherical droplet the Young-Laplace equation gives this pressure difference:

$$\Delta p = \frac{2\gamma}{r} \qquad 2.3$$

where γ is the interfacial tension and r the droplet radius. In qualitative terms, the surface tension tends to compress the droplet, increasing its internal pressure. For an emulsion droplet this pressure difference may alter the chemical potential of the material inside, thus increasing the solubility of the dispersed phase in the continuous phase.

If the radius of a droplet increases from r to r + dr, the interfacial area will also increase from $4\pi r^2$ to $4\pi(r+dr)^2$ (i.e. by $8\pi dr$). The corresponding increase in surface free energy will be $8\pi\gamma r dr$. If dn moles of liquid are

transferred from a planar surface of solubility S_∞ to a droplet of solubility S_r the free energy increase is equal to $dnRT\ln S_r/S_\infty$. (R being the gas constant and T the absolute temperature). Equation 2.4 equates these free energy increases:

$$dnRT\ln\frac{S_r}{S_\infty} = 8\pi\gamma r dr \qquad 2.4$$

Since $dn = 4\pi r^2 dr\rho/M$ (ρ is the density and M is the molar mass of the liquid) equation 2.5, equivalent to the Kelvin equation for vapour pressure, is derived. This relates the chemical potential (and hence solubilty) of the dispersed molecules to the radius of curvature of the droplet.

$$\mu^r - \mu^\infty = RT\ln\frac{S_r}{S_\infty} = \frac{2\gamma M}{\rho r} = \frac{2\gamma V_m}{r} \qquad 2.5$$

Here μ^r is the chemical potential of the molecule inside the droplet, μ^∞ is the chemical potential of the same molecule in a bulk fluid with a planar interface and V_m is the molar volume of the liquid in the droplet. It can be seen that the smaller the droplet the higher the solubility of the molecules contained within.

As the dispersed phase will establish, at equilibrium, a concentration in the dispersed phase S_r, difference in droplet size is crucial. Any resultant increase in the mean droplet size of the emulsion will enhance creaming or sedimentation which encourages coagulation and coalescence. Ostwald ripening however, can be slowed by addition of a second, more insoluble component (refer to section 5.1.1). If the dispersed phase is of very low solubility then the attainment of equilibrium is often a slow process and Ostwald ripening is not observed.

2.3 Interdroplet Interactions: Droplet Coagulation

2.3.1 Electrical double–layer interactions

The surface charge of an oil droplet in water is acquired through ionisation of groups at the oil/water interface of the droplet. This surface charge will affect the distribution of ions near the surface in the aqueous phase. This arrangement of ions near the surface leads to the formation of an electric double layer, as first described by Gouy and Chapman [4,5].

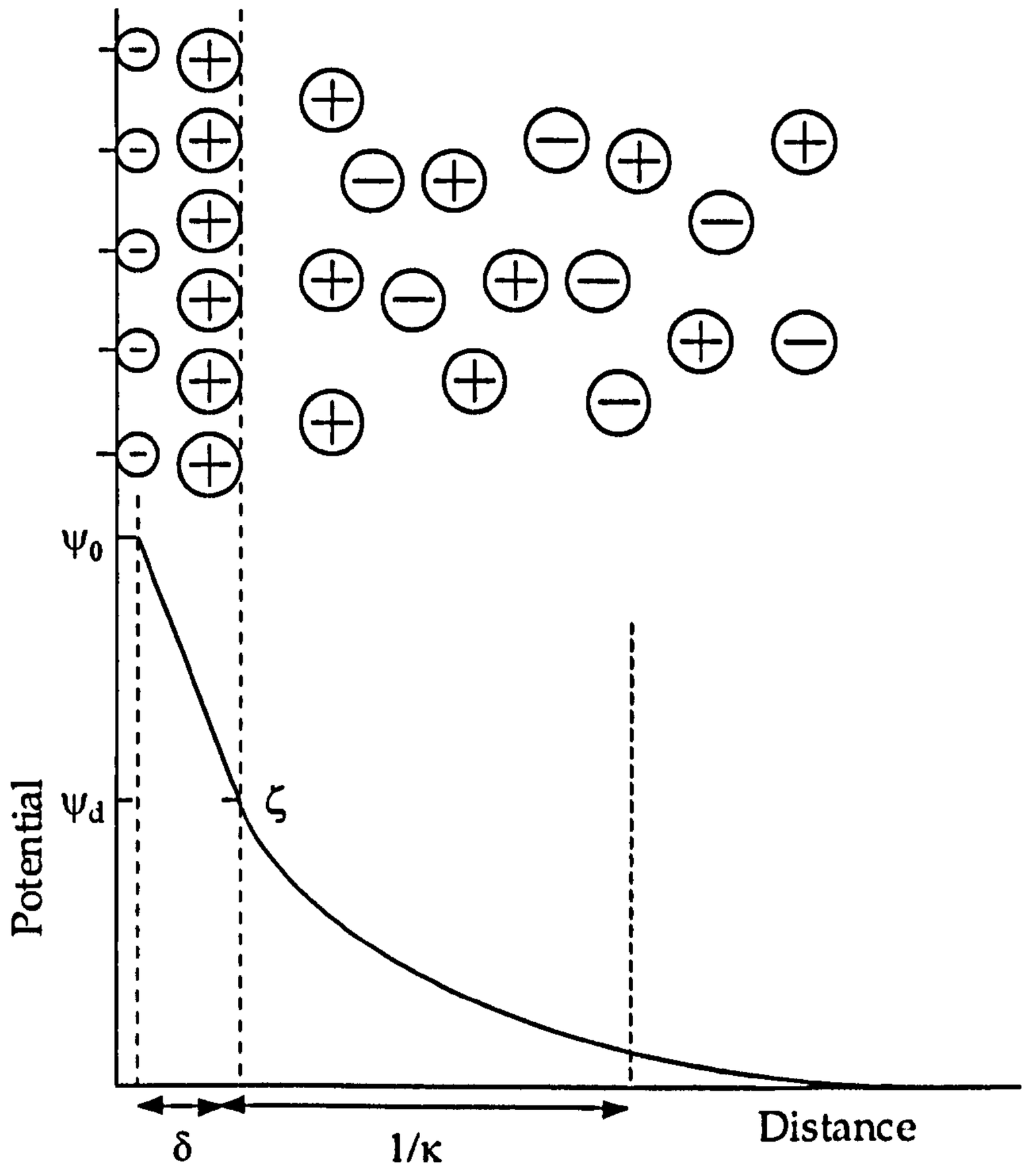

Figure 2.2: Structure of the electrical double layer

Figure 2.2 depicts the structure of the double layer. The electric double layer has been extensively discussed [6,7] and only a brief description is given here. The double layer is made up of the surface charge (σ_o) giving rise to a surface potential (ψ_o) and a diffuse layer. There may be a layer of counter ions specifically adsorbed next to the surface in the aqueous phase (the Stern layer). The potential at this point has a value ψ_d. This is usually experimentally determined as the zeta (ζ) potential [7]. This is the measured potential at the plane of shear as the surface moves in an electric field. The unequal distribution of ions in the bulk phase surrounding the surface forms the diffuse layer.

It is assumed that the potential decreases exponentially away from the Stern layer. The potential is described by:

$$\psi = \psi_d \exp(-\kappa x) \qquad 2.6$$

Here x is the distance from the surface, $1/\kappa$ is the Debye–Hückel length, which depends on the permittivity of the medium and the electrolyte concentration. The Debye–Hückel length is, in effect, the extension of the double layer and is given by the following expression:

$$1/\kappa = \left(\frac{\varepsilon_r \varepsilon_o kT}{2e^2 N_A c z^2} \right)^{\frac{1}{2}} \qquad 2.7$$

where ε_r is the dielectric constant of the medium, ε_o the permittivity of free space, k the Boltzmann constant, T the absolute temperature, N_A Avogadro's number, e the electronic charge, c the bulk concentration of electrolyte and z the valency of the ions. The size of the surface charge and the nature and extent of the electric double layer determines the electrostatic repulsion between the droplets and also many experimental observations (e.g. electrokinetic effects, refer to section 4.3).

With increasing electrolyte concentration κ increases and the extension of the double layer decreases. For a 1:1 electrolyte $1/\kappa$ is of the order of about 1 nm for a 10^{-1} mol dm^{-3} solution and 10 nm for a 10^{-3} mol dm^{-3} solution.

For the calculation of the interaction energy, V_E, which results from the overlapping of the diffuse parts of the electric double layer of two identical particles of radius a, the following expression is derived for large κa [8]:

$$V_E = 2\pi\varepsilon a\psi_o^2 \ln(1+\exp[-\kappa h]) \qquad 2.8$$

where h is the shortest distance between the two surfaces and ε is the permitivity of the dispersion medium. From equation 2.8 it is apparent that V_E at a distance h depends on the value of κ. Note that this interaction is repulsive for two identical overlapping double layers.

2.3.2 London–van der Waals interactions

Van der Waals forces arise from dipole–dipole (Keesom) interactions, dipole–induced dipole (Debye) interactions, and fluctuations in the electronic fields of atoms and molecules (dispersion or London interactions). Hamaker derived the interaction energy (V_A) between two identical droplets of radii a, separated by a distance h, which can be simplified to [9]:

$$V_A = -\frac{A_{12}a}{12h} \qquad h << a \qquad 2.9$$

A_{12} is the effective Hamaker constant. The Hamaker constant can be calculated from dielectric data of a material over a wide frequency range [10,11]. This can be achieved by the macroscopic (Lifshitz) approach. The other approach of pairwise additivity makes assumptions that ignore the influence of neighbouring atoms on the interaction between any pair of atoms, which is a source of error when considering condensed media. Lifshitz theory derives the Hamaker constant in terms of the bulk properties. If υ_e, the characteristic absorption frequency of the media is assumed to be the same the following expression for the non–retarded Hamaker constant for two identical phases (1) acting across a medium (2) [11]:

$$A_{12} = \frac{3}{4}kT\left(\frac{\varepsilon_1 - \varepsilon_2}{\varepsilon_1 + \varepsilon_2}\right)^2 + \frac{3h\upsilon_e}{16\sqrt{2}}\frac{\left(n_1^2 - n_2^2\right)^2}{\left(n_1^2 + n_2^2\right)^{3/2}} \qquad 2.10$$

where ε is the static dielectric constant and n is the refractive index for the respective media ($n^2 = \varepsilon_{vis}$).

The van der Waals force for two identical phases acting across a medium is attractive, as A_{12} is always positive. The first term of equation 2.10 is the zero–frequency term. For media dispersed in water this is the dominant term. This is because water has a high static dielectric constant (ε = 80) whereas the dielectric constant for PDMS is much lower (ε ≈ 1.9 [12]). This, added to the non–zero (dispersion) frequency term (the second term of equation 2.10), gives a total value of $A_{PDMS\text{-}water}$ of 0.35×10^{-20} J at 300 K. The Hamaker constant for D_4, the major constituent of the silicone phase, estimated from refractive index data [13] was 5×10^{-20} J.

The Hamaker constant decreases with increasing distance from the surface of the media. This is known as the retardation effect and is due to a fast decay in the dispersion energy between two atoms as separation increases. Electrostatic screening can also affect A_{12} by reducing the zero–frequency contribution. This is due to the electrostatic fields of the interacting atoms being screened by polarising ionic charges in the medium.

2.3.3 Steric interactions

Emulsions can also be stabilised by adsorbed polymer or surfactant at the oil/water interface. At equilibrium, adsorbed molecules may protrude into the continuous phase (all adsorbed polymer layers have a 'tails and loops' morphology). When two droplets approach each other a repulsive force is generated when these two layers interact. This stabilising effect is known as steric stabilisation.

With the PDMS/water emulsions, droplet stability is provided by a fraction of the oil phase behaving as an *in–situ* surfactant. This resides in the PDMS droplet with the charged end groups residing at the interface. Thus, two droplets approaching each other will only be subjected to electrical and van der Waals type of interactions. Steric interactions, in this instance, can be ignored.

2.3.4 Total potential energy of interaction

Deryaguin–Landau–Verwey–Overbeek (DLVO) theory [8],[14] describes the total energy of interparticle interactions for colloidal particles. In the case of PDMS emulsions the forces to consider are the attractive van der Waals forces and the repulsive interaction between the two charged electric double layers. The theory describes the total interaction energy as a function of interparticle distance, h. The general form of the potential energy–distance curve is shown in figure 2.3

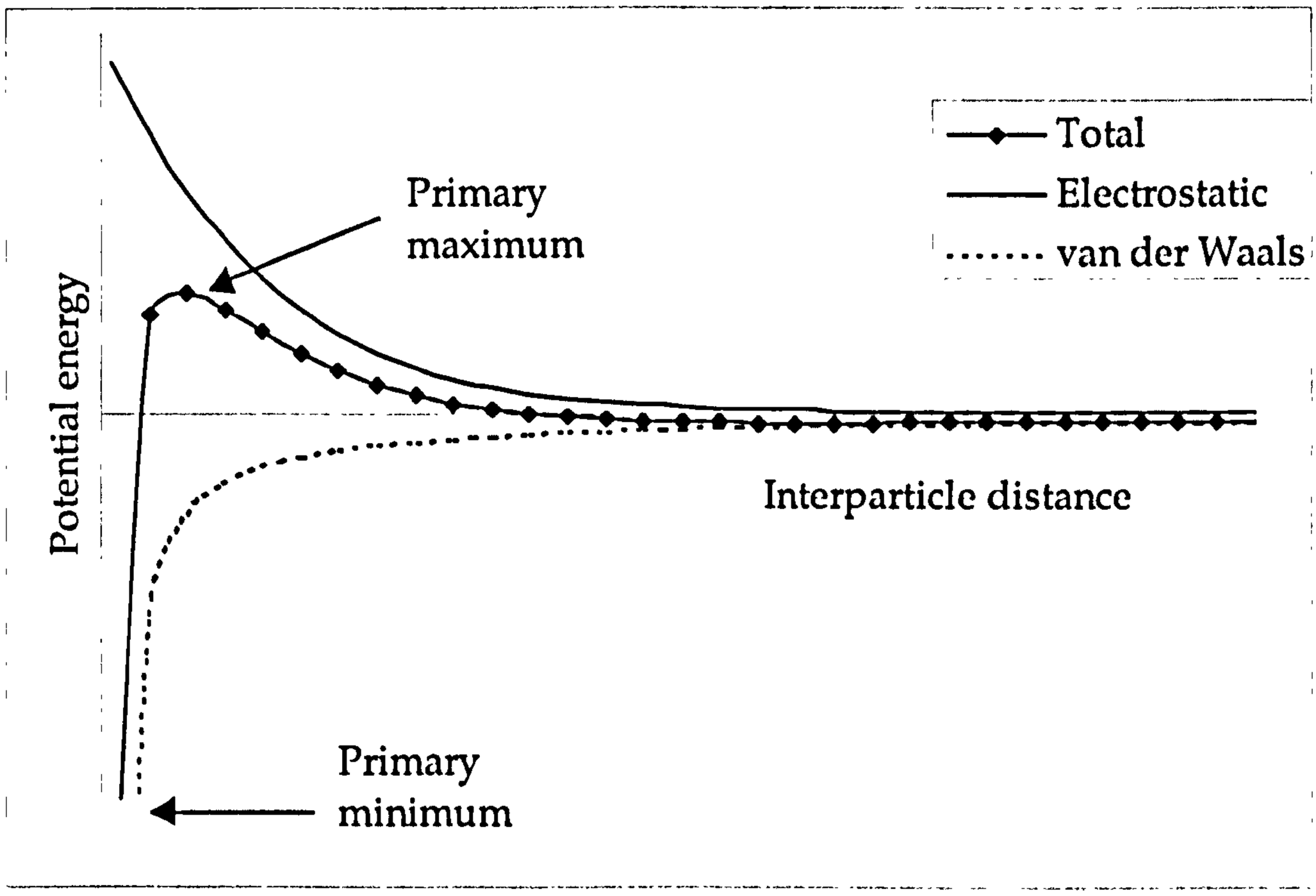

Figure 2.3: Schematic of the potential energy curves for a pair of emulsion droplets

The total potential energy of interaction (V_h) is obtained by summing equations 2.8 and 2.9. The electrostatic interaction decays exponentially with distance, with a range of the order of $1/\kappa$, and the van der Waals interaction decreases as an inverse power of the interparticle distance. As can be seen in figure 2.3 van der Waals attraction predominates at small and at large interparticle distances. At intermediate distances the electrostatic term dominates, for low electrolyte concentrations. In figure 2.3 the total potential energy curve shows a primary maximum. If this is large compared with the thermal energy, kT, of the droplets the emulsion should be stable. This maximum depends on the value of ψ_o and upon the range of the force (i.e. upon $1/\kappa$). If it is not large enough (25 kT and below [15]) then the emulsion will coagulate and the system will enter the primary minimum (at very small values of h). Droplets in the primary minimum will be irreversibly coagulated. Note that there is also a secondary minimum at much larger

interparticle distances. If this minimum is sufficiently deep it may give rise to reversible coagulation.

As electrolyte acts as a screen for surface charge, increasing the concentration of electrolyte will decrease the electrostatic repulsion. There exists a critical concentration at which coagulation will occur when the size of the primary maximum is insufficient to ensure droplet stability. Thus, to improve the colloid stability of a dispersion, one needs to increase the surface potential and decrease the electrolyte concentration.

2.4 Thin Film Thinning: Droplet Coalescence

2.4.1 Introduction

Emulsions have an additional instability, compared to solid colloidal particles, namely coalescence. When two droplets come into close proximity with one another by Brownian collision, coagulation or creaming/sedimenting, a thin liquid film of the dispersion medium forms between the two interfaces [16]. This film will drain to a metastable thickness depending on a complex process involving hydrodynamic and interfacial force interactions. Disruption and elimination of the film will result in the two droplets uniting together into a single droplet. If the film is unstable then coagulation will always result in coalescence.

Figure 2.4 shows the general features of the lamella between two PDMS droplets. The PDMS–water–PDMS film can be considered as a type B_1 film as defined by Hunter [17]. When the radius of the droplets is large compared to the separation distance, b, then the Derjaguin approximation [18] is applicable. Under such conditions, elements on each sphere interact as

parallel plane elements at the same separation; the total interaction is a sum over the infinitesimal elements.

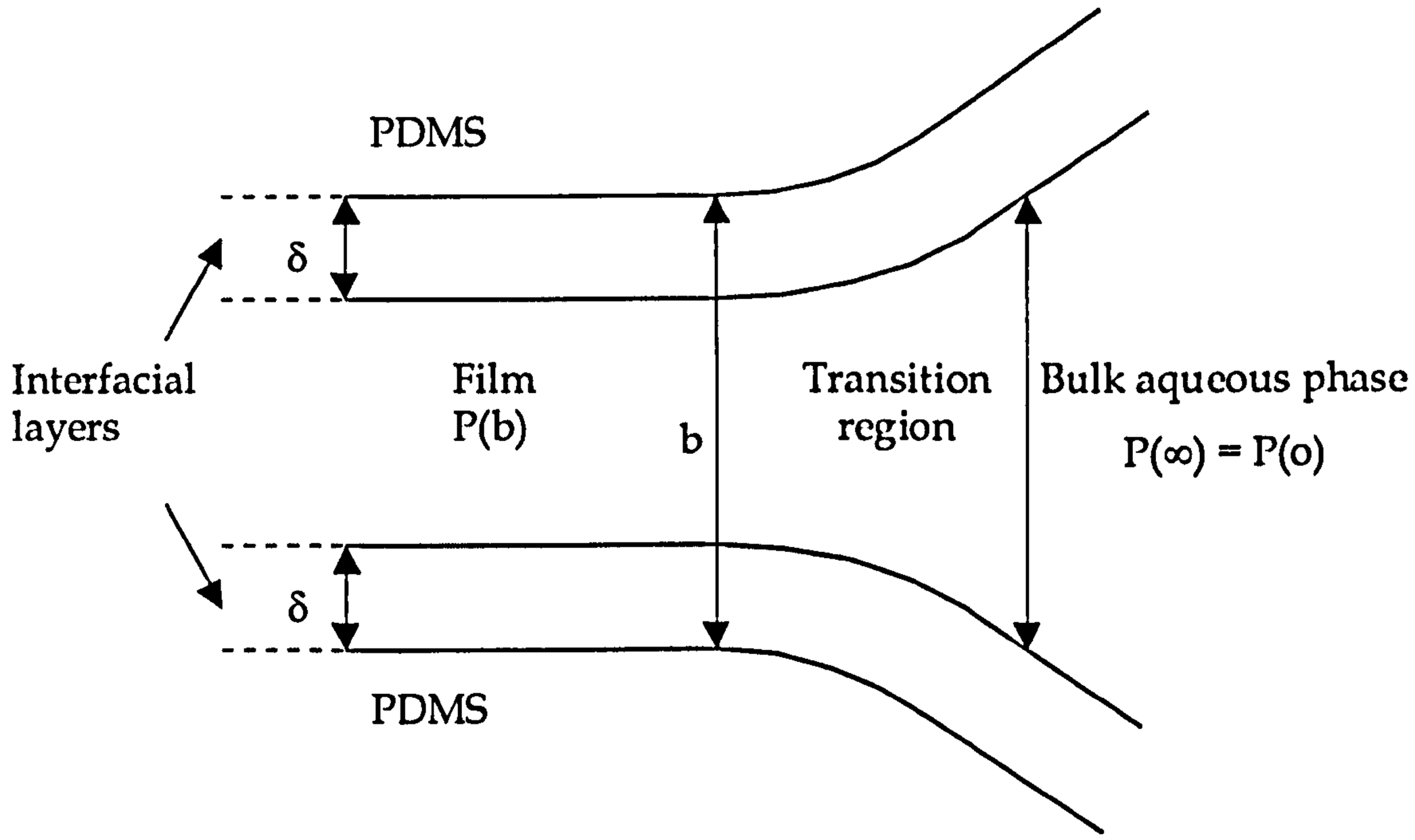

Figure 2.4: Diagrammatic representation of the thin film and border regions between two PDMS droplets (from [19]*)*

Here P(b) is defined as the normal pressure in a film of thickness b, and P(∞) is the normal pressure in a film where the interaction energy across the film is zero. Thus, P(∞) is equivalent to the isotropic pressure in the adjacent bulk phase P(o). The interfacial layers are the regions of thickness δ in the film where the electrical double layer (refer to figure 2.2) applies; i.e. where there is an amount of interfacial structure.

2.4.2 Thermodynamics of film thinning

Emulsion coalescence is a thermodynamically favourable process (as opposed to emulsion formation). The variation in the free energy of the film is dependent on the DLVO (refer to section 2.3.4) calculation, i.e. $G(b) = G_{electrostatic} + G_{van\ der\ Waals}$. As the film thins, so the surface area of the droplets must increase. If a surfactant is present this results in an increase in the interfacial tension, which is unfavourable to the process. If the approaching droplets have sufficient kinetic energy to surmount this free energy barrier (G_{max}) then they will coalesce. If this barrier is sufficiently high then the emulsion droplets will remain in the coagulated state. In addition to the surface forces of intermolecular origin, two colliding droplets in a liquid medium will also experience hydrodynamic interactions due to the viscous friction of the thinning film.

2.4.3 Forces acting across a thin film: disjoining pressure

For a coagulated pair of droplets there are two stable film thicknesses. These are when the film is sitting in either the primary or the secondary minimum. In these states the net force on the film is zero ($dG_i/db = 0$). The variation of the potential energy of interaction with film thickness is dependent on van der Waals attractive forces and electrostatic repulsive forces (as for coagulation) with an additional very close range repulsive force. This force is only significant when a film that is in the primary minimum tries to thin further (i.e. $b < 2\delta$). It is normally a very steep repulsive force, usually associated with the molecules adsorbed in the interfacial areas. In the case of the PDMS/water films, the rigidity without adsorbed polymers or surfactants

at the interface is very low. As discussed in section 2.3.3 there are no steric interactions as such.

Much of the experimental work on thin liquid films is discussed in terms of the hydrostatic pressure in the interior of the film. This pressure, acting normal to the plane of the film is called the disjoining pressure [20].

The excess normal pressure (P(b) - P(o)) in the film is balanced by the disjoining pressure, $\pi(b)$. $\pi(b)$ is the net force per unit area acting across the film ($\pi(b) = -dG_i(b)/db$). A film will tend to thin spontaneously until $\pi(b)$ is zero (in the primary or secondary minima). The disjoining pressure can be considered to be made up from the contributions listed in section 2.4.2 such that:

$$\pi(b) = \pi_A(b) + \pi_E(b) + \pi_S(b) \qquad \textbf{2.11}$$

i.e. the disjoining pressure is made up of van der Waals (π_A), electrostatic (π_E) and steric (π_S) contributions. A stable film has a positive disjoining pressure, such that $\pi_E + \pi_S > \pi_A$. Other forces, such as gravity, may also act on the film, but, in the consideration of a horizontal film, these can be ignored. In the transition zone P(b) < P(o) ($\pi(b)$ is negative) due to the high interfacial curvature in the region. Here P(b) is lower than P(b) in the film so liquid tends to get sucked into the transition region from the film by a capillary force acting parallel to the flat interfaces. This does not affect $\pi(b)$ as the disjoining pressure is described normal to the film.

Another method by which the forces acting on a thin film can be described is the interfacial tension, which contributes to a tangential pressure P_t across the film. It should be noted that the interfacial tension in the film is not the same as in the bulk as the film is under stress. As a film thins, the area increases. As the interface expands so the tension must increase. With adsorbed surfactants the Gibbs–Marangoni effect helps to restore equilibrium. This is achieved by a combination of adsorption of more surfactant from the bulk to replenish the interface (Gibbs effect) and flow of the monolayer along the interface driven by the tension gradient (Marangoni effect).

It should be noted that the mere fact of the existance of thermodynamically metastable states does not guarantee that the film will actually reach this state. Therefore, the concept of kinetic stability is used to denote the resistance of the film against rupture, the major factor providing kinetic stability of emulsions is the presence of adsorbed surfactant monolayers at the droplet surface.

2.4.4 Hydrodynamics of film thinning

How rapidly a film drains can affect the rate of coalescence. However, accurate analysis of the hydrodynamic flow of liquid from between two droplets is difficult due to the distortion of the form of the droplets. The radial flow of liquid exerts a shearing force, which will lead to internal circulation within the droplet. As a result a phenomenon known as 'dimpling' can occur.

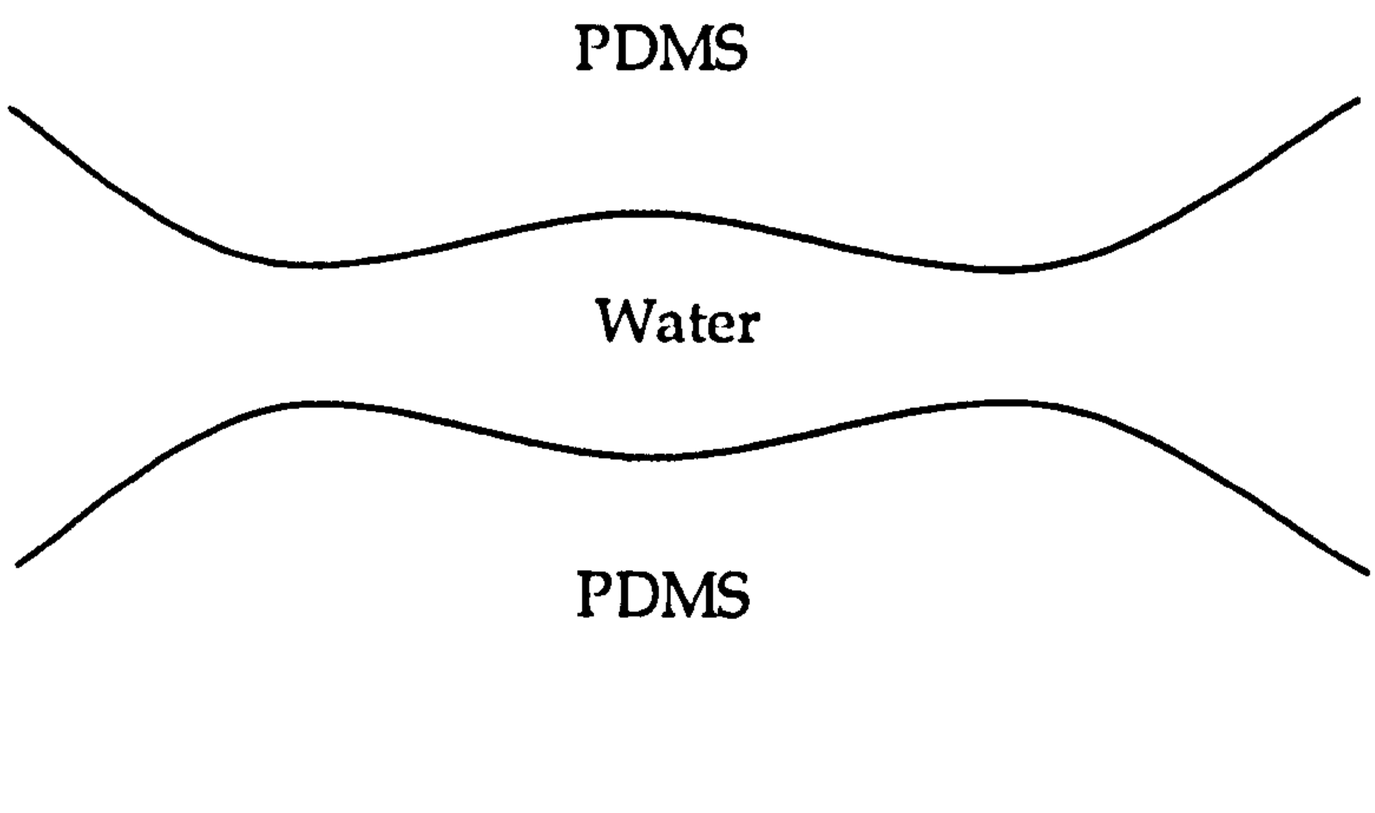

Figure 2.5: Schematic representation of the 'dimple' between two emulsion droplets

As can be seen from figure 2.5 the thinnest region of a dimple does not necessarily occur along the axis of approach. Instead, it may occur at the periphery of the contact zone. Dimpling is lessened by the presence of an adsorbed surfactant or polymer at the interface, which causes increased

rigidity. The dimple does not usually occur for small drops (< 1 μm) and a planar film forms [16].

The actual rate of thinning was first examined by Reynolds [21]. He solved the Navier–Stokes equation, neglecting gravitational and inertia forces. The hydrodynamics of film thinning is expressed as a relation between the droplet velocity and the driving force. A good summary of this is given by Hunter [17].

2.4.5 Film rupture

Thermal or mechanical fluctuations in the film thickness may occur in the region of closest approach. These waves can grow in magnitude until, at the point of closest approach the apexes may join, causing coalescence. Reduction in the film thickness results in increased van der Waals attraction, which causes more thinning with the ultimate disruption of the whole film. This will occur if the attractive contribution outweighs the electrostatic repulsion and the opposing increase in the interfacial tension due to expansion, i.e:

$$\frac{d\pi_A}{db} > \frac{d\pi_E}{db} + \frac{d\pi_\gamma}{db} \qquad 2.12$$

If the condition expressed in equation 2.12 is met then the film is unstable, the fluctuation will grow and rupture occurs. This will tend to occur at a critical film thickness.

2.5 Surfactant Stabilised Emulsions

As stated in section 1.2, it is usually necessary to employ an emulsifying agent of some sort so that a stable emulsion can be produced. The nature of this agent affects the stability and the form of the emulsion. The emulsion formed could be either O/W or W/O, as depicted in figure 1.1.

The first attempt to draw together simple rules connecting the emulsion stability with the surfactant properties was the Bancroft rule [22]. This states that "in order to have a stable emulsion the surfactant must be soluble in the continuous phase". Griffen [23,24] introduced the concept of the Hydrophile–Lipophile balance (HLB) which is a numerical scale that determines the likelihood of a surfactant to form W/O or O/W emulsions. Shinoda and Friberg [25] showed that the HLB number was not only dependent on the surfactant molecules but also on the temperature, type and concentration of electrolytes, type of oil, etc. They proposed that the phase inversion temperature (PIT) be used instead of HLB for the characterisation of the emulsion stability.

These emulsions, which contain a solute that can adsorb at the interface, are subject to a number of dynamic effects that do not occur in pure liquid/liquid systems. The finite rate at which such a solute responds to either: (i) approach of another interface; (ii) local deviations in curvature; or (iii) formation of new surface, influences the rate of coagulation and coalescence and determines the emulsion stability. These effects include the Gibbs–Marangoni (surface elasticity) effects and surface viscosity. Surface elasticity refers to the fact that adsorbed surfactants resist changes in the surface area in either direction. Even at low concentrations of surfactant the interface becomes essentially rigid so that there is little or no transfer of momentum from the exterior liquid to the interior of a drop [17]. Emulsion droplets thus behave like solid particles in the presence of surfactants.

2.6 References

1. Israelachvili, J. *Colloids and Surfaces a-Physicochemical and Engineering Aspects* **91**, 1 (1994).

2. Kabalnov, A. S. and Shchukin, E. D. *Advances in Colloid and Interface Science* **38**, 69 (1992).

3. Tadros, Th.F. and Vincent, B., *in* "Encyclopaedia of Emulsion Technology" (P. Beecher, Ed.), Vol. 1, Chaps. 1 and 3. Marcel Dekker, New York, 1983.

4. Gouy, G. *Journal of Physical Chemistry* **9**, 457 (1910).

5. Chapman, D.L. *Philosophical Magasine* **25**, 475 (1913).

6. Hunter, R.J., "Foundations of Colloid Science.";Vol. 1, Clarendon Press, Oxford, 1986.

7. Hunter, R.J., "Zeta Potential in Colloid Science.", Academic Press, London, 1981.

8. Verwey, E.J.W. and Overbeek, J.Th.G., "Theory of the Stability of Lyophobic Colloids.", Elsevier, Amsterdam, 1948.

9. Hamaker, H.C. *Physica* **4**, 1058 (1937).

10. Gregory, J. *Advances in Colloid and Interface Science* **2**, 396 (1969).

11. Israelachvili, J., "Intermolecular and Surface Forces." 2nd ed., Academic Press, London, 1991.

12. Hunter, M.J., Hyde, J.P., Warrick, E.L. and Fletcher, H.J. *Journal of the American Chemical Society* **68**, 667 (1946).

13. Clever, H.L. and Taylor, M.L. *Journal of Chemical and Engineering Data* **16**, 91 (1971).

14. Derjaguin, B.V. and Landau, L. *Acta Physiochem USSR* **14**, 633 (1941).

15. Tadros, Th.F. *Advances in Colloid and Interface Science* **46**, 1 (1993).

16. Ivanov, I.B. and Kralchevsky, P.A. *Colloids and Surfaces A: Physicochemical and Engineering Aspects* **128**, 155 (1997).

17. Hunter, R.J., "Foundations of Colloid Science.";Vol. 2, Clarendon Press, Oxford, 1991.

18. Derjaguin, B.V. *Kolloid - Zeitshrift* **69**, 155 (1934).

19. Tadros, Th.F. and Vincent, B., *in* "Encyclopaedia of Emulsion Technology" (P. Beecher, Ed.), Vol. 1, Chap. 3. Marcel Dekker, New York, 1983.

20. Derjaguin, B.V. and Obuchar, E. *Journal of Colloid Chemistry* **1**, 385 (1935).

21. Reynolds, O. *Philosophical Transactions of the Royal Society* **177**, 157 (1886).

22. Bancroft, W.D. *Journal of Physical Chemistry* **17**, 514 (1913).

23. Griffen, J. *Journal of the Society of Cosmetic Chemists* **1**, 311 (1949).

24. Griffen, J. *Journal of the Society of Cosmetic Chemists* **5**, 249 (1954).

25. Shinoda, K. and Friberg, S., "Emulsions and Solubilisation.", Wiley, New York, 1986.

Chapter 3: Polydimethylsiloxane Emulsions

3.1. Silicones

3.1.1. Introduction

One of the most commonly investigated of the silicone polymers is polydimethylsiloxane (PDMS). PDMS and other silicone polymers are widely used in the manufacture of cosmetics, food-processing materials and medical preparations. They are highly valued for their lubricity, their low surface energy and their ability to act as antifoam agents.

The first silicones were manufactured by Kipping [1]. These were formed from the condensation of diphenylsilanediol. They were initially erroneously thought to bear a structural resemblance to ketones of general formulae R_2CO. The name 'silicone' denotes a polymer of the form:

$$(R_nSiO_{\frac{4-n}{2}})_m \qquad 3.1$$

where n is between 0-3 and m is 2 or larger. PDMS exhibits the basic structure shown below in figure 3.1.

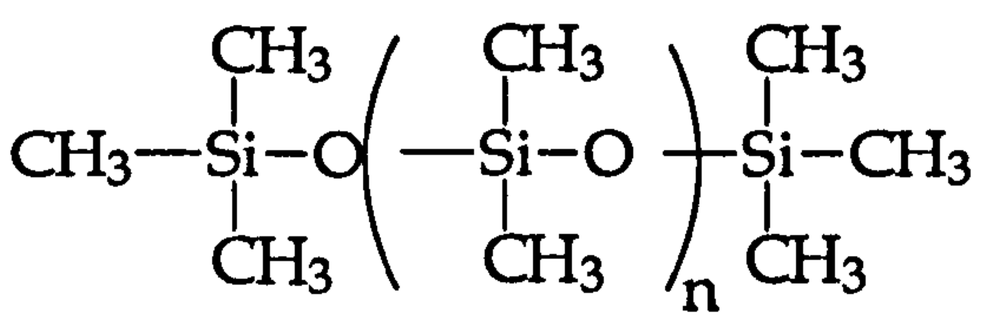

Figure 3.1: The basic structure of PDMS

The repeating unit of the polymer is referred to as a 'D' unit [2]. The termination unit is known as an M unit, so the above structure is referred to

as MD_nM. Branch points where cross–linking units (i.e. O– sites) occur are denoted as a T group for a trifunctional unit and Q for the quaternary unit. These branching units have the effect of introducing rigidity into the chain structure. Colloidal silica is effectively a network of Q units. This relatively simple chemistry leads to fluids in the case of low molecular weight PDMS. At higher molecular weights silicone fluids become gums which, when cross–linked, can form elastomeric products.

3.1.2. Synthesis of silicones

Silicones are generally synthesised by the hydrolysis of the highly reactive Si–Cl bond [3] as shown in figure 3.2. The silicones made by the reaction in figure 3.2 can be either linear or a cyclic.

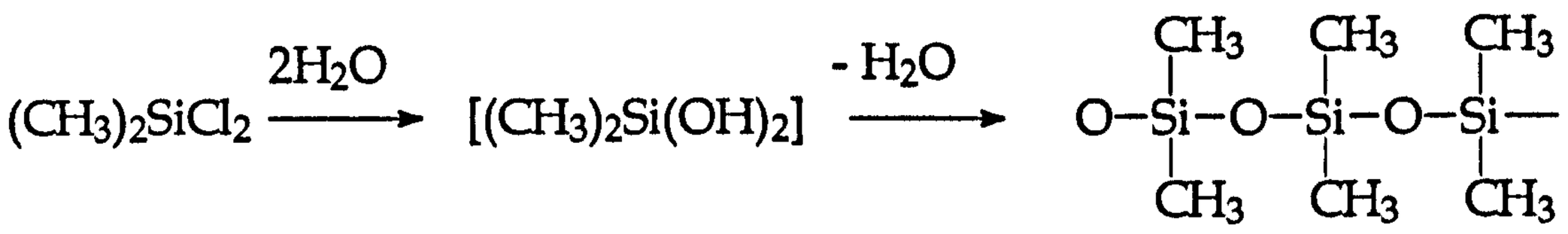

Figure 3.2: General synthesis of silicones

Alternative monomers can be used, for example dimethyldiethoxysilane $(CH_3)_2Si(OC_2H_5)_2$ which is the starting monomer used in this work. The hydrolysis and polymerisation of this monomer was first described in 1945 [4]. Hydrolysis, in acidic alcohol, results in mainly cyclic polymers being produced. It was noted that the proportion of cyclic to linear (from 15%–70% cyclic) polymer could be altered by changing the reaction conditions.

The cyclic polymers formed contain a minimum of 3 D units linked together in the form shown in figure 3.3.

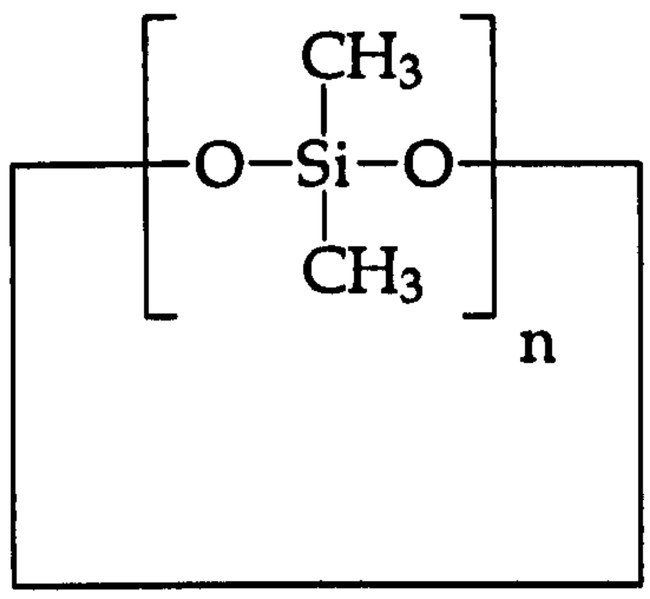

Figure 3.3: The general structure of cyclic silicones

Kipping [1] and later Patnode [3] found cyclo–octamethyltetrasiloxane (D_4, n=4 in figure 3.3) to be the predominant molecule formed in the hydrolysis reaction (~ 47 % of the product). Due to the larger size of the silicon atom, and the nature of the Si–O bond, larger rings are allowed with silicon compared to carbon chemistry. These cyclic molecules and low molecular weight silanols (PDMS with –OH end groups) are used as intermediates in the synthesis of higher molecular weight polymers. In fact, D_4 is the most commonly used oligomer for the production of higher molecular weight silicones [5,6]. It readily reacts with hexamethyldisiloxane (M_2) in concentrated sulphuric acid at room temperature, or with tetraalkylammonium hydroxides at 80 °C in what is termed 'linearisation' of the siloxanes. If D_4 is dispersed in aqueous media by a quaternary ammonium hydroxide, which acts as a catalyst, then very high molecular weight silicones are obtained [7,8]. The resulting silicone emulsion is stable and of a small droplet size. Such silicone emulsions can be employed as release agents or for coating compositions. The silicone polymers can be extracted at the end of the polymerisation by breaking the emulsion.

3.1.3. Properties of silicones

Silicones do not have a carbon–based backbone. Their inorganic chain of alternate silicon and oxygen atoms gives rise to their unique physical characteristics. Silicones generally have the physical properties listed below:

Low surface energy	High gas permitivity
Thermal and oxidative stability	Good weather resistance
Chemically inert	Wide service temperature
Shear stability	Non–flammability

These are all due to the silicone polymer backbone having certain chemical properties. Table 3.1 below compares some key properties of PDMS and two carbon–based polymers, poly(ethylene) and poly(tetraflurocthylene) (PTFE) [9].

Polymer	Poly(ethylene)	PTFE	PDMS
Backbone bond length (Å)	C–C=1.54	C–C=1.54	Si–O=1.65
Backbone bond angle (degrees)	112°	112°	Si–O–Si=130°
Min. distance between two backbone atoms (Å)	2.53	2.53	2.99
Energy of rotation ($J\ mol^{-1}$)	14	20	0
Surface free energy ($mJ\ m^{-2}$)	34	19	22

Table 3.1: Comparison of PDMS with other polymers

The Si–O bond energy is very high (799.6 KJ mol^{-1}), making the polymers chemically inert. The bond is also longer than the carbon–carbon bond. The silicone chain has enhanced flexibility due to the length of the Si–O bond, resulting in virtually no energy barrier for backbone rotation. This results in PDMS having one of the lowest glass transition temperatures for any polymer. The high 'mobility' of the PDMS chain ensures that the molecule is very efficient at presenting low surface energy methyl groups at the polymer/air interface. This results in many of the characteristics associated with low surface energy, such as the absorption and adhesion behaviour of other materials onto the polymer [9]. The low polarity of the molecule also means that there are very weak intermolecular forces in PDMS and other silicones. These give rise to the polymers having a low variation of viscosity with temperature and pressure and a high gas permittivity for oxygen and nitrogen. The surface tension of PDMS is low enough to cause the polymer to spread as a liquid film on many surfaces.

3.1.4. Applications of silicones

Silicones have many uses due to their unique nature and low toxicity. Silicones are easily dispersed in many solvents and their surface–active properties enable them to be used in many coating treatments and cooling applications. Cyclic silicones find use in personal deodorant sprays. The so–called 'dry feel' is a direct consequence of their low volatility. Higher molecular weight silicones are used more as lubricants, sealants and as conditioners in shampoos.

Industrially, functionalised silicones are used in many applications such as detergents and petroleum extraction [10]. In detergents, it is their specific anti–foaming ability that is utilised. Again in the extraction of crude oil and natural gas there is a need for anti–foaming agents with mixtures of

oil, gas and water all present. Silicone surfactants are used to de-emulsify W/O crude oil emulsions. Functionalised silicone polymers, which have been given additional properties by substitution of methyl groups have many practical advantages. One example is in the textile industry where silicones help to impart smoothness, bounce and resiliency to fibres.

Silicones are also important in many personal care products. Their chemical inertness and biological safety, together with good spreading and lubricative properties, give rise to use in many formulations. They are used in hair products such as shampoos, conditioners and hair sprays to reduce resistance to wet and dry combing, to reduce static build up, enhance gloss and provide a soft silky feel. They are important components of many skin-care products where again a soft smooth silky feel and ease of spreading and application are highly desired attributes.

Other uses are as diverse as medical implants, contact lenses, adhesives, cosmetics, electrical systems, diffusion pumps, damping oils, polishing oils and heat exchange [11]. All rely on some of the specifically unique properties associated with silicones.

3.2. PDMS (Silicone oil) in Water Emulsions: Experimental

3.2.1. Materiäls

Dimethyldiethoxysilane (DMDES) (97%) was obtained from Aldrich chemicals (UK) and distilled prior to use. Dimethyldimethoxysilane (DMDMS) was obtained from Fluorochem and methyltriethoxysilane (MTES) was supplied by Strem Chemicals (USA). Ammonia '880' solution (35% w/w), potassium chloride (AnalaR grade), and sodium azide (AnalaR grade) were supplied by BDH (UK). Volumetric standard solutions of hydrochloric acid (0.1008 N) and sodium hydroxide (0.1015 N) were used as supplied from Aldrich. Dextran (molecular weight 505,000 g mol^{-1}) was obtained from Sigma (UK). Visking dialysis tubing (19 mm internal diameter) was obtained from Medicell International (UK). All water was purified using a Millipore 'Milli–Q', and later a 'Mill–Q Plus' filtration system.

3.2.2. Preparation of PDMS emulsions

All the PDMS emulsions studied in this investigation were made in essentially the same way: by the polymerisation of a silane monomer in an aqueous alkali solution. This process proceeds via a nucleation and growth mechanism from a homogeneous aqueous phase. The most common monomer used was DMDES, a difunctionally active molecule. Alternative monomers used included DMDMS (similar to DMDES, but with methoxy groups instead of ethoxy) and MTES, a trifunctionally active and hence, cross-linking monomer. The structure of these monomers is shown in figure 3.4.

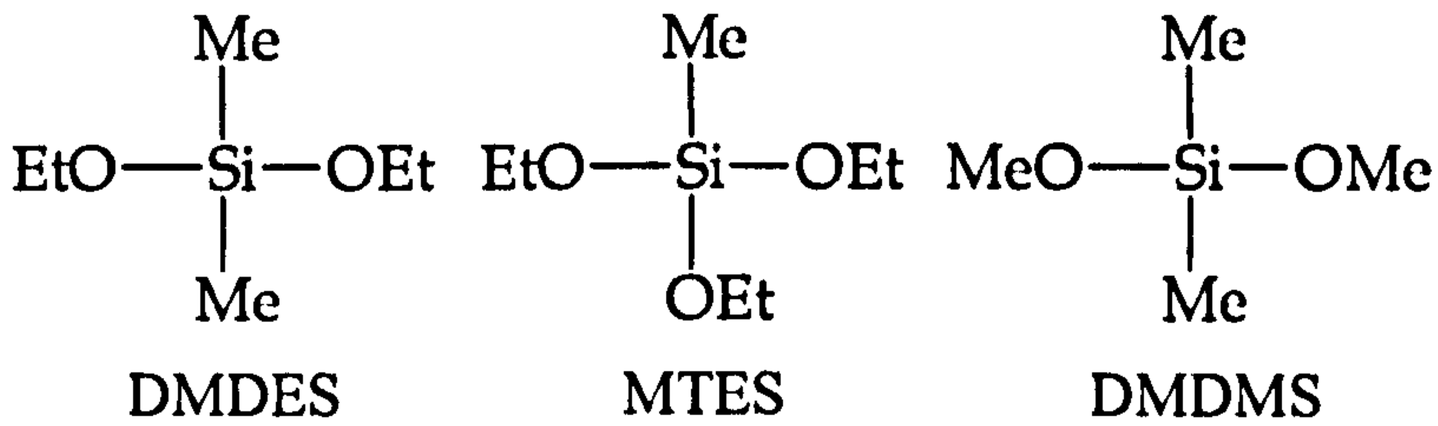

Figure 3.4: The chemical structure of the silane monomers used

In figure 3.4 above 'Me' denotes a methyl group (CH_3) and 'Et' an ethyl group (CH_2CH_3). The alkalinity of the aqueous phase was adjusted by using ammonia solution. The polymerisation proceeds via initial hydrolysis of the active ethoxy (or methoxy) groups to form ionic precursors to the oligomeric molecules. The reaction scheme is presented in figure 3.5.

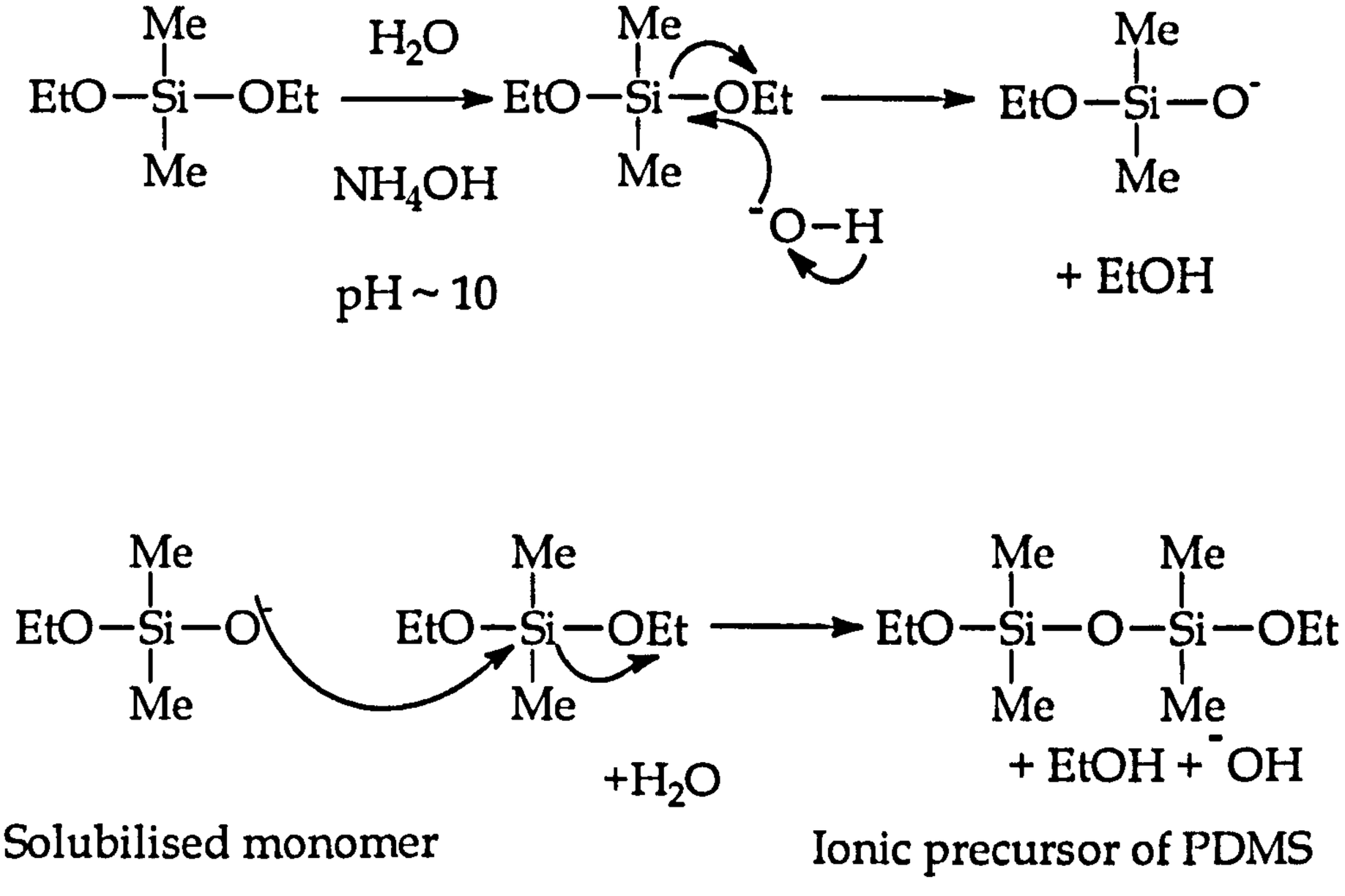

Figure 3.5: Proposed reaction scheme for the formation of the PDMS

The concentrated ammonia '880' solution was initially diluted with pure water to 0.1 v/v, which in turn was diluted to 0.02 v/v. This was used as the 'stock' solution. Most emulsions were prepared using solutions of 0.01

v/v monomer in 0.01 v/v ammonia solution. This was only varied when the amount of monomer in the starting mixture was increased to 0.075 v/v. No other concentration of ammonia was used, since it has a purely catalytic role in the polymerisation. Obey [12] investigated the effect of ammonia concentration on emulsion droplet size. Emulsions were made, using the stated concentrations, in varying quantities from 5 mL samples up to 1 dm^3. When MTES was added to the starting monomer mixture it was mixed in the appropriate proportions with the DMDES before addition to the ammonia solution. For example, a 0.2 v/v solution of MTES in DMDES would be prepared, from which 0.1, 0.05, 0.025 and 0.01 v/v solutions, as required, would be made by dilution with DMDES. When the required amount of monomer had been added to the ammonia solution the mixture was then shaken manually for 30 seconds and left to stand at room temperature. In the case of higher volumes of monomer it was found that the mixture had to be repeatedly shaken vigorously until most of the droplets had dissolved. Eventually a clear solution with a bluish tinge would develop. Over the next few hours this would become increasingly turbid as the PDMS precipitates in the form of small droplets which begin to grow. The larger the droplets, the 'whiter' in appearance the emulsions become.

The polymerisation reaction producing the emulsion was left to continue for 18 hours. At this stage the emulsion was either left as it was or it was dialysed. Dialysis was achieved by inserting the crude emulsion into cleaned Visking dialysis tubing (the tubing was first boiled in distilled water approximately 8 times, using fresh water for each subsequent boiling cycle) and dialysing it against pure water. The water was changed for fresh, pure water approximately 12 times over a 48 hour period. This dialysis procedure was carried out in the case of all the experiments involving emulsion stability, electrolyte and pH (refer to chapter 4).

Black and white photographs of the PDMS emulsions were taken using the Nikon 'Optiphot' optical microscope with a Nikon FX–35 camera and a long focal distance × 40 lens, two of which are shown in plate 3.1.

3.2.3. Isolation of the PDMS phase

The liquid phase of the droplets needed to be isolated from the emulsion in order to facilitate analysis. Creaming or sedimentation under gravity is dependent upon whether the dispersed phase is less dense (creams) or more dense (sediments) then the continuous phase. Indeed, a phase density matched emulsion is very difficult to separate. When there is a significant difference in density between the dispersed and continuous phase then gravity is a sufficient force to separate the two phases. This process is accelerated by centrifugation. However, this was found not to be the most efficient method of separation with a creaming emulsion. The amount of time taken to isolate small amounts was deemed to be too long and so the method described below was adopted.

Most of the PDMS isolated was obtained by making 0.8 dm^3 of 0.05 v/v DMDES, leaving the emulsion undialysed for a week and then neutralising the ammonia by adding 0.1 mol dm^{-3} HCl (prepared from concentrated HCl) until the pH dropped to a value around 3. If left to stand, the PDMS droplets coalesce and rapidly cream. When the aqueous phase had cleared a distinct layer of PDMS could then be removed via careful pipetting. Water and other impurities would often be present in the PDMS as a water in oil (W/O) emulsion. This was removed by repeatedly freeze–thawing the emulsion in an ethanol bath, cooled by the addition of solid carbon dioxide. It was found that if the PDMS was cloudy it soon cleared after 4 or 5 freeze/thaw cycles. Typically about 15–20 mL of silicone oil was obtained, representing approximately 40–50 % yield from the starting monomer. This procedure ensured that the PDMS oil isolated from the emulsion was in as similar form to the oil in the droplets as possible.

3.2.4. Physical properties of the PDMS phase

Measurements on the isolated PDMS were performed in order to assess the effect of cross-linker on the density, viscosity, surface and interfacial tension of the PDMS.

Viscosity measurements were carried out using a Cannon–Fenske capillary viscometer in a glass–fronted water bath, thermostatted at 25 ± 0.5 °C. This technique has been described by Matthews [13]. The volume of sample measured was kept constant at 12 mL. The viscometer was calibrated with pure water. It was cleaned with ethanol and purified water and dried in an oven between measurements. Efflux times were observed visually and recorded on a stopwatch. Errors were estimated at less than 0.5 s.

Density measurements were carried out in a 10 mL density bottle, supplied by BDH. The volume of the bottle was accurately calibrated using pure water at 25 °C. After measuring each sample, the density bottle was cleaned and rinsed with water and acetone and then dried in an oven.

Surface and interfacial tensions were measured by the DuNouy ring method using a Krüss 'K12' processor tensiometer. The ring was calibrated against pure water to check cleanliness. The ring was washed with acetone and water and then flamed in a blue Bunsen flame between each measurement to remove impurities. All glassware was rigorously cleaned by insertion in a 20% HNO_3 bath overnight and thoroughly rinsed with 'Milli–Q' purified water. The oil phase was themostatted at 25 ± 0.2 °C at all times in the experiments.

Melting and freezing points were visually determined using a Linkam themostatted microscope hot–stage, cooled with liquid nitrogen and a Nikon 'Optiphot' microscope with a × 20 long focal distance lens.

The nature of the PDMS and its solvency in organic liquids was examined. It was found that the PDMS was miscible with all hydrocarbons and most common solvents available except ethylene glycol and water.

3.2.5. Determination of PDMS volume fraction in the emulsion

The initial volume fraction of monomer in any preparation was known; typically 0.01 v/v for the majority of the experiments. However, what was not known was the exact final volume fraction of the PDMS formed. Being an emulsion the 'dry weight' cannot be determined as both liquid phases evaporate. Another technique had to be used therefore to determine the volume fraction.

It was initially thought that it would be possible to measure the dry weight of solid PDMS by freeze drying the emulsion. However, it was found that the entire system sublimed, no matter how carefully the temperature was controlled.

High temperature distillation was tried. If the emulsion was distilled then the water phase could be removed and the remaining PDMS phase content recorded. Problems arose in that the PDMS was too difficult to separate from the water; it appeared in the distillate as well as the residue. A solution would have been to carry out a very precise fractionated distillation. However, the tendency of PDMS to absorb on glass surfaces would lead to some inaccuracy.

A possible method to use is the 'Coulter Counter' technique of particle counting. This works on the principle that particles (droplets) passing through a small orifice, across which an electrostatic potential is applied, will cause a change in the resistivity of the medium across that gap. If a certain volume of the medium containing the droplets is passed through the orifice, then the number of droplets in that aliquot is simply related to the number of 'spikes' in the measured current across the gap. Obviously, the dispersion has to be fairly dilute and the medium has to be of moderate conductivity. In order to facilitate this, an ionic strength of 0.18 mol dm^{-3} NaCl was used.

There were three major problems found with this technique when applied to the PDMS emulsions. The first is that the reported lower particle diameter threshold of the apparatus is 1 μm, which is of the same order of size

as the droplets to be studied. The second is that at a background electrolyte concentration of 0.18 mol dm^{-3}, any droplet collisions will result in coalescence (see section 4.2.1), giving rise to a false number concentration. Thirdly, the diameter of the orifice needed for the highest resolution (30 μm) is so small that small dust particles can result in it being blocked. The nature of the apparatus is such that it was very difficult to ensure that the dispersion was entirely dust free, even after filtration through a 5 μm filter.

Another method for determining the volume fraction involved creaming and coalescing the emulsion, and then extracting the PDMS phase in a more volatile liquid (e.g. diethyl ether) which could then evaporate, leaving behind the PDMS. However, problems were encountered with this method. The evaporation of the diethyl ether proved difficult to control without simultaneous loss of PDMS. Also, the PDMS droplets were found not to be transferring into the diethyl ether. Creamed and coalesced droplets were visible at the water / ether interface and would not disappear, suggesting that not all the dispersed phase was present in the ether. It was not apparent why this should occur since it had been shown earlier that previously isolated PDMS was miscible with most solvents available in the laboratory (refer to section 3.2.4).

Finally, it was investigated whether viscosity measurements could be used to determine droplet volume fractions. Emulsions at low or moderate concentrations behave as Newtonian fluids. It is possible to calculate the volume fraction (ϕ) (for $\phi < 0.01$) of the dispersed phase from a knowledge of the viscosity of the emulsion [14,15].

$$\eta_r = 1 + 2.5\phi \qquad 3.2$$

Einstein's equation [16] applies to hard sphere dispersions, where ϕ is the volume fraction and η_r is the relative viscosity. For deformable droplets the internal motion inside the droplet will effect the viscosity [17]. If the internal viscosity of the droplet is significantly larger than the viscosity of the external medium, then Einstein's equation still applies. Similarly, presence of

surfactant at the oil–water interface can cause hard sphere–like behaviour due to interfacial tension gradients and surface viscosity.

Unfortunately, no difference in viscosity could be determined between a 1 % DMDES emulsion and the continuous medium. This is probably due to the thermostatted water bath only being accurate to ± 0.5 °C. Any fluctuation in temperature of this margin would result in an inaccurate reading especially as ϕ, the volume fraction is very low.

From the isolation of PDMS from 800 mL of 0.05 v/v DMDES emulsion a final volume of 15 mL of PDMS was obtained. This represents an approximate volume fraction, ϕ, of ~ 0.019. Thus the oil volume fraction in a typical 0.01 v/v DMDES emulsion may be estimated. Given the change in density from DMDES (ρ=0.865 g cm^{-3}) to PDMS (ρ=0.955 g cm^{-3}), this represents a yield of 41 % by mass. In a 0.01 v/v DMDES emulsion therefore, assuming identical polymerisation, a final oil volume fraction, ϕ, of 0.00375 would be attained.

3.3. Measurement of Droplet Size by PCS

3.3.1. Introduction

Photon Correlation Spectroscopy (PCS), or Dynamic Light Scattering, has been a major technique for determining the average particle size of monodisperse colloidal dispersions [18-20].

The principle of the technique is that the light scattered by a dispersion, at a given angle, has a net intensity resulting from interference in the light scattered from each illuminated particle. Dispersed colloidal particles move due to Brownian motion, which results in a change in the phase and polarisation of the scattered light. Summed over all particles, there are

fluctuations in the net scattered light intensity of a given polarisation. These fluctuations are thus related to the translational diffusion coefficient (movement) and hence the size and shape of the particles. PCS relies on detecting the scattered photons in a series of short time intervals and the digital autocorrelation of the intensity of the fluctuations of the scattered light.

3.3.2. Theory

The autocorrelation function $G_2(\tau)$ of the time–dependent intensity of the scattered light is given by:

$$G_2(\tau) = \lim_{T\to\infty} \int_0^T I(t)I(t+\tau)dt \qquad 3.3$$

T signifies the time over which the correlation is performed and I(t) and I(t+τ) are the scattered light intensities at times t and t+τ. The value of τ must be small relative to the characteristic time of the fluctuations in I. The digital correlator then records the intensity at times separated by successive intervals of $\Delta\tau$.

For short time intervals the particle positions and hence scattered light intensities are highly correlated so that $G_2(\tau)$ tends to a value of 1. As time progresses I(t) and I(t+τ) become increasingly less correlated and the value of equation $G_2(\tau)$ decays as a single exponential [21] of the form:

$$G_2(\tau) = A + B\exp\left(-2q^2Dt_c\right) \qquad 3.4$$

Here A is an instrument constant, B is the baseline value and D is the diffusion coefficient. t_c is the single characteristic correlation time and may be equated to the time taken for a scatterer to move the distance 1/q (where q is the scattering vector, which is constant at a given wavelength, λ, of light and scattering angle, ϑ). The scattering vector is given by equation 3.5:

$$q = \frac{4\pi n}{\lambda} \sin \frac{\vartheta}{2} \qquad 3.5$$

where n is the refractive index of the medium. The correlation time t_c is inversely related to the diffusion coefficient:

$$t_c = \frac{1}{2q^2 D} \qquad 3.6$$

The hydrodynamic radius r_h of a spherical particle is related to the translation diffusion coefficient D by the Stokes–Einstein relationship [16].

$$D = \frac{kT}{6\pi\eta r_h} \qquad 3.7$$

PCS thus provides a measure of the average hydrodynamic radius of the scattering particles. It is assumed that the particle concentration is sufficiently dilute to neglect multiple scattering and particle–particle interactions. The particles have to be spherical in shape, have a low polydispersity (i.e. a narrow size distribution) and possess negligible interactions.

3.3.3. Analysis of droplet size

All droplet diameters were measured using PCS. Two instruments were used. The first was comprised of a CL-4 Cambridge Lasers argon-ion laser tuned to λ = 514.5 nm with PS 100 Malvern Optics and a K7027 Malvern multibit correlator. Later on in the investigation, the apparatus used was a Brookhaven 'Zetaplus' with a B1-9000 AT Digital Correlator. Close agreement was found between measurements made with both instruments. A typical PCS set–up is shown in figure 3.6.

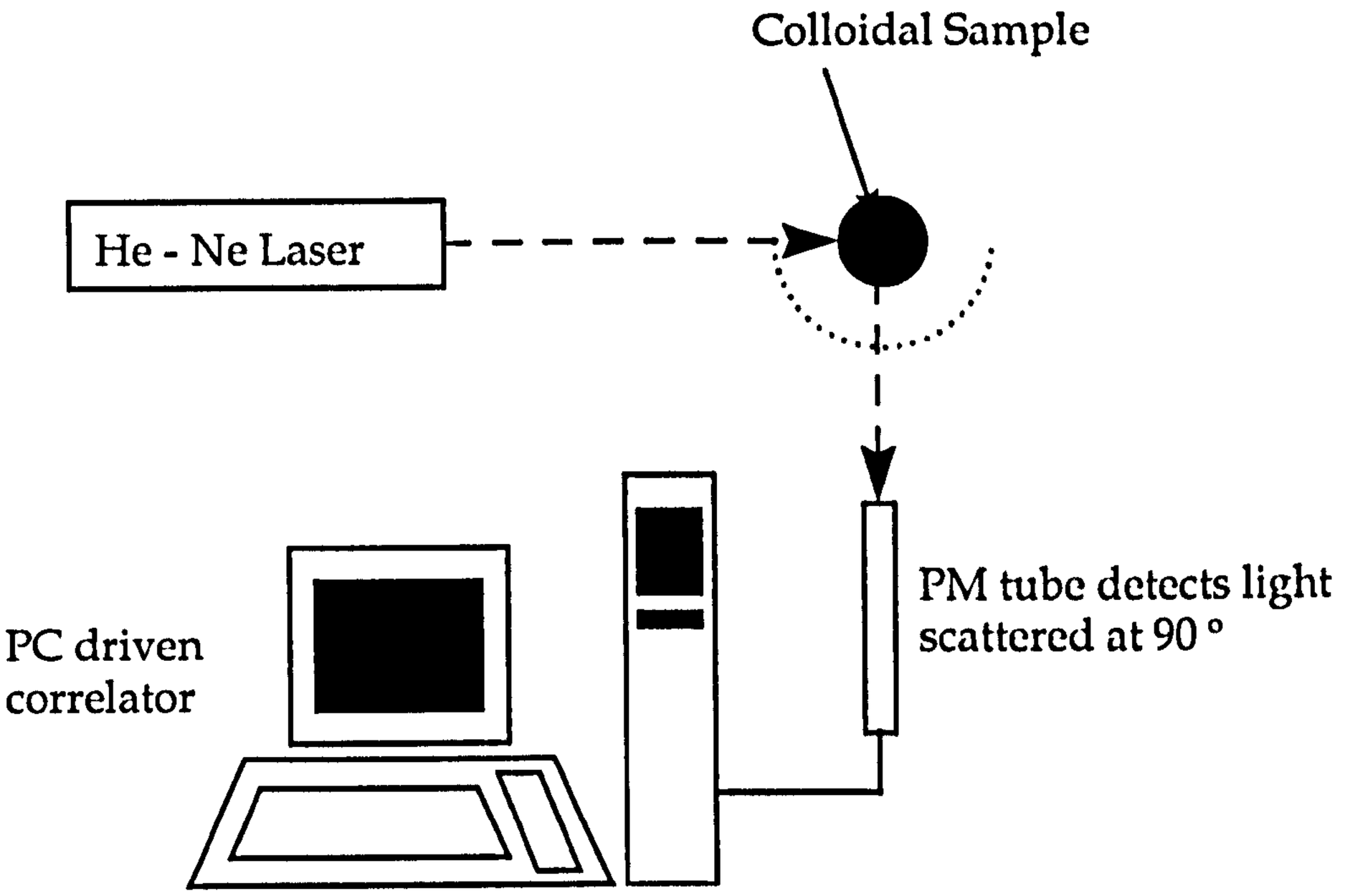

Figure 3.6: Typical PCS set-up

Most PCS samples needed to be diluted before measurement due to the problem of multiple scattering caused by a too concentrated dispersion. Multiple scattering is detectable by observing a broad, diffuse beam when the laser shines through the sample. In most cases, extensive dilution did not significantly effect the droplet diameter. However, difficulties did arise in certain cases, notably with very large swollen droplets (refer to section 5.1.1 on swelling with hydrocarbons). The optimum concentration was determined visually as being the point at which the dispersion was optically clear but with a definite bluish tinge. It should be noted that some of the sizes of the large swollen droplets will be at the upper range of most PCS instruments (typically 3μm in diameter) [22]. Measurements of droplets of sizes near to this limit should therefore be considered as somewhat approximate.

3.4. PDMS (Silicone Oil) in Water Emulsions: Results and Discussion

3.4.1. Emulsion preparation

Depending on the starting synthetic conditions, liquid PDMS emulsion droplets or 'gel'–like silica particles can be made with controllable properties. It is possible to synthesise large 'monodisperse' droplets from about 1 μm in diameter up to 2.5 μm in diameter. Droplets as small as 250 nm in diameter can also be formed. Properties such as density, surface charge and internal viscosity are all controllable simply by changing the monomer mixture at the start of the polymerisation.

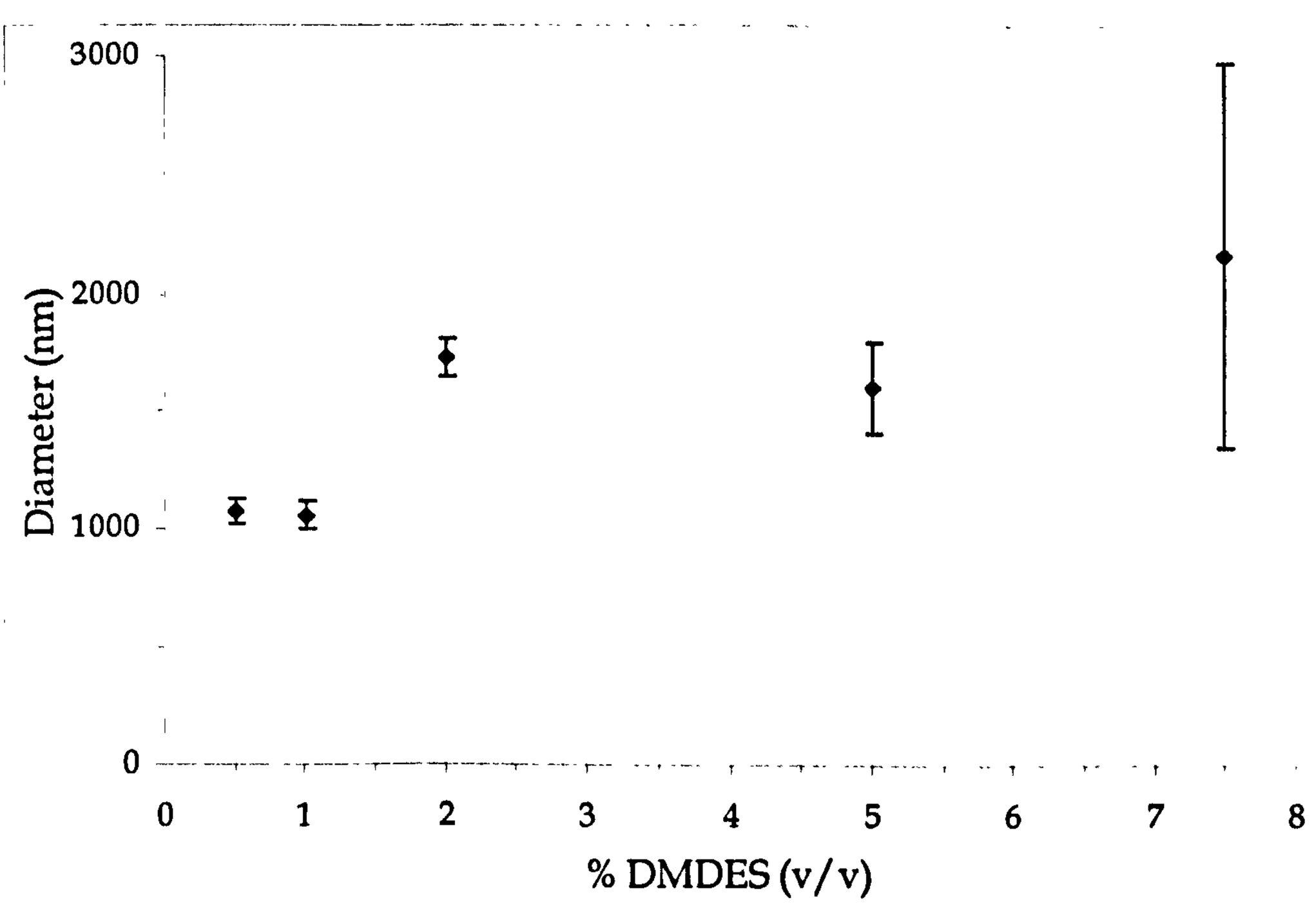

Figure 3.7: Variation of droplet size for PDMS emulsions with initial monomer concentration

Figure 3.7 illustrates how droplet size can be varied in a purely DMDES–derived emulsion by varying the initial monomer concentration. As can be seen, the average droplet size and the droplet polydispersity increase with increasing monomer concentration. Over a threshold limit of approximately 0.07 v/v an excess phase of monomer remains undissolved. As the PDMS emulsion begins to form and precipitates out of solution in the nucleation and growth mechanism, more DMDES dissolves to replace it. Thus droplets appear and swell with PDMS at the same time as an appreciable amount of monomer is starting to react. This is thought to be the origin of the increased polydispersity at high initial monomer concentrations.

Plate 3.1 displays images of PDMS emulsions at 1 % v/v and 4 % v/v DMDES. The droplets in plate 3.1 (a) are just distinguishable using a × 40 objective. They are clearly 'monodisperse'. The emulsion droplets in plate 3.1 (b) at least are more polydisperse. Large, medium and small PDMS droplets are clearly visible in this image, causing a high polydispersity index. It is apparent that there is a solubility limit for the DMDES monomer in water, which causes this polydispersity. It is also possible that the polydispersity results from unreacted monomer solubilising inside forming PDMS droplets. It is not possible to synthesise a monodisperse PDMS emulsion with monomer concentrations greater than 0.02 v/v under these particular conditions (as described in section 3.2.2).

(a)

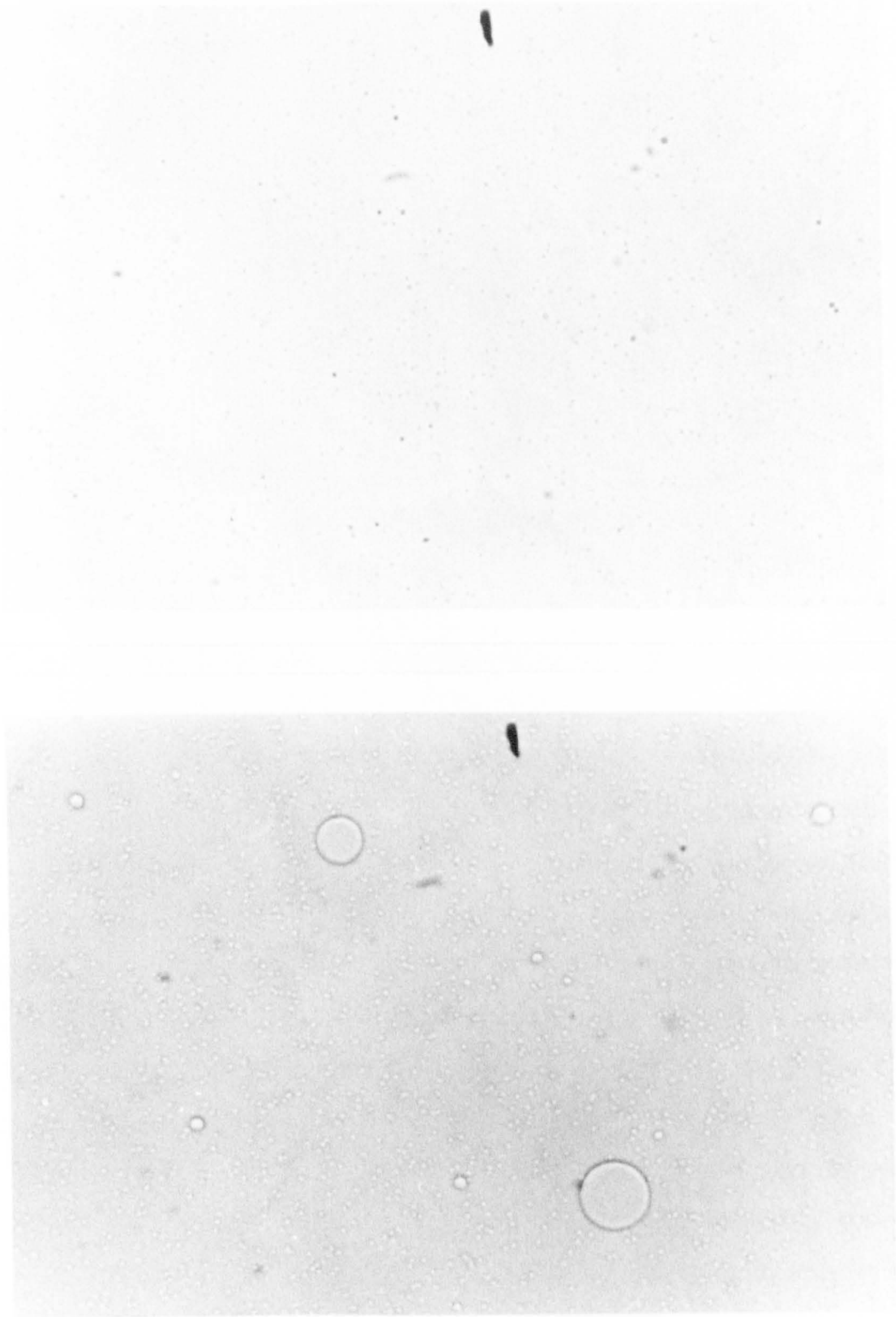

(b)

Plate 3.1 (a): 0.01 v/v PDMS emulsion (diameter = 1081 ± 134 nm)

(b): 0.04 v/v PDMS emulsion (diameter = 1556 ± 272 nm)

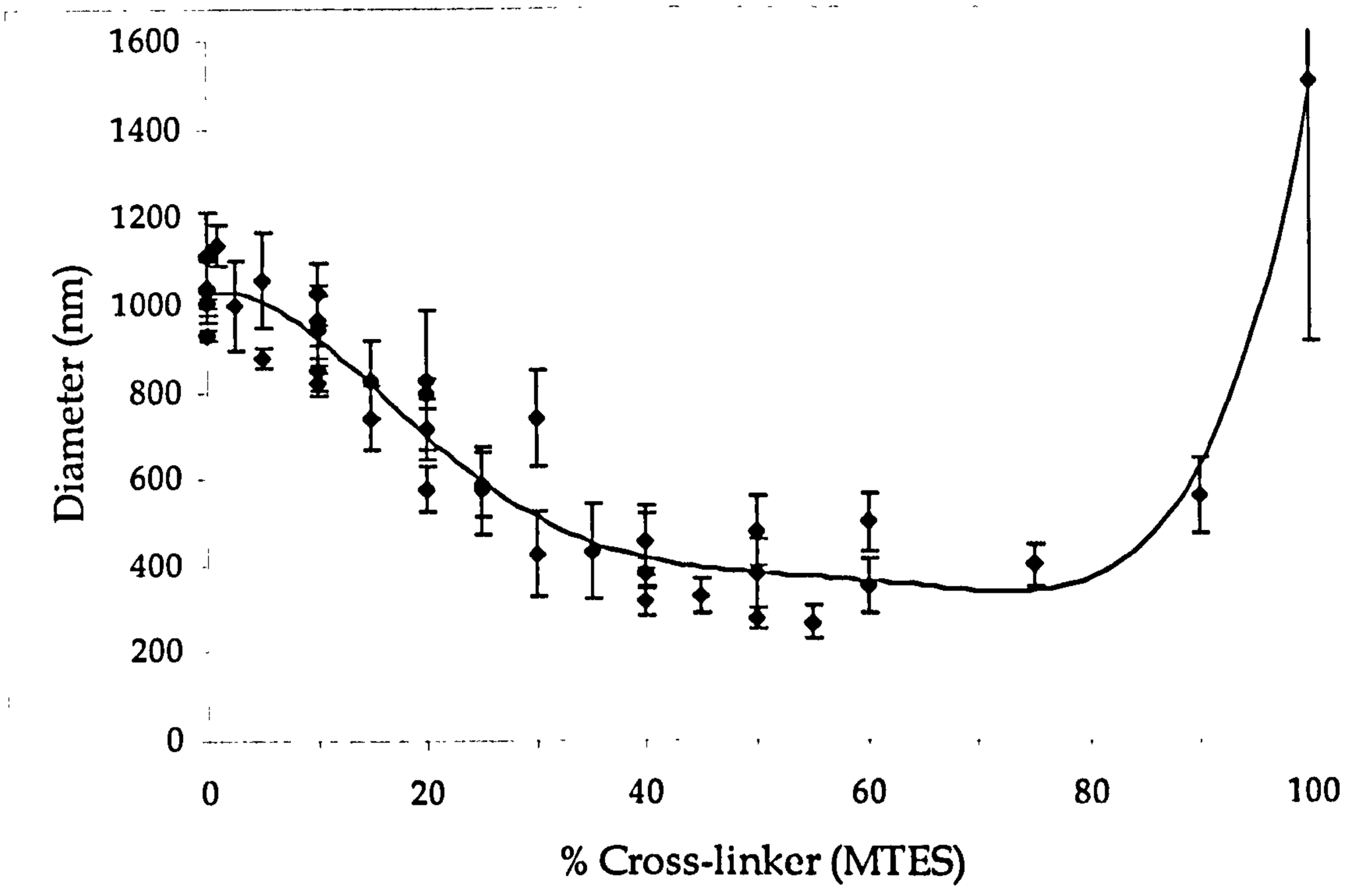

Figure 3.8: Effect of cross–linking monomer on droplet size

Figure 3.8 shows the effect of adding MTES (the trifunctionally active, cross-linking monomer), to form mixtures with DMDES, on droplet size. All the dispersions were formed from 0.01 v/v monomer. The droplet or particle size was determined using PCS, typically 18 hours later. Droplets with DMDES only, synthesised in 0.01 v/v ammonia, are typically of the order of 1 μm in diameter. Up to 5 % v/v MTES in DMDES there is no significant change in the size. The polydispersity in this region is typically below 10 % and hence the droplets can be considered to be reasonably 'monodisperse'. At higher cross-linker concentrations (> 5 %) the average droplet size decreases to around 400 nm in diameter at 50% MTES. Concurrently, the polydispersity increases to around 10 to 15 %. The reason for the decrease in droplet size may be attributed to an enhanced rate of production of nucleation sites for emulsion growth due to reduced solubility of the cross–linked PDMS oligomers. Beyond 70 % MTES the samples become more silica like in appearance. Wegener [23] showed that the particles in this region are no

longer spherical. Hence accurate measurement of the diameter using PCS is unreliable.

If the emulsions are dialysed, there is no alteration in the size or polydispersity over time. If they are left undialysed the droplets continue to grow. This is shown above in figure 3.9 for 0.01 v/v DMDES/MTES emulsions. This shows how the volume (V) changes for four sets of emulsions with different amounts of cross–linker, compared to their starting volume (V_o). Typically, the maximum volume is attained after approximately 11 to 14 days growth for the lower MTES concentration emulsions. The reason for the continued growth may be attributed to residual polymer left in the aqueous phase continuing to precipitate out of solution and being incorporated into the droplets. The rate of this growth is obviously dependent on there being PDMS still available; when this source runs out the droplets cease to expand.

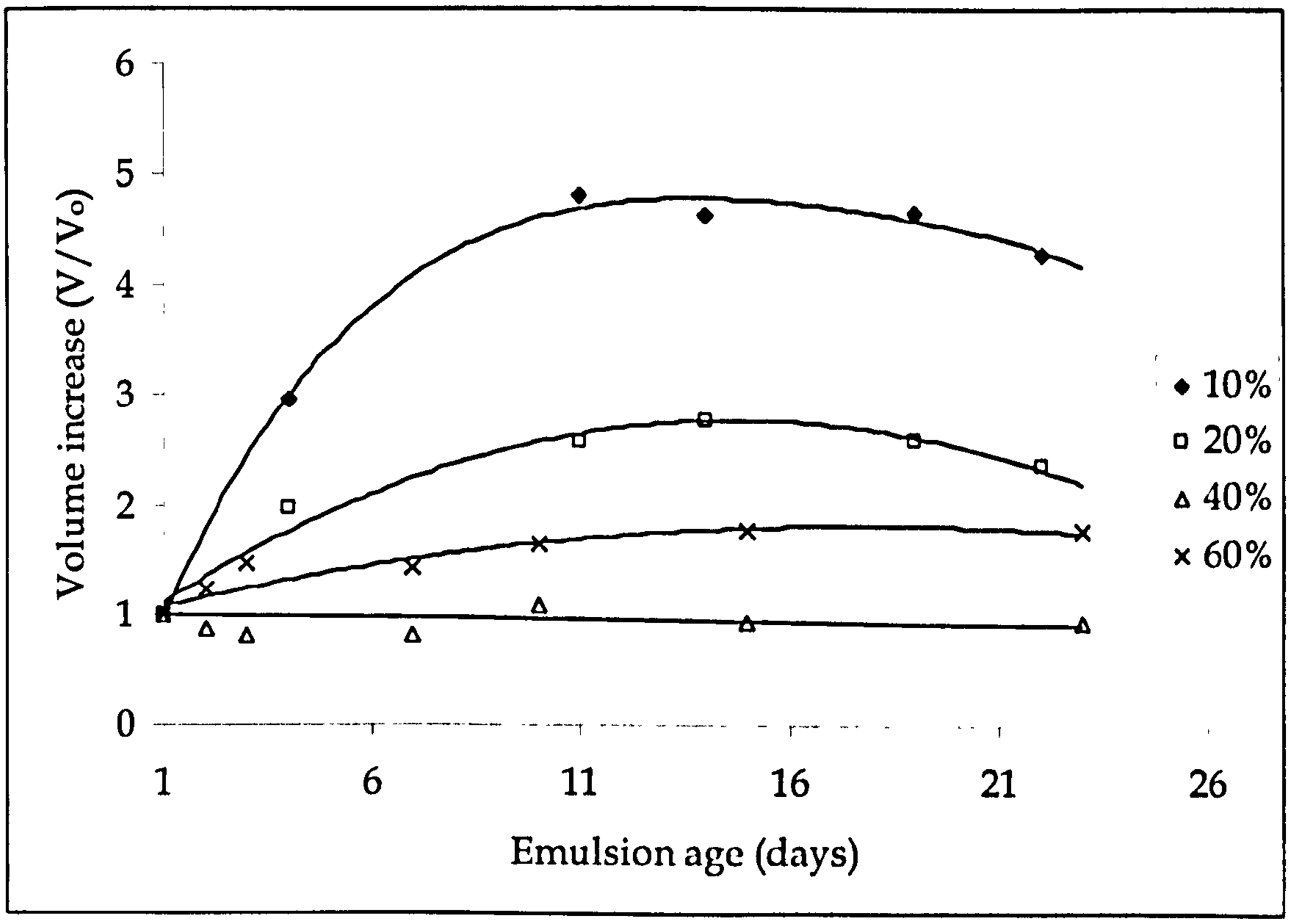

Figure 3.9: Growth in size of undialysed emulsions with effect of cross–linker

With reference to figure 3.7, the greater the starting concentration of monomer, the more rapidly and larger the droplets will grow. The results for higher concentrations of cross–linker also support the notion that the reaction in this region is more rapid, due to there being more nucleation sites. No appreciable droplet growth is seen in either the 40 % or the 60 % MTES emulsions.

Another possibility for the growth shown in figure 3.9 is Ostwald ripening. However, if this phenomenon were occurring there would be an expected breakdown in the emulsion structure. This is not the case. If Ostwald ripening did occur it would also be observed in the dialysed emulsions, which exhibited no such behaviour.

When the emulsion was synthesised with the dimethoxy monomer (DMDMS), there was no appreciable difference in the size of PDMS droplet produced compared to the diethoxy monomer. Nor was there any significant effect of the temperature at which the polymerisation was carried out. PDMS was synthesised at 5, 25 and 40 °C across the range of MTES concentrations, and similar sized droplets were produced at each temperature. Consequently all the PDMS emulsions were synthesised at room temperature with the diethoxy monomer.

3.4.2. PDMS characterisation

It is possible to control the properties of the PDMS in the emulsion produced by varying the amount of MTES, the cross-linking monomer, present in the starting mixture. As can be seen in figure 3.8, the presence of the MTES can have a profound effect on the droplet size. Several samples (typically between 12–15 mL) of PDMS at cross–linker concentrations between 0 and 20 % MTES were isolated. Properties of the isolated PDMS

determined included viscosity, density, surface tension, interfacial tension and freezing/melting point measurements.

Obey [12] and Wegener [23] have extensively studied isolated PDMS by ^{1}H and ^{29}Si NMR. Obey showed that the PDMS obtained from a 0.05 v/v DMDES emulsion consisted of 88.6 % cyclic D_4, with 11 % being linear PDMS and D_3 representing only 0.4 % of the total oil phase. The high dilution of the monomer during polymerisation minimises the chance of oligomers reacting with each other. Cyclisation is, therefore, favoured over the inter–oligomeric reaction. Gel–permeation chromatography gave a number–average and a weight–average molecular weight of 420 g mol^{-1} and mass spectrometry a number–average molecular weight of 320 g mol^{-1}.

As can be seen in figure 3.10 there is a near–linear increase in the density of PDMS from a value very close to that of pure D_4 (octamethyltetrasiloxane). The density coincides with that of water at a MTES concentration of about 12–13%. The value at 100% DMDES confirms that D_4 is the dominant molecular species present; the small difference in density is probably due to the linear fraction.

Figure 3.11 shows the viscosity of the isolated PDMS as a function of increasing cross–linker concentration. As expected, the silicone oil becomes more viscous with increased amounts of MTES.

As cross–linker is added, so more complex and larger oligomeric silicone molecules are formed, with a corresponding increase in the density and the viscosity of the oil. Janke [24] has proposed several types of cyclic cross–linked silicone oligomers, which may be formed at low MTES concentrations. As the droplets become increasingly gel–like electron micrographs of the particles become possible. This reflects the corresponding increase in molecular weight of the silicone oil.

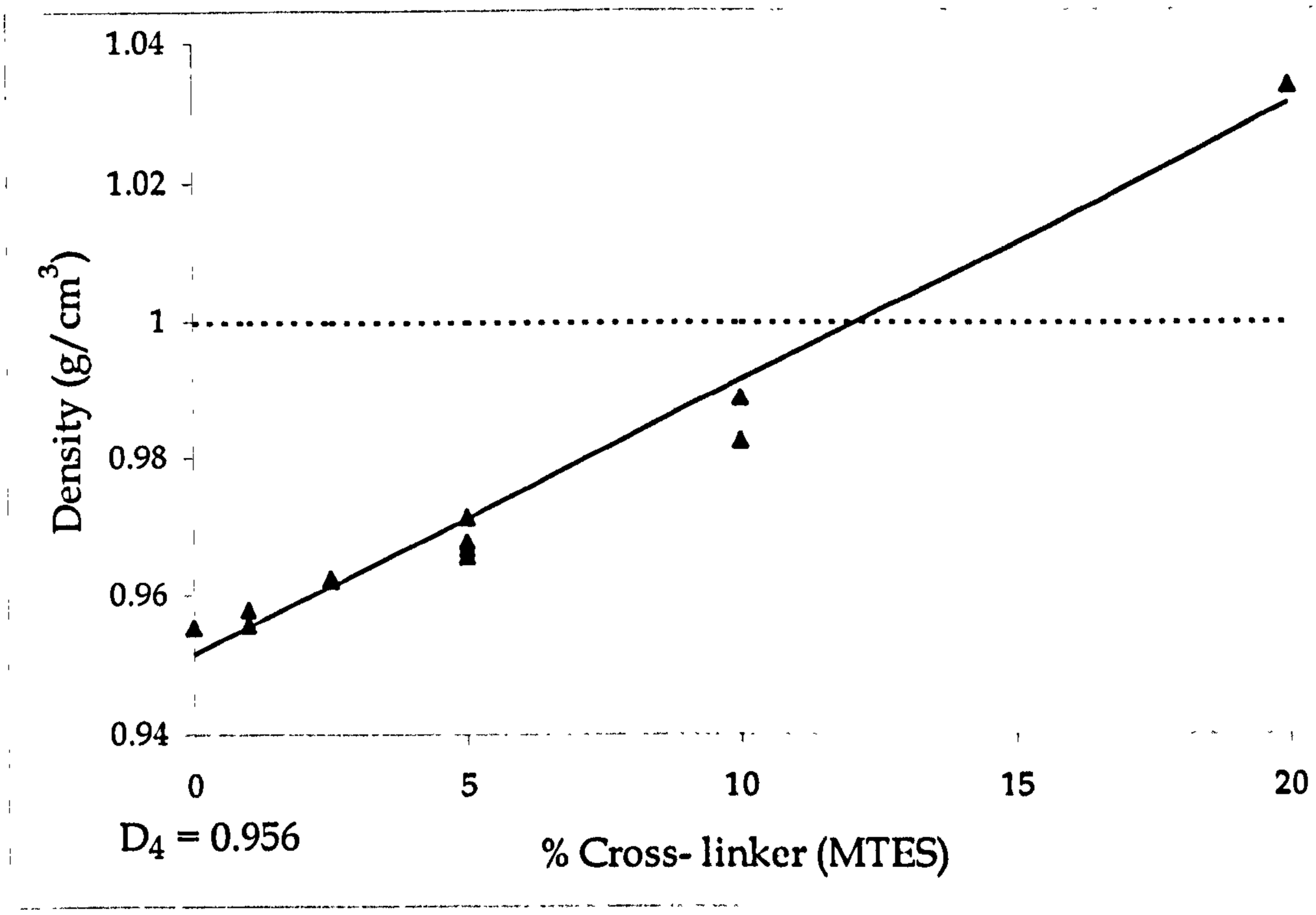

Figure 3.10: The effect of cross–linker on the density of the PDMS phase

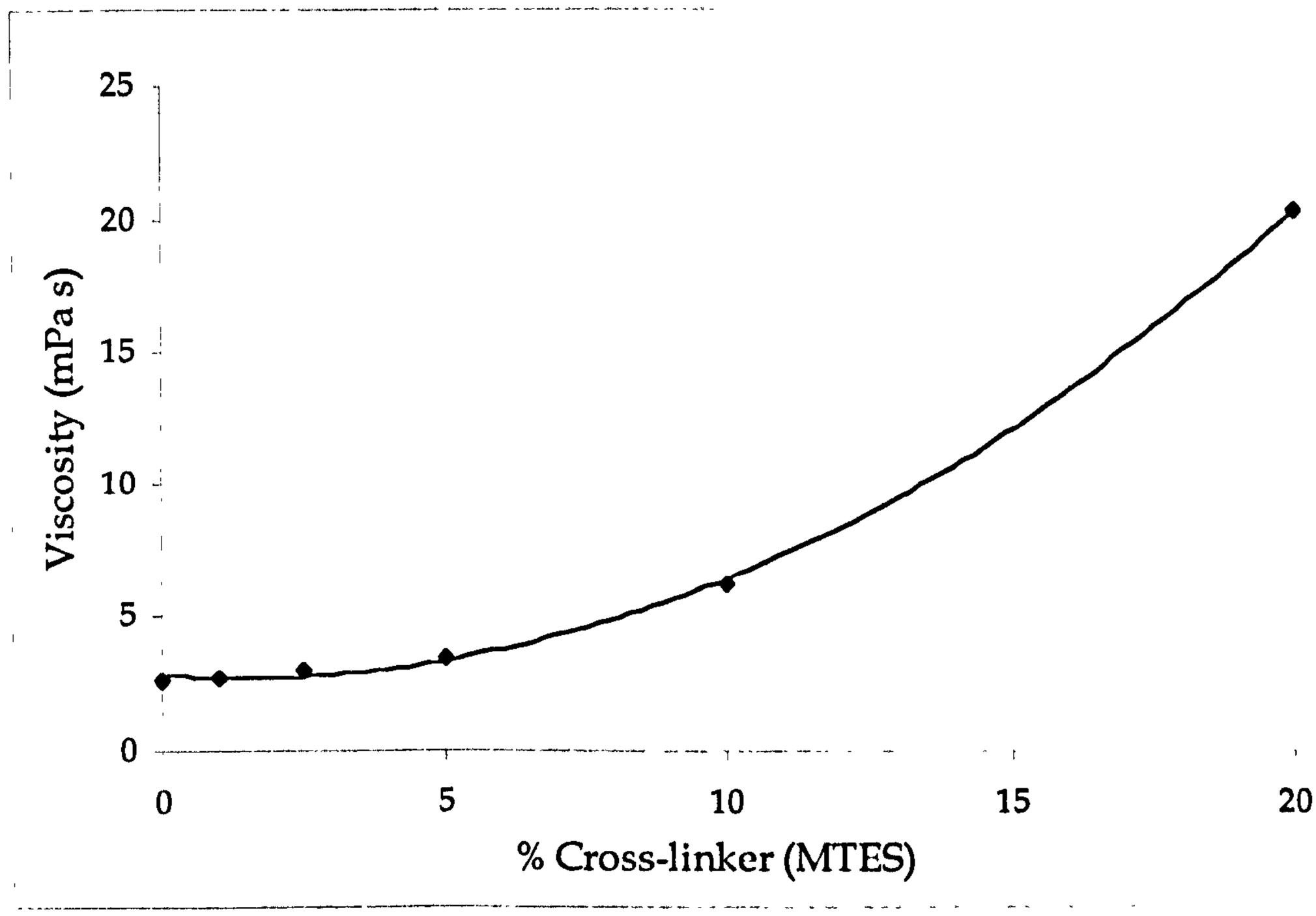

Figure 3.11: The effect of cross–linker on the viscosity of the PDMS phase

Adding cross–linker to mixtures of monomer has no significant effect on either the surface or the silicone oil/water interfacial tensions. The results are presented in figure 3.12. This is unsurprising given the efficiency of PDMS at presenting low energy methyl groups at the air or water interface.

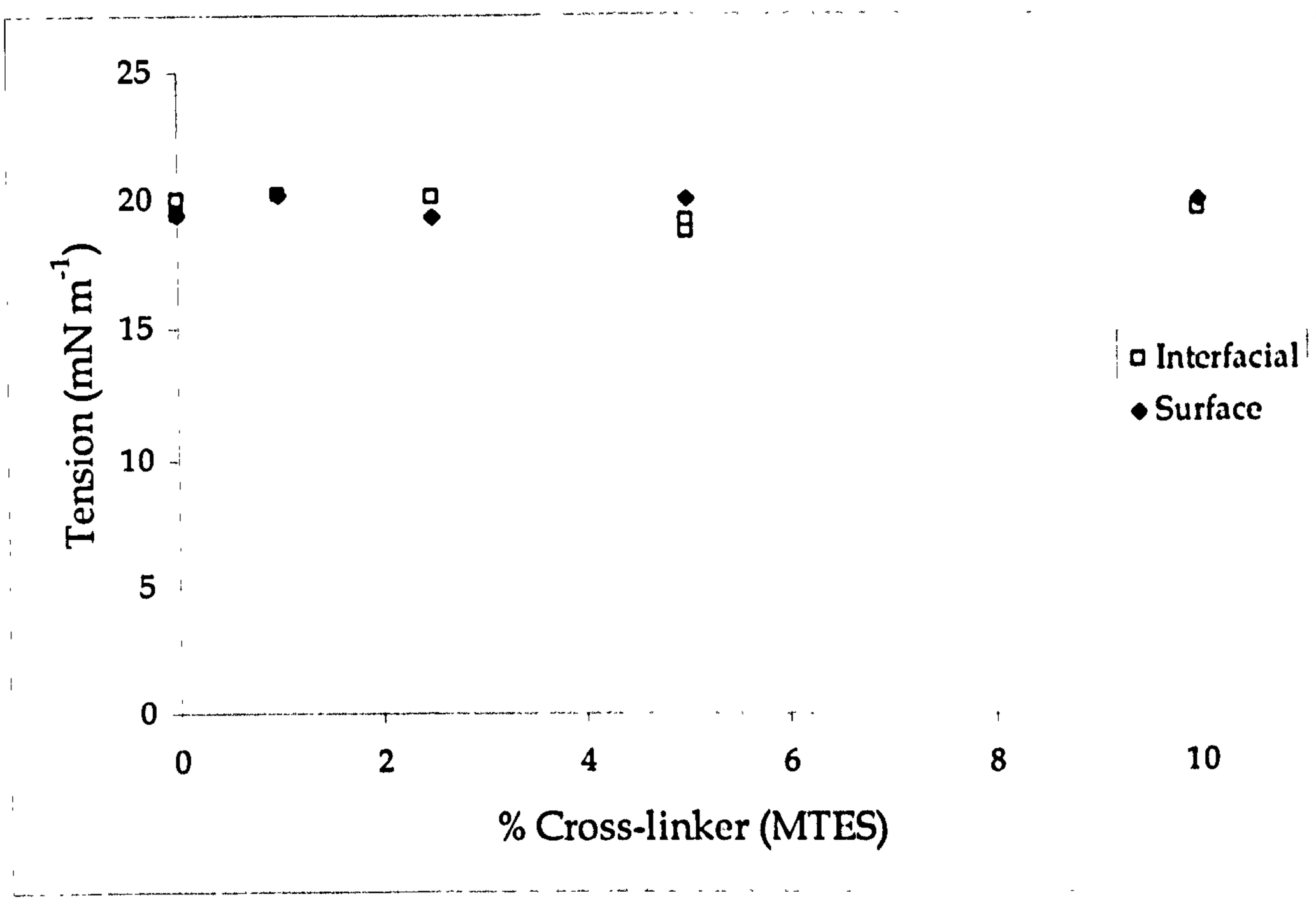

Figure 3.12: Effect of cross–linker on the surface and interfacial tension of the PDMS phase

One implication of the data shown in figure 3.12 is that the small fraction of ionically terminated PDMS oligomers present do not lower the interfacial tension as other, more conventional ionic surfactants would. This has important implications especially with hydrodynamic phenomena such as viscosity and electrophoresis [15,17,25], where the nature of either a hard sphere equivalent droplet or a soft, deformable droplet has a direct consequence on the interpretation of the results obtained. Anderson [26] reported that addition of a surfactant resulted in smaller droplet sizes. This is due to a lowering of the interfacial tension (hence less energy is required to

increase the interfacial area) thus favouring the production of smaller droplets.

Figure 3.13 shows that the measurement of the freezing and melting point of the isolated PDMS was difficult to visually determine as the temperature range over which the solid–liquid transition took place was broad.

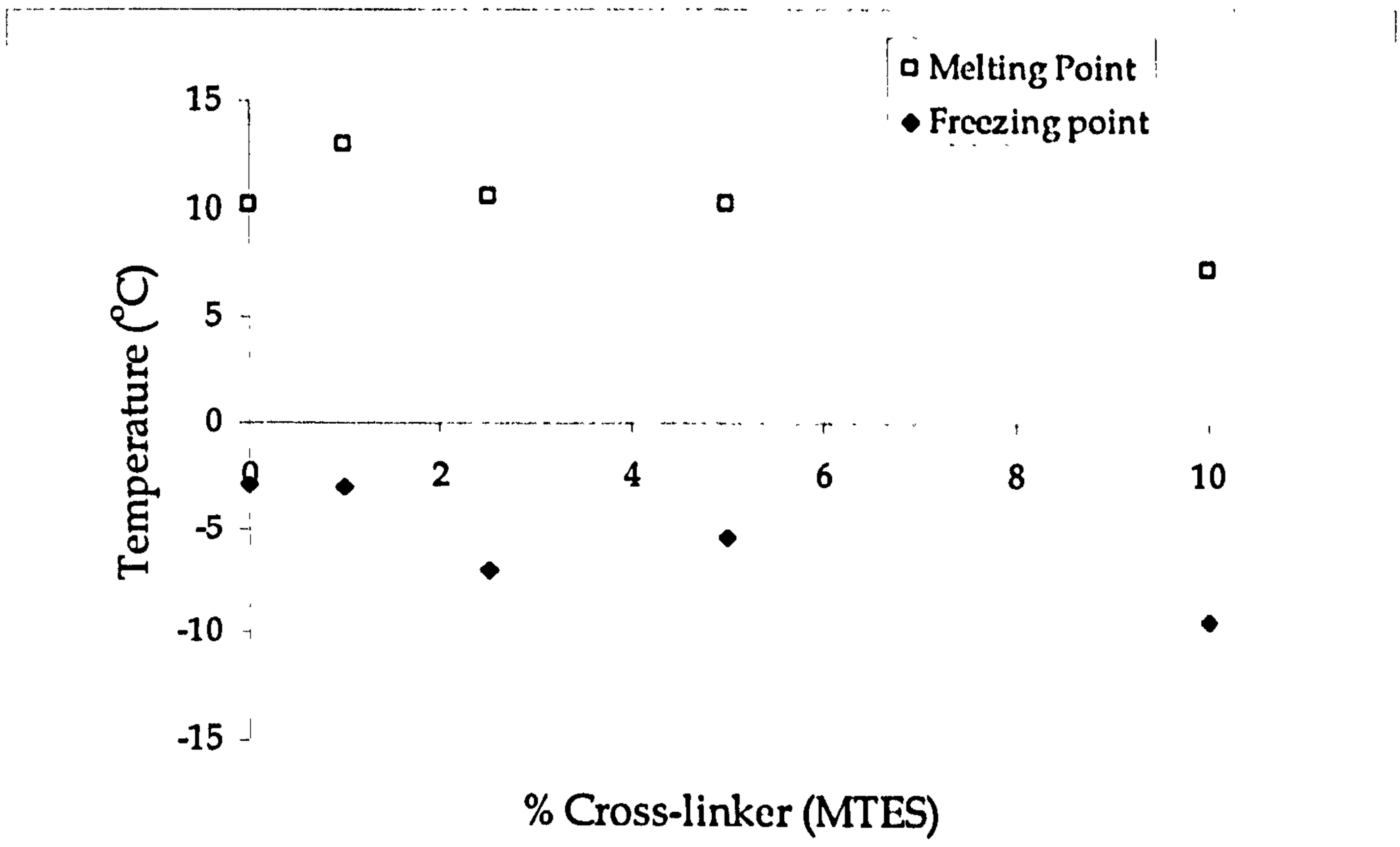

Figure 3.13: Effect of cross–linker on the freezing and melting points of the PDMS phase

An observable trend is the rise to a maximum, followed by a decrease, as cross–linker concentration is increased. This follows for increasing molecular weight of cyclic siloxanes [27]. There is a consistent discrepancy between the melting and freezing point for each concentration of MTES. Further work is required, especially by differential spinning calorimetry (DSC) to investigate the thermodynamics of this phase change.

Table 3.2 summarises the data acquired for PDMS characterisation.

Characteristic	% Cross-linker in monomer mixture					
	0	1	2.5	5	10	20
Density ($g\ cm^{-3}$)	0.955 $\pm 3\times10^{-4}$	0.957 $\pm 3\times10^{-4}$	0.962 $\pm 3\times10^{-4}$	0.968 $\pm 3\times10^{-4}$	0.986 $\pm 3\times10^{-4}$	1.034 $\pm 3\times10^{-4}$
Viscosity (mPa s)	2.578 $\pm 3\times10^{-3}$	2.724 $\pm 5\times10^{-3}$	2.961 $\pm 5\times10^{-3}$	3.462 $\pm 6\times10^{-3}$	6.224 $\pm 6\times10^{-3}$	20.35 $\pm 7\times10^{-2}$
Freezing Point (°C)	-3 ±0.2	-3 ±0.2	-8.5 ±1.4	-8.5 ±1.4	-9 ±1.2	–
Melting Point (°C)	10 ±4	13 ±4	11 ±5	10 ±3	7 ±3	–
Surface Tension ($mN\ m^{-1}$)	19.5	20.2	19.3	20.0	19.9	–
Interfacial Tension ($mN\ m^{-1}$)	19.7	20.2	20.1	18.9	19.6	–

Table 3.2: Experimental data of PDMS phases

The surface and interfacial tensions of 20% MTES in DMDES monomer mixture were not measured due to insufficient quantities of isolated oil.

3.5. References

1. Kipping, F.S. *Journal of the Chemistry Society* , 2125 (1912).

2. Rochow, E.G., "Chemistry of the Silicones.", John Wiley, New York, 1946.

3. Patnode, W. and Wilcock, D.F. *Journal of the American Chemical Society* **68**, 358 (1946).

4. McGregor, R.R. and Warrick, E.L. *United States Patent* **No. 2384384** (1945).

5. Scott, D.W. *Journal of the American Chemical Society* **68**, 2294 (1946).

6. Kantor, S.W., Grubb, W.T. and Osthoff, R.C. *Journal of the American Chemical Society* **76**, 5190 (1954).

7. De Gunzbourg, A., Favier, J.C. and Hémery, P. *Polymer International* **35**, 179 (1994).

8. Hyde, J.F and Wehrly, R. *United States Patent* **No. 2891920** (1959).

9. Brady, R.F. *Journal of Chemistry and Industry* , 219 (1997).

10. Brown, S.S., Kendrick, T.C., McVie, J. and Thomas, D.R., "Silicones.";Vol. 2, Pergammon, 1995.

11. Arkles, B. *Chemtech* **13**, 542 (1983).

12. Obey, T.M. and Vincent, B. *Journal of Colloid and Interface Science* **163**, 454 (1994).

13. Matthews, G.P., "Experimental Physical Chemistry.", Clarendon Press, Oxford, 1985.

14. Pal, R. *Colloids and Surfaces a-Physicochemical and Engineering Aspects* **84**, 141 (1994).

15. Tadros, Th.F. *Colloids and Surfaces a-Physicochemical and Engineering Aspects* **91**, 39 (1994).

16. Einstein, A., "Investigations on the Theory of Brownian Movement.", Dover, New York, 1956.

17. Taylor, G.I. *Proceedings of the Royal Society of London, Series A* **138**, 41 (1932).

18. Stepanek, P. and Konak, C. *Advances in Colloid and Interface Science* **21**, 195 (1984).

19. Randle, K.J. *Chemistry in Industry* **2**, 74 (1980).

20. Finsy, R. *Advances in Colloid and Interface Science* **52**, 79 (1994).

21. Brown, J.C., Pusey, P.N. and Dietz, R. *Journal of Chemical Physics* **62**, 1136 (1975).

22. Orr, C., *in* "Encyclopaedia of Emulsion Technology" (P. Becher, Ed.), Vol. 3, p 137. Marcel Decker, New York, 1988.

23. Wegener, M., M.Sc. thesis, University of Bristol (1993).

24. Janke, H., Engelhardt, M., Magi, M. and Lippmaa, E. *Zeitschrift für Chemie* **13**, 392 (1973).

25. Barchini, R. and Saville, D.A. *Langmuir* **12**, 1442 (1996).

26. Anderson, K.R., Obey, T.M. and Vincent, B. *Langmuir* **10**, 2493 (1994).

27. Petrarch Systems Silanes & Silicones Catalogue, "Silicon Compounds: Register and Review", ABCR GmbH & Co, Karlsruhe, 1987.

Chapter 4: Physical Properties of PDMS Emulsions

4.1 Experimental Methods

For a complete list of all the materials used in the experiments reported here refer to section 3.2.1.

4.1.1 PDMS droplet stability to coagulation

Experiments were performed on a series of cross–linked PDMS emulsions to determine the threshold coagulation concentration of electrolyte and the effect of pH on the stability at fixed background electrolyte concentration. In all experiments potassium chloride (KCl) was used as background electrolyte and hydrochloric acid (HCl) as acid. Coagulation can be defined as the process in which two droplets come into close enough proximity to each other to form a thin liquid film. Coalescence results in the formation of a single, large droplet due to thinning and break–up of the thin liquid film separating the two initial droplets [1]. Droplet size and size distribution was measured and followed, with time, using PCS and UV–Vis turbidity (refer to section 3.3.3 for a description of the PCS technique).

Turbidity–wavelength measurements [2] have been used to follow the onset of coagulation as a function of particle concentration in the dispersion. A plot of $\log_{10}$ (turbidity, τ or optical density) against $\log_{10}$ (wavelength, λ) should be linear for the appropriate wavelength range providing the Beer–Lambert law is obeyed. For the PDMS droplets of diameter *ca* 1 micron this range of wavelengths was found to be between 570 and 800 nm. By

following changes in the gradient and linearity of the $\log_{10}(\tau)$–$\log_{10}(\lambda)$ plot the onset of coagulation in the emulsion could be monitored. Hence, the critical electrolyte coagulation (CCC) concentration could be determined.

All emulsions were prepared as 0.01 v/v monomer in 0.01 v/v ammonia '880' as stated in section 3.2.2. After 18 hours the emulsions were then dialysed against pure water for 48 hours. Following dialysis 9 mL of the sample emulsion was pipetted into a 10 mL vial. The sample was then made up to 10 mL by addition of 1 mL KCl solution of the required concentration to produce the final desired electrolyte concentration. The turbidity of the samples was measured between 570 and 800 nm using a Perkin Elmer "Lambda 5" UV-vis spectrophotometer. Initial turbidity readings together with some PCS measurements, were taken within an hour of sample preparation and subsequently every other day. Samples were diluted, where necessary, with water containing KCl at an equivalent concentration to the sample in order to achieve the desired photon count rate for the correlator.

The emulsion stability at low pH was also monitored using the turbidimetric technique. All emulsions were prepared with a background electrolyte concentration of 1×10^{-3} mol dm^{-3} KCl, which was found to be below the CCC. HCl was then added at a concentration of 1×10^{-3} mol dm^{-3} or 1×10^{-2} mol dm^{-3} depending on the desired final pH. The pH value was measured using an Orion 420A pH meter. This was calibrated for each measurement between pH 4 to 7 using pH buffer solutions.

4.1.2 PDMS droplet stability to freeze–thawing

Many emulsions and colloidal dispersions can be induced to coagulate by repeated freeze–thawing of the suspension [3]. When the water phase of an O/W emulsion freezes, ice crystals appear and grow, thus forcing the oil droplets into narrow spaces between crystals. This has the double effect of concentrating the emulsion and any electrolyte present in the as yet unfrozen water. Eventually oil droplets are forced into contact with each other and coalescence may occur.

A 0.01 v/v PDMS emulsion was slowly frozen in an ethanol bath cooled by addition of solid carbon dioxide. After the sample had solidified the emulsion was subsequently thawed to room temperature. The size and polydispersity of the emulsion was followed using PCS after each freeze–thaw cycle. This cycle was repeated three times. Neither the average droplet size nor the polydispersity of the emulsions were significantly changed by freeze–thawing.

4.1.3 PDMS emulsion stability to increases in osmotic pressure

Further experiments were performed on the stability of PDMS emulsions with respect to change in osmotic pressure. Osmotic stress is an experimental technique, which may be used for the direct measurement of interparticle forces [4]. The experiments described below were performed using this osmotic stressing technique [5].

Dextran is a commonly used polymer in this type of experiment. The osmotic pressure (Π) of solutions of dextran is not significantly dependent on the molecular weight within the range 250000–2000000 g mol^{-1}, except at concentrations below a few wt. %. Π values measured directly using a

membrane osmometer at room temperature and at 7, 30 and 37 °C show little significant change [6,7].

Using a variation of the 'secondary osmometer' [8], (refer to figure 4.1), 4 mL of dialysed PDMS emulsion was placed in sealed dialysis tubing which was immersed in approximately 80 mL of a dextran solution (MW 505,000 g mol^{-1}).

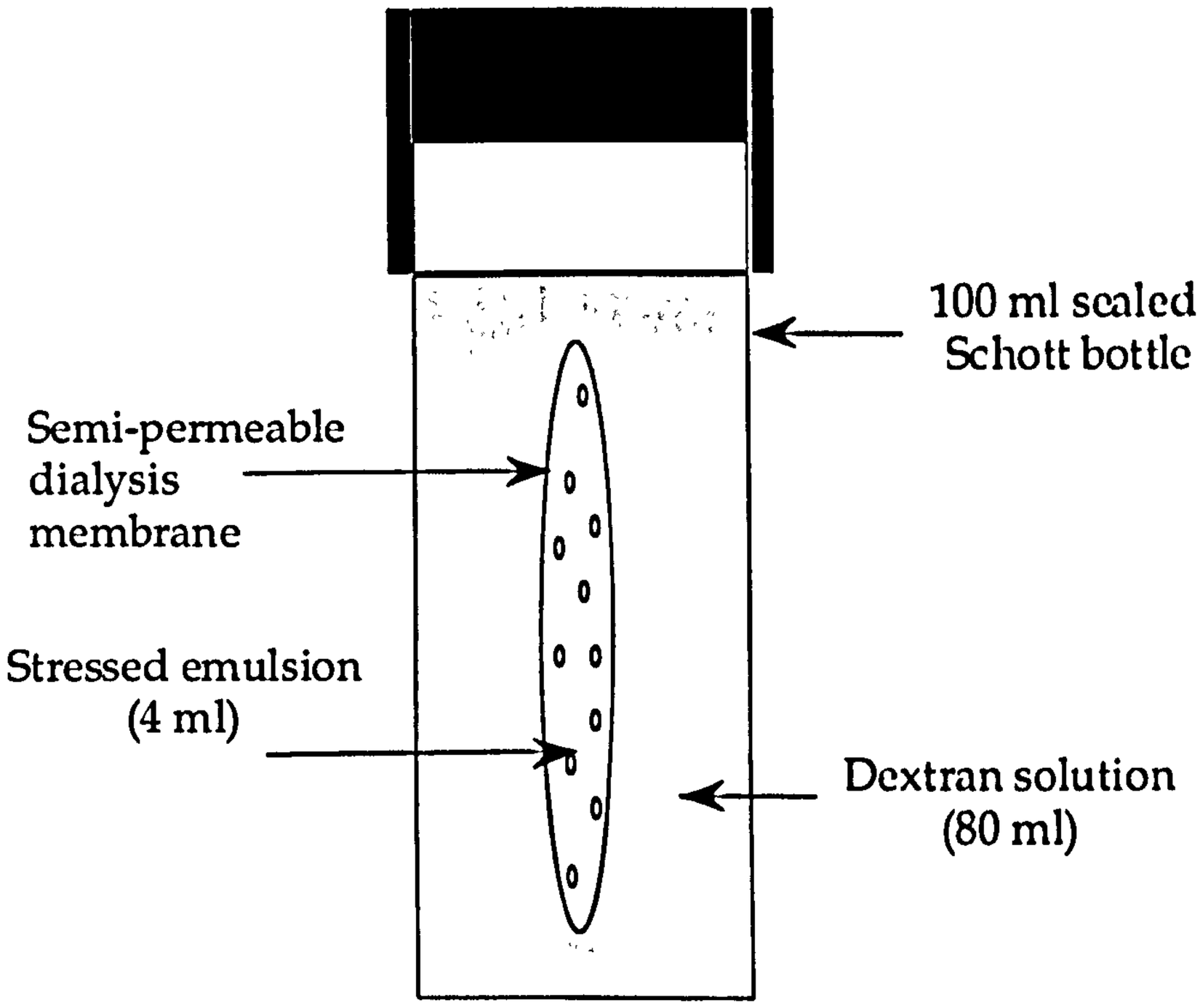

Figure 4.1: The 'Secondary Osmometer'

The samples were placed in a shaker water bath equilibrated at 25 °C for a week. The samples had to be shaken to ensure that equilibrium could be established as concentrated aqueous polymer solutions are often viscous. This may result in solvent that has been osmotically pulled through the membrane absorbing as a layer around the membrane surface. This can slow or even halt the attainment of equilibrium via osmosis. Thus, by agitating the samples in the water bath and removing any forming solvent layer next to the membrane, this problem is avoided.

The samples were analysed visually and by optical microscopy to determine whether the emulsion had broken or not. The final equilibrium dextran concentration was determined using a Hilger–Watts differential interferometer, thermostatted at 25°C ± 0.05°C. The method and necessary precautions have been discussed previously by Adams [9]. The instrument was calibrated with dextran samples of known concentration, the reference solution was pure water in all cases and a white tungsten light source was used.

Plots of log Π versus weight % [4] (ω, in equation 4.1) show little scatter and are represented by equation 4.1. This is shown in graph form in figure 4.2.

$$\log_{10}\left[\Pi_{dex}(\omega)\right] = 2.75 + 1.03\omega^{0.383} \qquad 4.1$$

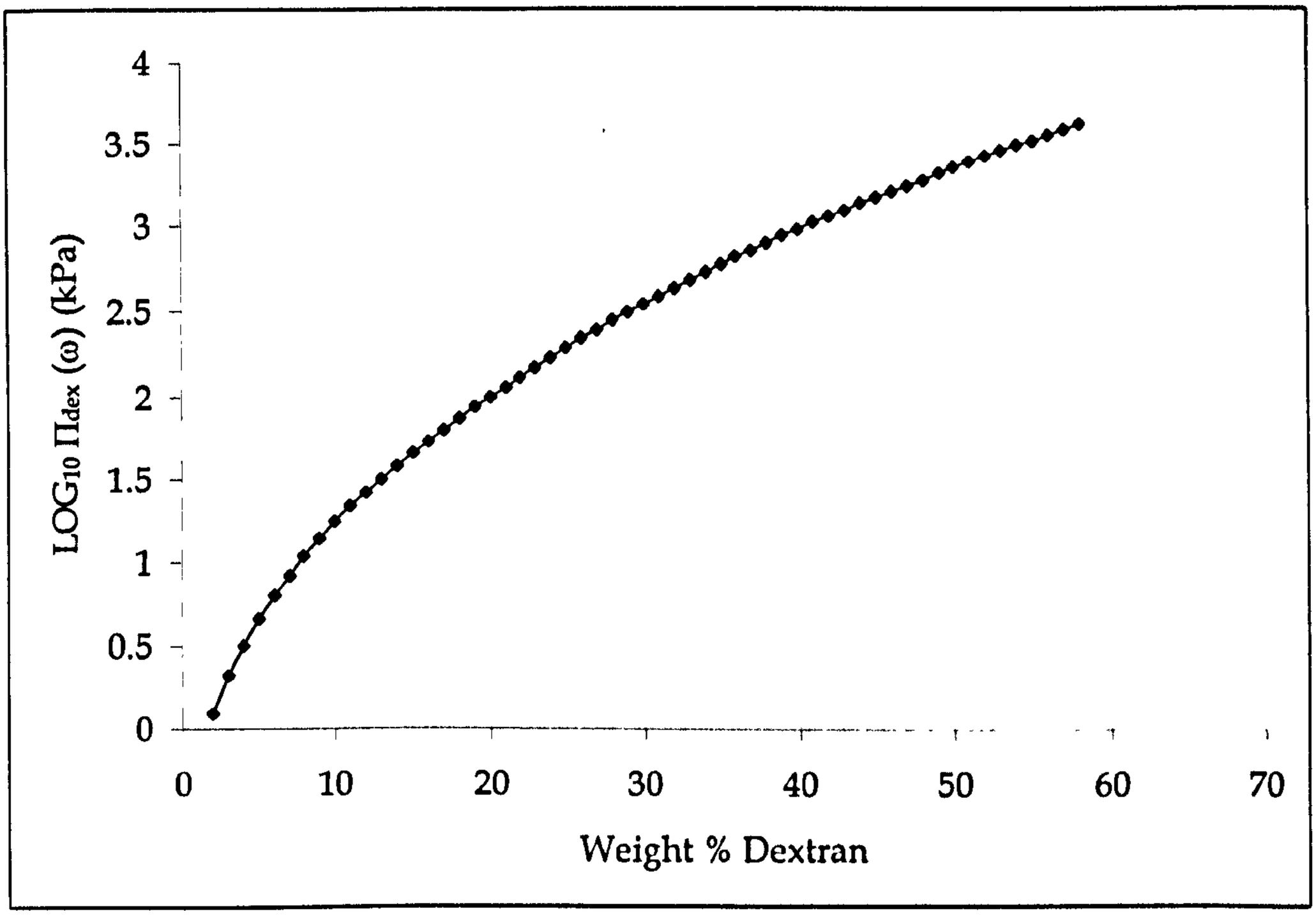

Figure 4.2: The osmotic pressure of dextran polymer solutions

Thus, the osmotic pressure exerted on the emulsion can be easily calculated from measuring the equilibrium concentration of aqueous dextran.

4.1.4 Surface charge measurements

It was thought that it would be possible to measure the surface charge of the droplets using a conductimetric charge titration technique. In order to ensure that all the bound counter ions are H^+, the sample to be measured was first dialysed against $1x10^{-3}$ mol dm^{-3} HCl. The sample was then re-dialysed against pure water until the conductivity was equivalent to that of pure water. A sample of emulsion was then titrated against $1x10^{-2}$ mol dm^{-3} NaOH in a stirred degassed vessel and the conductivity was determined using a Wayne-Kerr "B224" conductivity bridge. This enables the determination of the end point of the titration, which occurs when sufficient NaOH has been added to neutralise all the surface charge groups. The concentration of the NaOH was calibrated by performing an equivalent experiment with 5 mL of $5x10^{-4}$ mol dm^{-3} sulphamic acid instead of the emulsion sample.

The experiments were not successful since the results were inconsistent, some emulsion samples appearing to have no charge at all. This can be attributed to the fact that exchanging the surface group ions to H^+ caused the emulsion to coalesce, reducing the total interfacial area, leading to a large variation in the apparent surface charge density.

4.2 Results

4.2.1 PDMS droplet stability to coalescence by electrolyte

Stability to coagulation and consequent coalescence was observed as a function of potassium chloride (KCl) concentration. This was determined by measuring the turbidity of the samples over a range of light wavelengths between 570 and 800 nm (refer to section 4.1.1). Figure 4.3 shows an example of the linear plot obtained for a typical 'monodisperse' PDMS emulsion.

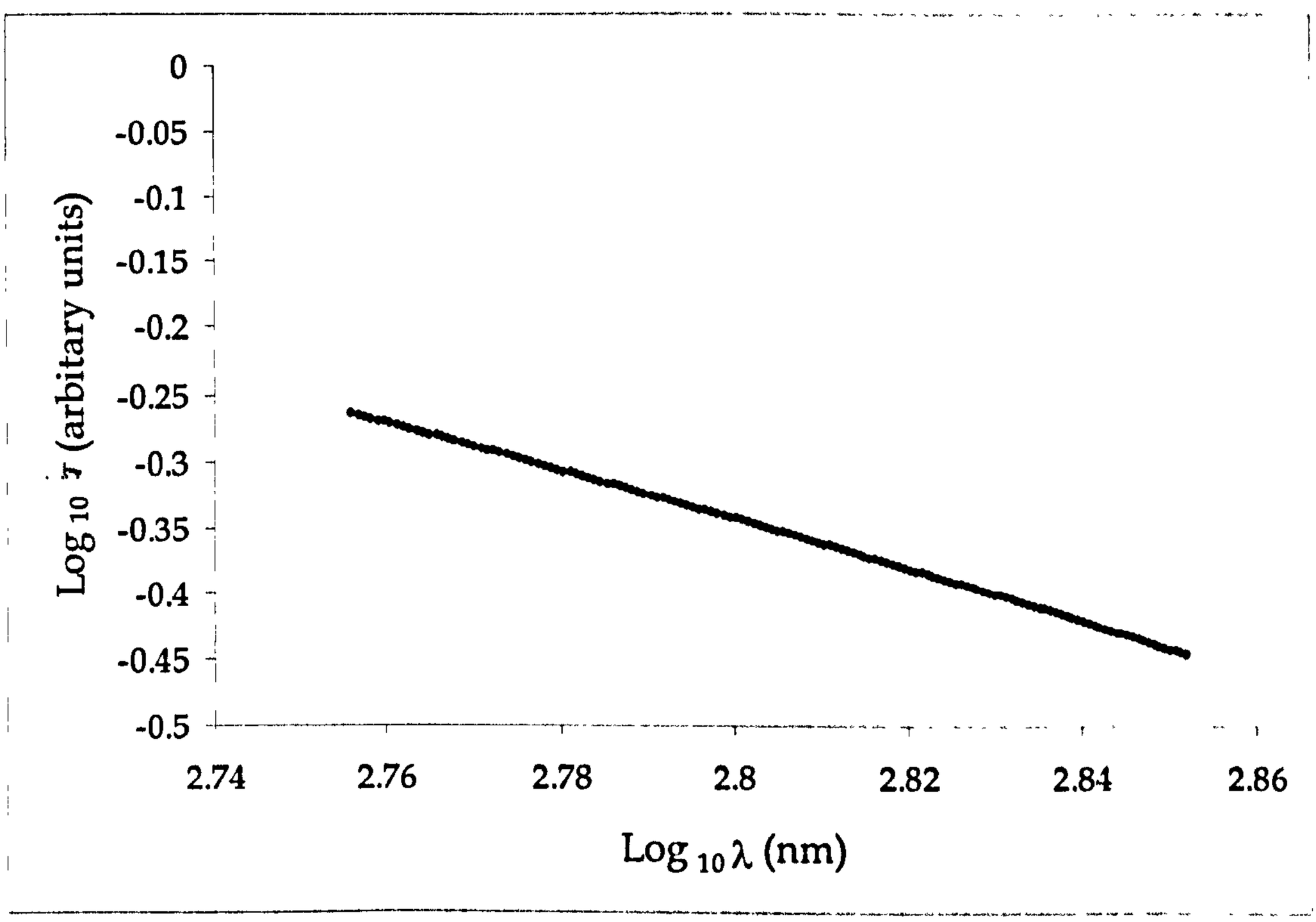

Figure 4.3. Example of the linear log τ / log λ for a PDMS emulsion

Over the wavelengths studied the log τ / log λ graph is linear. The gradient is -1.88 and the linearity fit is 0.999. The gradient and linearity are calculated from a least squares fit of the form y = mx + c.

Figures 4.4 and 4.5 show the effect of KCl concentration for a 0.01 v/v DMDES monomer emulsion. Both figures show graphs of the same experimental data. Figure 4.4 shows the change in the gradient of the $\log_{10}$ (turbidity)–$\log_{10}$ (wavelength) plot whereas figure 4.5 shows the change in the linearity of the gradient of the $\log_{10}$ (turbidity)–$\log_{10}$ (wavelength) plot.

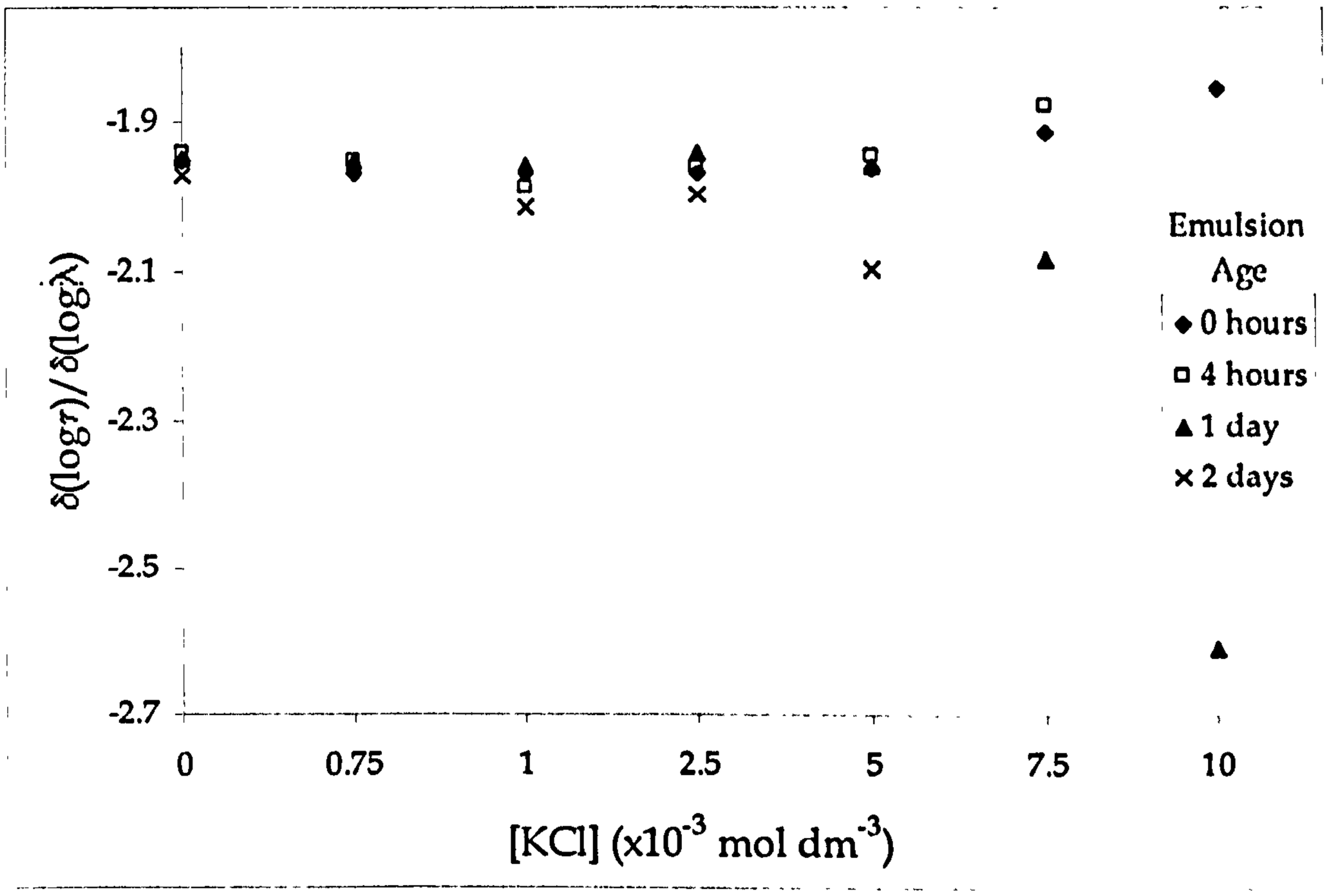

Figure 4.4: The effect of KCl on PDMS emulsion stability; $\delta(\log\tau)/\delta(\log\lambda)$ plot

The linearity factor (also known as the R^2 value) shown in figure 4.5 is defined in equation 4.2. A value of 1 indicates a straight line with no deviations. The lower the value, the less linear the fit. In equation 4.2 y_i is the experimental point, $\bar{y}_i$ is the fitted value and n the number of values.

$$R^2 = 1 - \frac{SSE}{SST} = 1 - \frac{\Sigma(y_i - \bar{y}_i)^2}{\left(\Sigma y_i^2\right) - \frac{\left[\Sigma y_i\right]^2}{n}} \qquad 4.2$$

SSE stands for sum of squares for error and SST sum of squares total.

As described in section 4.1.1, for a monodisperse emulsion the slope of turbidity against wavelength should be linear and constant. If the size

distribution of the emulsion changes then the gradient changes and the linearity fit ratio falls.

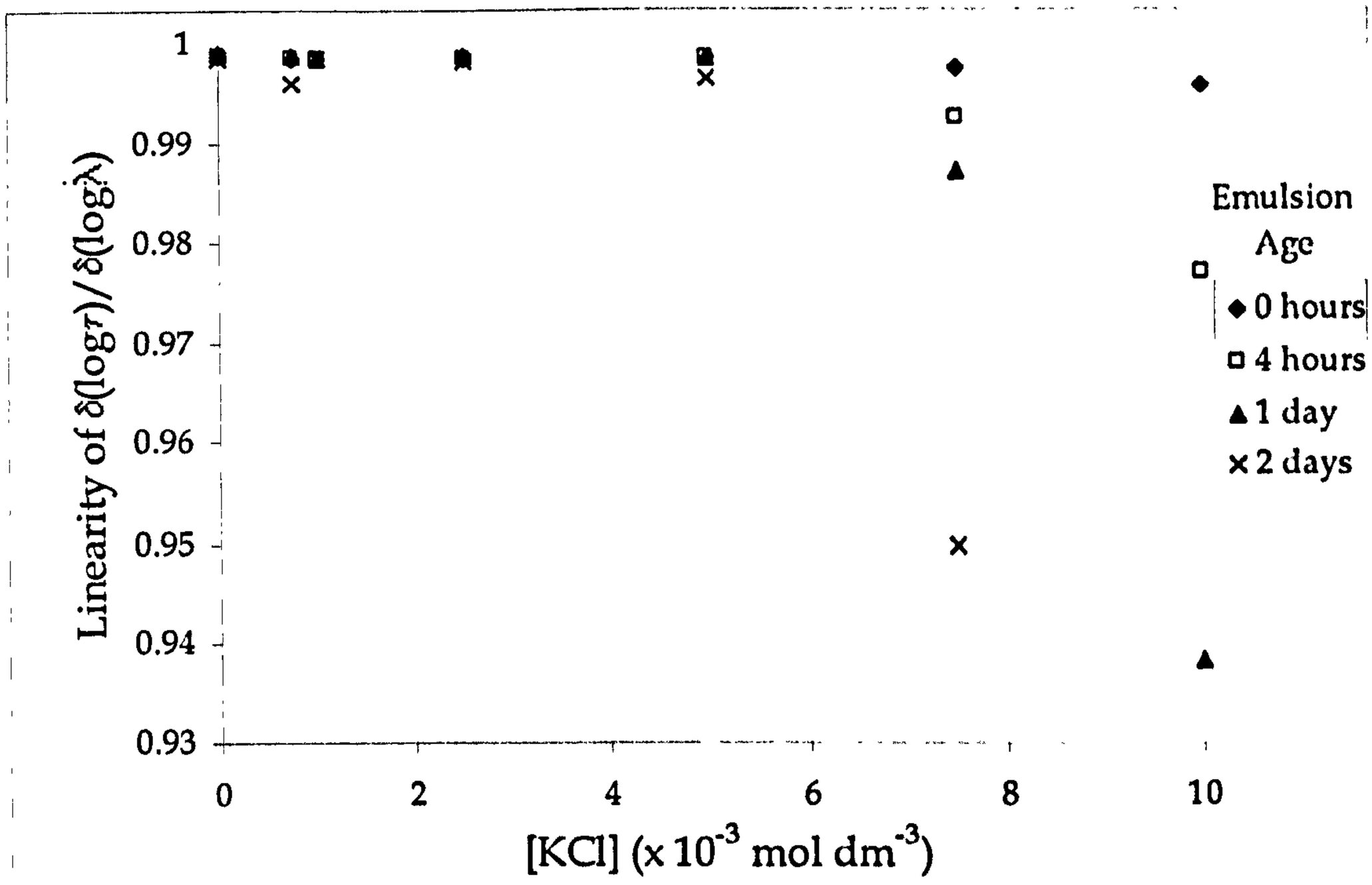

Figure 4.5: The effect of KCl on PDMS emulsion stability; linearity plot

Coalescence occurs after 4 hours for the droplets at KCl concentrations greater than 7.5×10^{-3} mol dm^{-3}. For these samples the gradient of the $\log_{10}$ (turbidity)–$\log_{10}$ (wavelength) changes after 4 hours as observed in figure 4.4. Coalescence is the instability occurring as the gradients for some samples increased. Coagulation is not observable as it results in lower values of the gradient [2]. If the linearity coefficient of the $\log_{10}$ (turbidity)–$\log_{10}$ (wavelength) is followed this change is even clearer to see. For coalescing emulsions the log–log plot loses its linear fit and the linearity coefficient falls below 1, as observed in figure 4.5. At weaker KCl concentrations (< 5×10^{-3} mol dm^{-3}) the emulsion is clearly stable (at least in the timescale studied) as shown by the constant gradients and linearity of the log–log plots.

The data displayed in figure 4.5 show more clearly the onset of coalescence, compared to the data in figure 4.4. As a consequence the remainder of the data from the UV–vis turbidimetric experiments are shown in the form displayed in figure 4.5.

In order to determine more accurately the CCC (critical coalescence concentration) more experiments were performed over a narrower range of KCl concentrations.

Figures 4.6, 4.7, and 4.8 show data from similar experiments for droplets containing cross–linker (MTES) at concentrations of 0, 0.1 and 0.2 v/v in DMDES monomer.

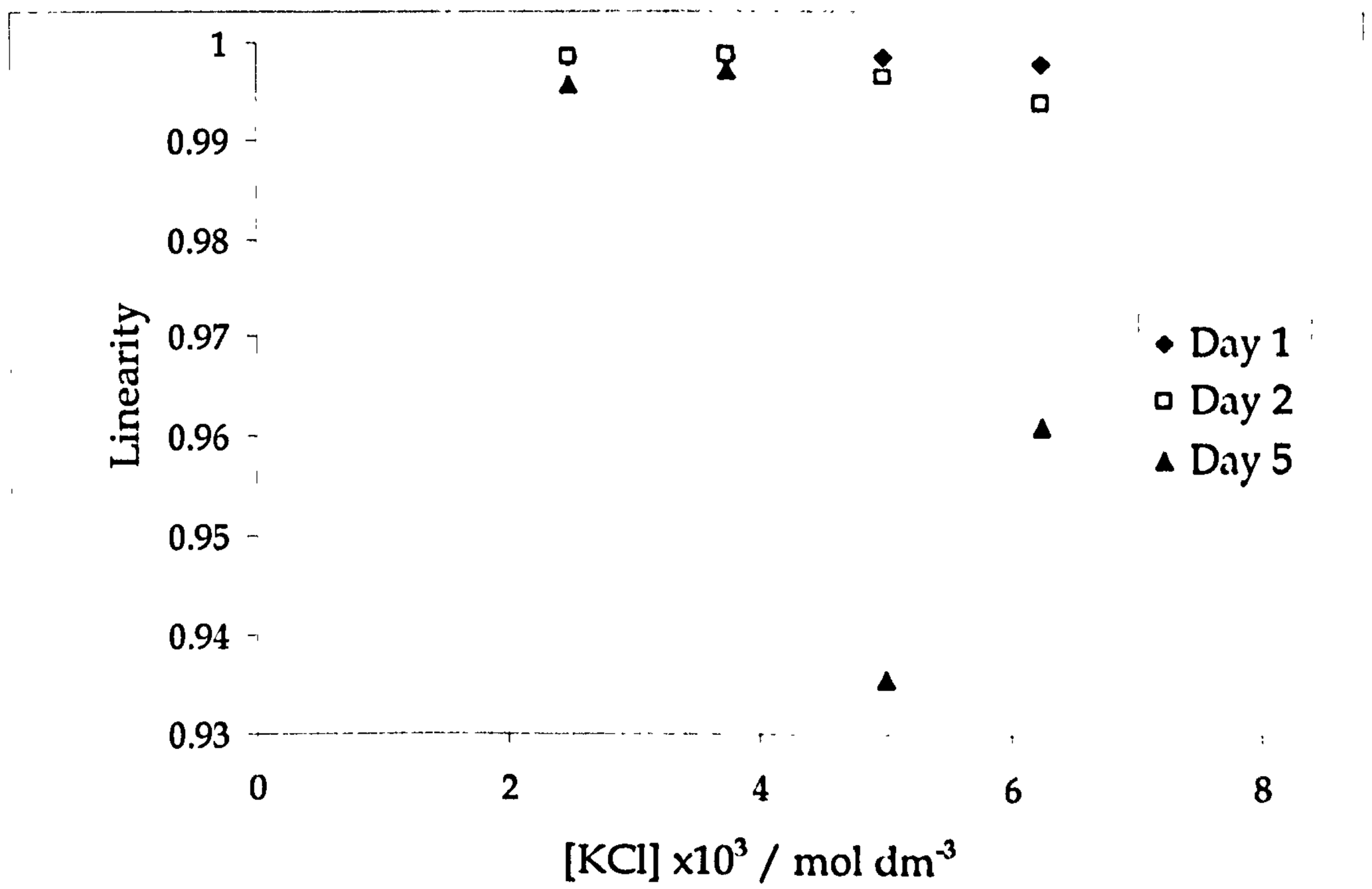

Figure 4.6: The CCC of a 0% MTES PDMS emulsion

As can be seen there is no difference in apparent CCC between the emulsions covering the three concentrations of cross–linker. Coalescence occurs at KCl concentrations of $5x10^{-3}$ mol dm^{-3} and above after a period of 5 days. At $7.5x10^{-3}$ mol dm^{-3} coalescence occurs within a day. One difference

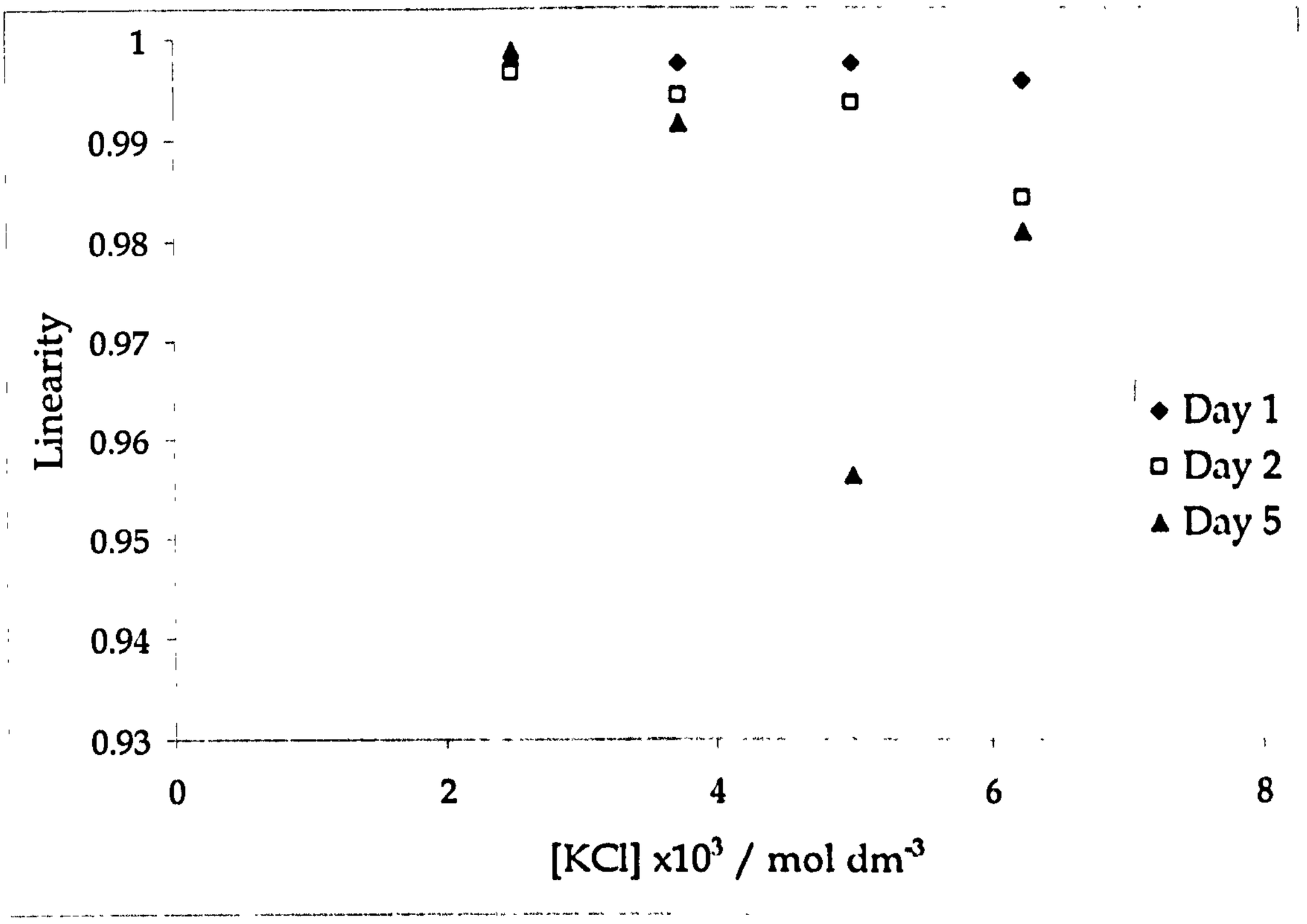

Figure 4.7: The CCC of a 10% MTES PDMS emulsion

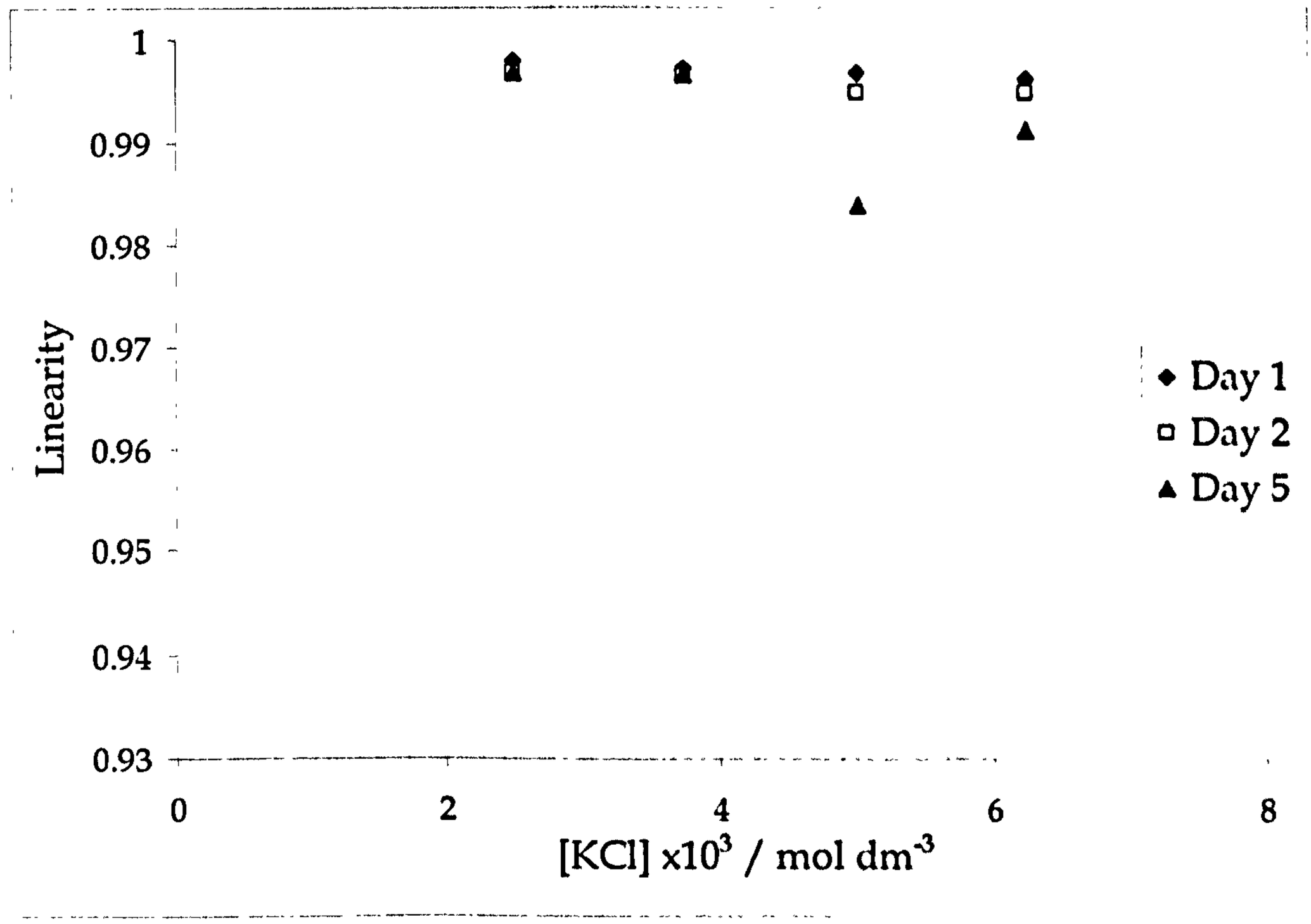

Figure 4.8: The CCC of a 20% MTES PDMS emulsion

that does occur with increasing cross–linker concentration is that the kinetics of coalescence are much slower for the 20% MTES PDMS emulsion. It is not until day five that a significant change in the linearity of the log_{10}–log_{10} graph occurs at electrolyte concentrations above the CCC.

4.2.2 PDMS droplet stability to coalescence by pH

Figures 4.9, 4.10 and 4.11 show the stability of PDMS emulsions of cross–linker concentrations of 0, 0.1, and 0.2 v/v in DMDES with low pH values over a 5 day period.

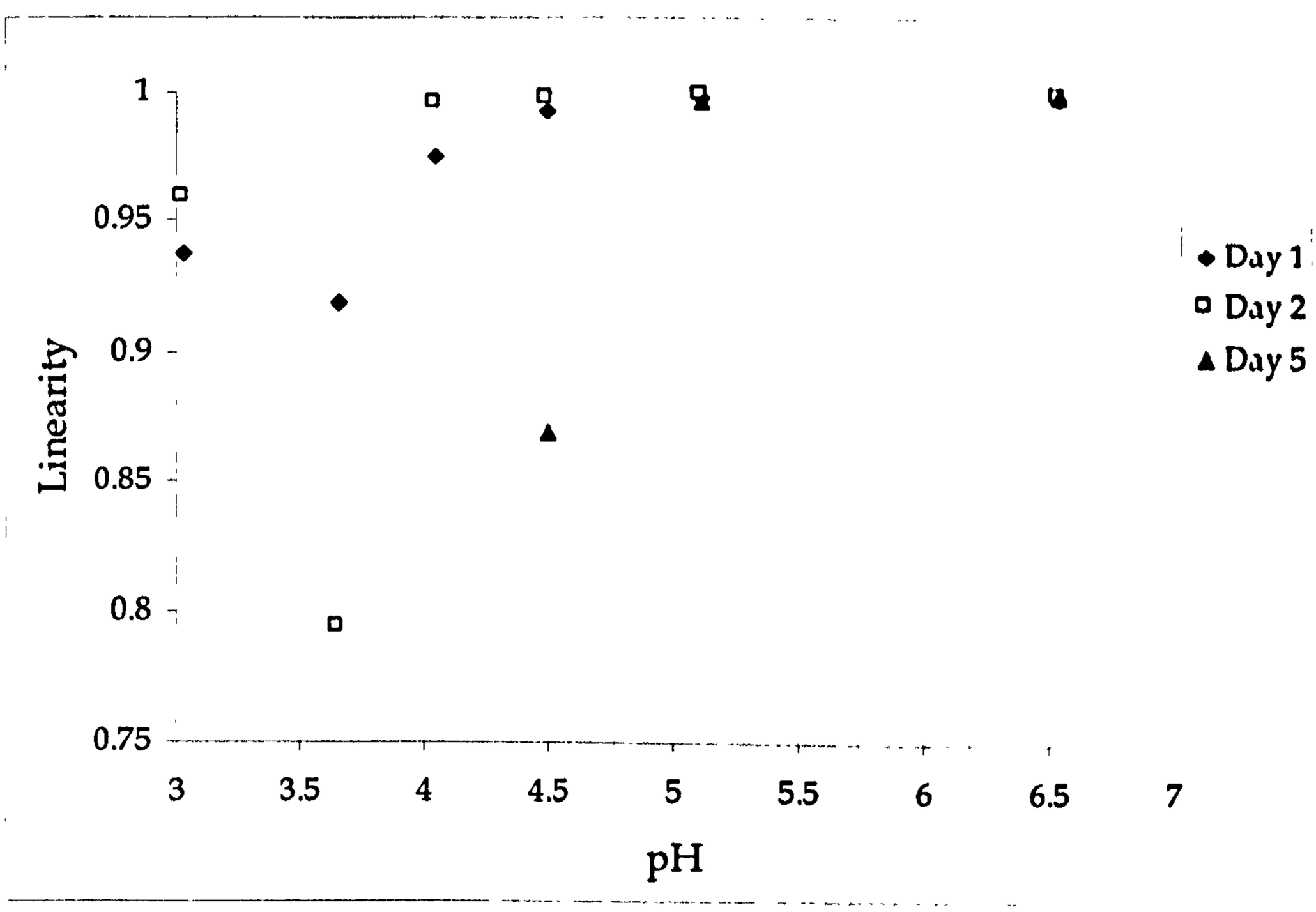

Figure 4.9: The coalescence of a 0% MTES PDMS emulsion at low pH

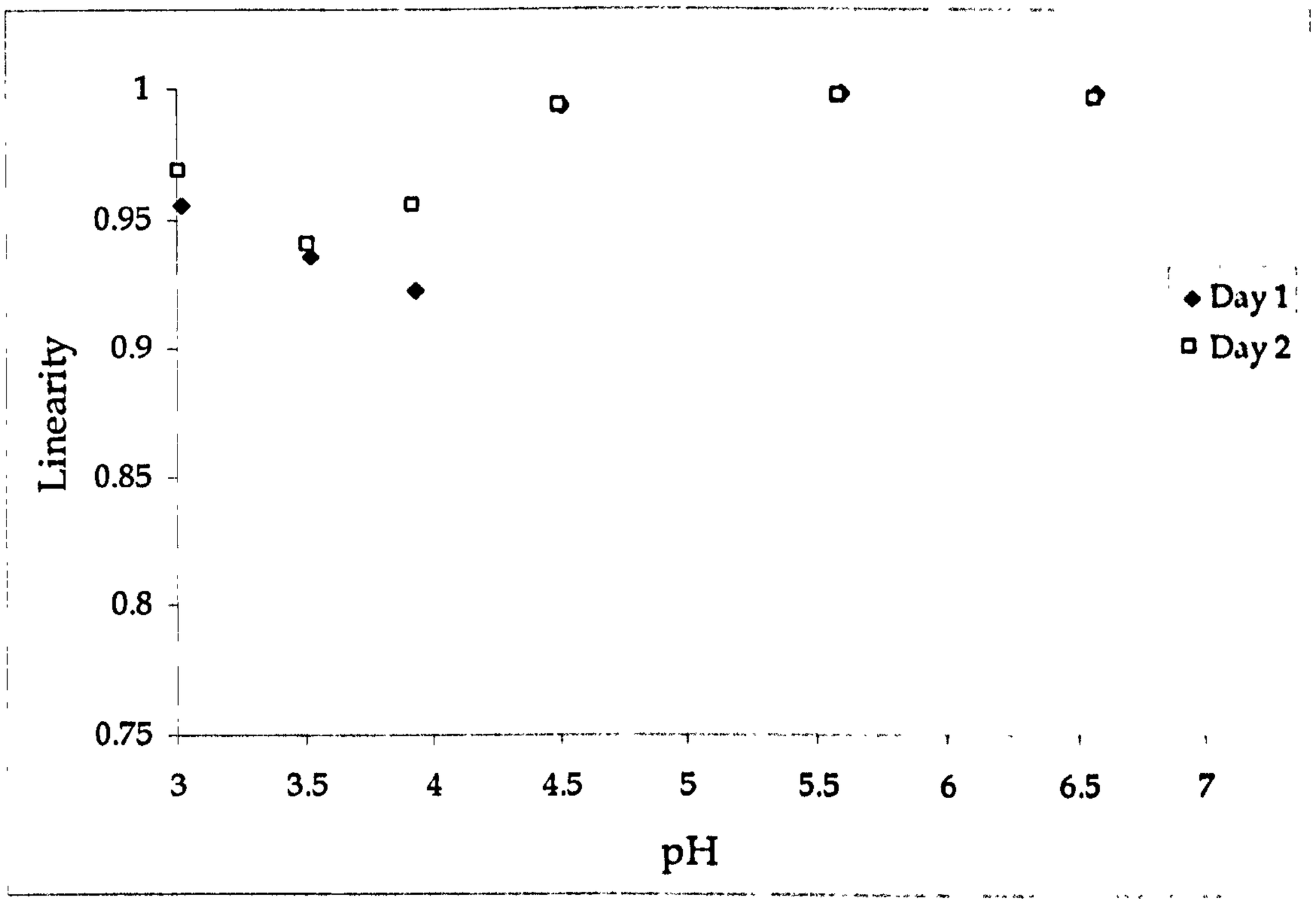

Figure 4.10: The coalescence of a 10% MTES PDMS emulsion at low pH

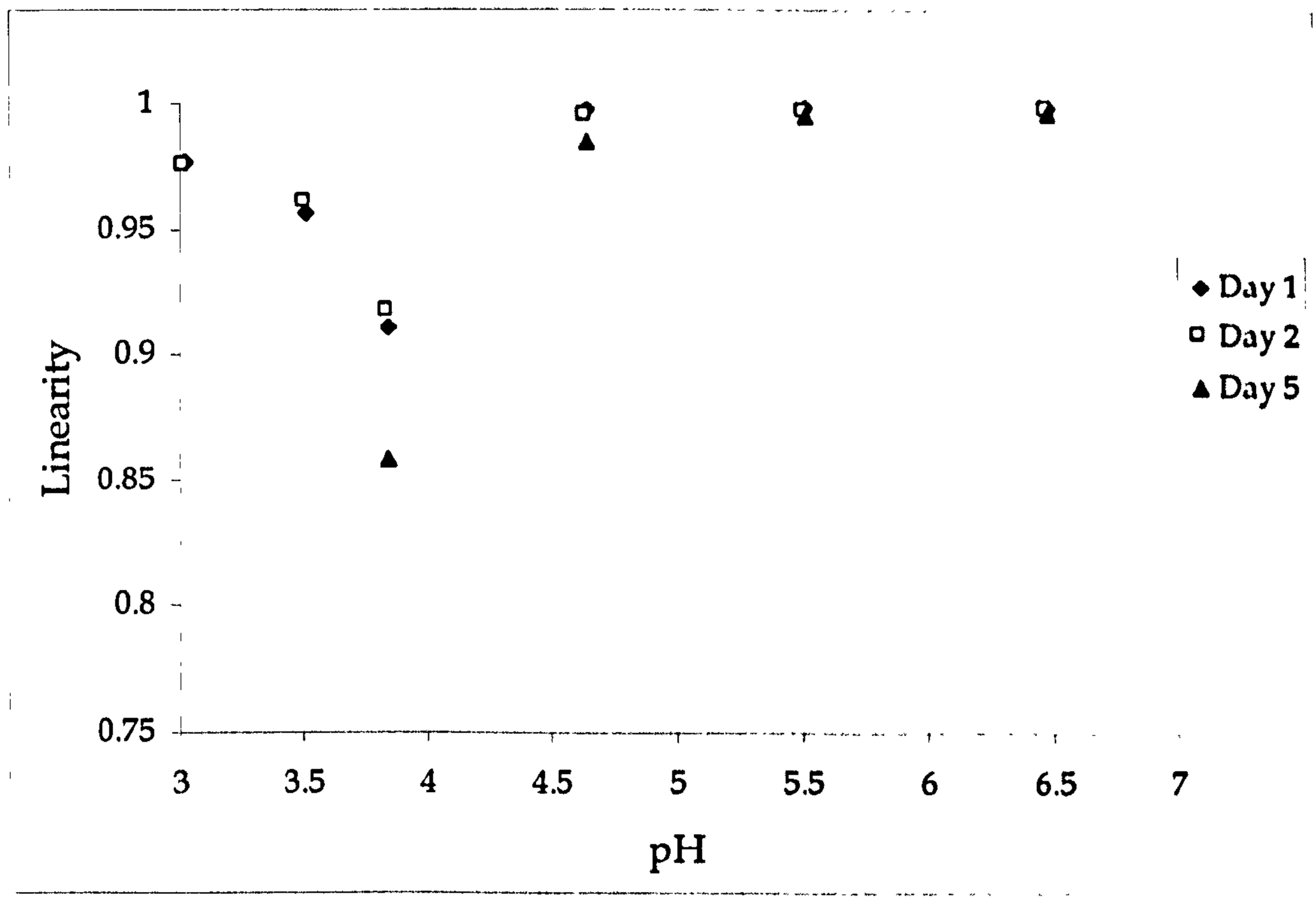

Figure 4.11: The coalescence of a 20% MTES PDMS emulsion at low pH

Figure 4.9 shows the stability of a 0% MTES PDMS emulsion. It is apparent that at or below pH 4.6 the emulsion is unstable, probably because there is insufficient charge on the droplet surface to prevent the droplets from coagulating upon collision. In figures 4.10 and 4.11 the emulsions appear more resistant to coalescence, particularly the 20% MTES emulsion where the linearity of the $\log_{10}$ (turbidity)–$\log_{10}$ (wavelength) graph is still high at pH 4.5. In all samples below a pH value of about 4 the PDMS emulsion is unstable and coalescence occurs within hours.

In these experiments only coalescence is observed. No flocs of coagulated droplets were evident. The results of both sets of experiments suggest that overall the higher the concentration of cross-linker in the PDMS emulsion the more resistant to coalescence the droplets are. This is shown by the linearity factors for the 20% MTES and 10% MTES emulsions remaining closer to 1 (i.e. there is a less significant change in the turbidity of the dispersion).

4.2.3 PDMS droplet stability to osmotic pressure

In these experiments a somewhat subjective criterion was used to determine whether or not the emulsion was stable or unstable under the experimental conditions. If droplets could be still be observed using optical microscopy following equilibration then the emulsion had not broken, irrespective of any change in the polydispersity (droplet size distribution) of the system. The equilibrium dextran concentration, not the initial value, was taken in order to derive the osmotic pressure of the medium (equation 4.1).

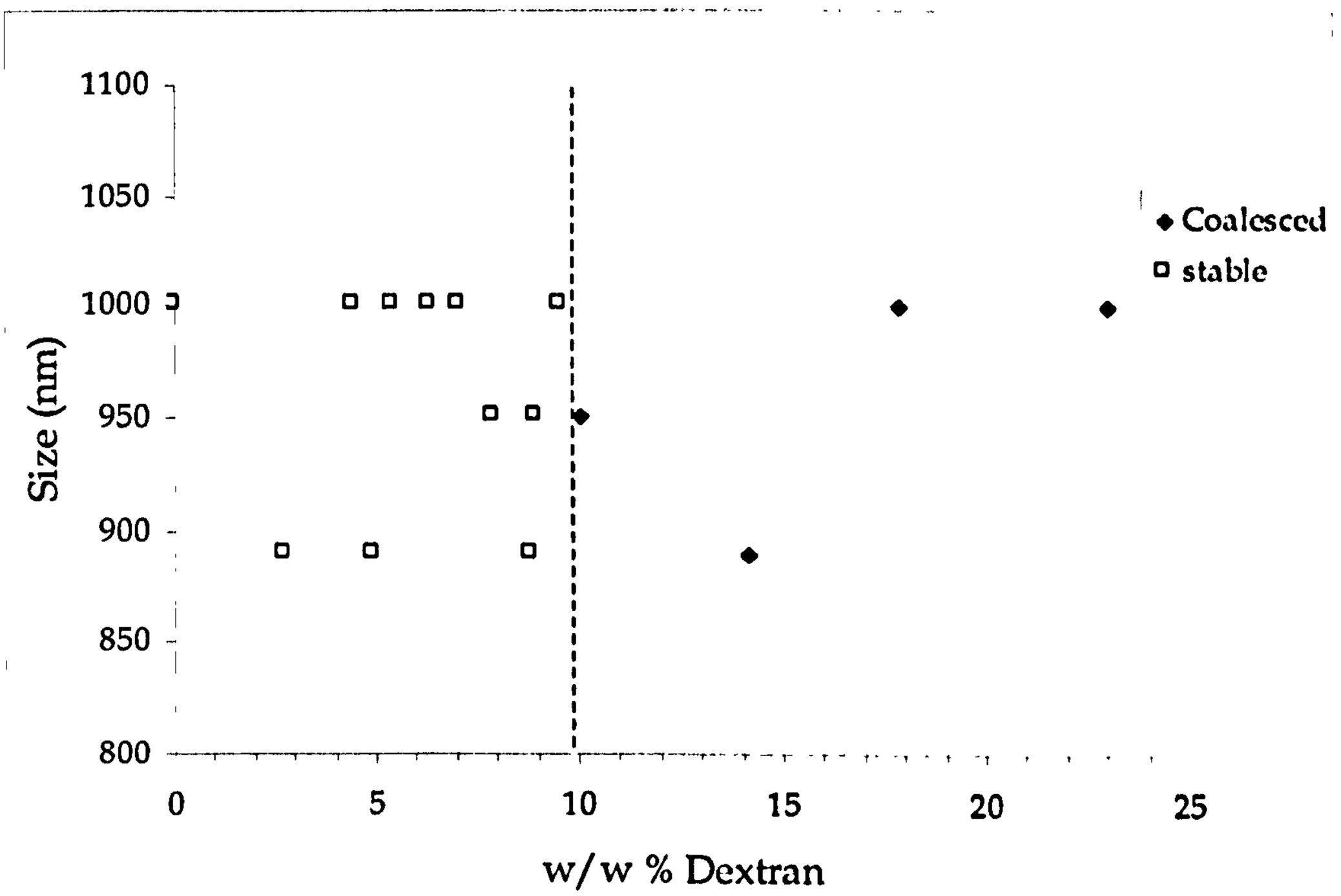

Figure 4.12: The coalescence of PDMS emulsions at high osmotic pressure

From figure 4.12 the threshold concentration for the onset of droplet coalescence is between 9 and 10 w/w % dextran as indicated by the dashed line. This dashed line corresponds to an osmotic pressure of 1.73×10^{1} N m^{-2} or about 0.17 atmospheres.

4.3 Electrophoresis

Electrophoresis is the movement of a charged particle or droplet in a liquid in an electric field.

In electrophoresis experiments the parameter usually determined is the electrophoretic mobility (u_E, velocity per unit electric field). A key parameter in calculating the zeta–potential (ζ, refer to section 2.3.1) from mobility values is the value of κa ($1/\kappa$ being the Debye–Hückel length and a the droplet radius). When κa is small a charged particle can be treated as a point charge; when κa is large the double layer can be treated as being flat in nature.

4.3.1 Theory

Hückel's equation (equation 4.3) describes the relation between the electrophoretic mobility, u_E, and the zeta–potential, ζ, for a point charge where ε is the permitivity of the medium and η_0 is the viscosity of the medium.

$$u_E = \frac{2\zeta\varepsilon}{3\eta_0} \qquad 4.3$$

The Hückel situation is only valid in extreme situations ($\kappa a << 1$). This is unlikely to occur in most aqueous colloidal dispersions where the sizes of the dispersed particles or droplets are large and electrolyte is present. Smoluchowski's [10] (equation 4.3) relates the mobility and zeta–potential under conditions of $\kappa a >> 1$.

$$u_E = \frac{\zeta\varepsilon}{\eta_0} \qquad 4.4$$

These two expressions are limits. Henry [11] derived a formula (equation 4.5) that took into account intermediate values of κa.

$$u_E = \frac{\zeta\varepsilon}{\eta_0} f(\kappa a) \qquad 4.5$$

In equation 4.5 f(κa) varies between 1 for small κa and 1.5 for large κa. The reason for this variance is electrophoretic retardation. This is caused by the double layer ions (and hence solvent around them) moving in an opposite direction to the particle. This is unimportant in equation 4.3 as the main retarding force is the frictional resistance of the medium, but becomes increasingly so for larger particles. In equation 4.5 the following assumptions are made: (i) the Debye–Hückel approximation is made; (ii) there is no surface conductance or relaxation (both are results of distorting the electric field around a droplet and (iii) ε and η are assumed to be constant throughout the mobile part of the electric double layer.

More recently the theory of electrophoresis has been developed further [12]. The O'Brien and White theory [13] allows the theoretical calculation of zeta–potentials from electrophoretic mobilities of spherical, rigid particles of any size. There are also theoretical considerations for the electrophoretic behaviour of non–rigid particles such as spherical polyelectrolytes [14] (e.g. a swollen microgel) and for liquid droplets. Booth [15] made several assumptions about the electrophoretic motion of a spherical fluid body. These included neglecting relaxation effects, assuming that the charge and potential distribution were spherically symmetrical and also that the dielectric constant, viscosity and conductivity of the liquids retain their macroscopic values. Levine and O'Brien [16] considered charged mercury drops dispersed in water in an electric field, a topic that has received further attention from Oshima. More recently Booth's theory has been extended to non–conducting droplets [17] where it has been shown that in some cases the effects of interior viscosity can be ignored. These cases include the presence of surfactant or some contaminant material at the liquid/liquid interface, which leaves the drop surface inextensible, as if the droplet were solid. 'Solidification' of the interface can also occur with drops with very thin double layers and very high zeta–potentials (above *ca* 150 mV) [17]. The same effect happens with

modest zeta–potentials in drops with thick double layers. The apparent rigidity is caused by the influence of ion concentration gradients on the interfacial tension.

For cases where 'solidification' was not evident, it was shown [17] for a liquid droplet of internal viscosity η_1 moving in a liquid of viscosity η_0 that:

$$u_E = \frac{3\varepsilon\eta_1\zeta}{\eta_0(3\eta_1 + 2\eta_0)} \qquad 4.6$$

for $\kappa a >> 0$. As κa approaches 0 the mobility becomes independent of the droplet viscosity.

4.3.2 Electrophoretic mobility measurements of PDMS emulsions

The electrophoretic mobility of the PDMS in water emulsions was measured using the phase analysis light scattering (PALS) technique developed by Miller and Schätzel [18]. Attempts were also made to measure mobility using a Penkem 3000 electrophoretic apparatus. This is a conventional style laser doppler electrophoresis (LDE) apparatus. This proved unsuccessful with the PDMS emulsions, as the apparatus requires relatively strong light scattering dispersions. PDMS emulsions do not scatter light strongly enough as the refractive index of PDMS is similar to that of water (R.I. D_4 = 1.3968 [19]; water = 1.333 [20]). PALS proved to be the most reliable technique as it does not require very strong light scattering dispersions . PALS is an extension of LDE, the difference being the analysis of the scattered light signal where PALS looks at the phase rather than the spectrum or autocorrelation.

With PALS the particles move relative to a moving interference fringe pattern. Two laser beams intersecting in the gap between parallel electrodes across which a sinusoidal electric field is applied generate this fringe pattern.

The cell set–up with parallel electrodes and crossed laser beams is displayed below in figure 4.13.

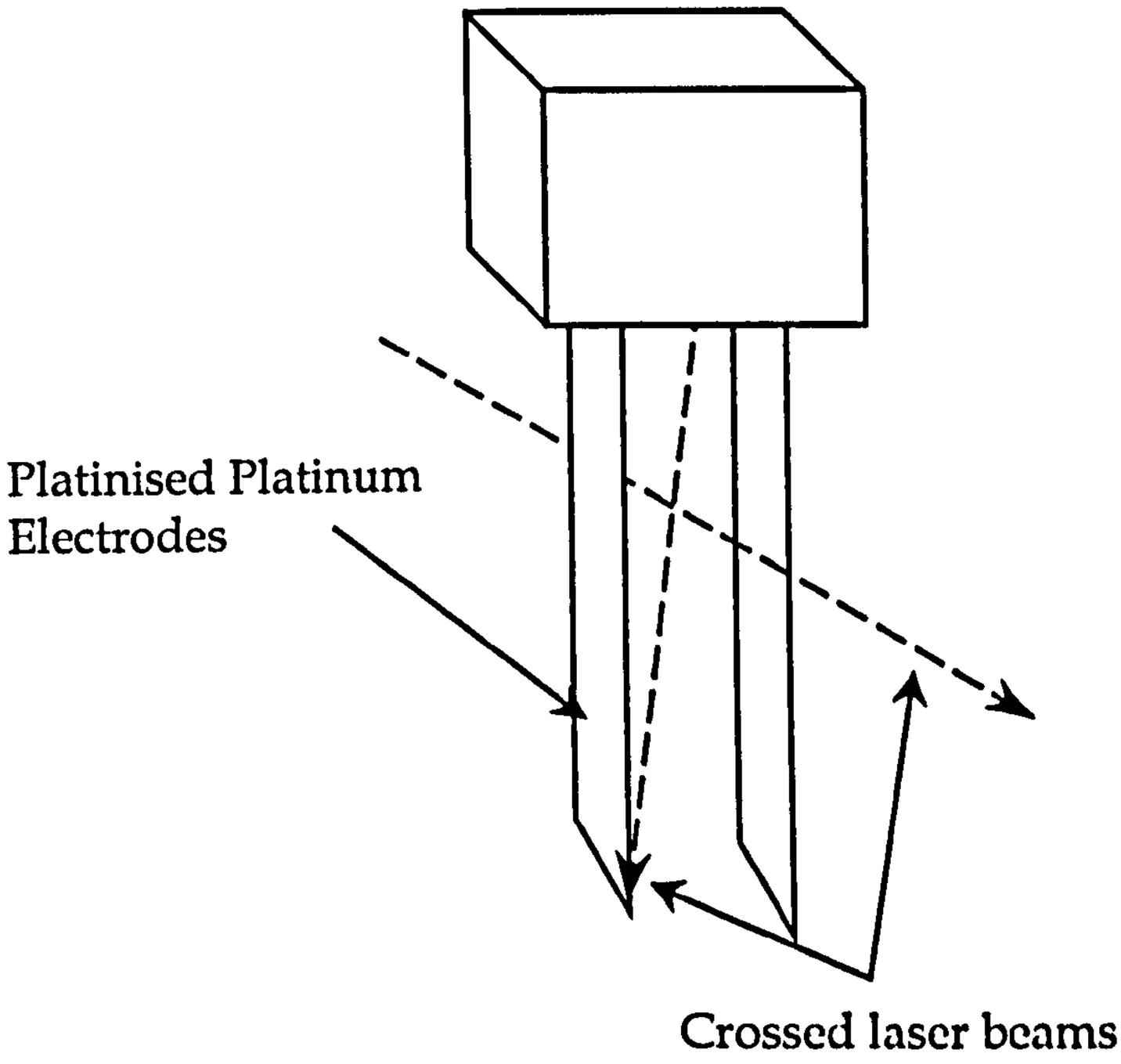

Figure 4.13: PALS cell and electrode design.

In LDE the colloidal particles must move over several fringe spaces during a single field pulse, so for samples of low mobility, large voltages are required, which can result in heating of the sample. PALS removes such restrictions by the use of phase demodulation of the laser Doppler signal. This allows the determination of very low mobilities with good precision (down to 10^{-12} m^2 s^{-1} V^{-1}) [18]. The crossed beams are set so that there is a low scattering angle (typically around 15°) which suits poor scatterers such as the PDMS emulsions and also very small colloidal particles such as microemulsions.

Experimental measurements were performed using 4 mm path–length quartz cuvettes. The cuvettes were thoroughly cleaned by sonication in acetone, toluene and ethanol. The dialysed PDMS emulsions contained KCl as a background electrolyte at a concentration of 1×10^{-3} mol dm^{-3}. As with the PCS measurements (refer to section 3.3.3) some samples required diluting

with aqueous electrolyte in order to avoid problems with multiple scattering. All samples measured were equilibrated at 25 ± 0.5 °C. Platinised black platinum electrodes were used in order to prevent electrolysis occurring on the electrode surface. Typical field strengths used were of the order of 1 V mm^{-1}.

Various experiments were carried out using the PALS technique. These included the effect of cross-linker on droplet mobility, the mobility of droplets swollen with hydrocarbons and the effect of pH on cross-linked emulsions to determine the isoelectric point of the surface charge groups.

Typically 3 sets of 5 readings were taken and averaged to give the quoted result. The one major disadvantage with the PALS technique is that it does not provide a standard deviation for each individual reading (this is a question of programming involved with the PALS software).

4.3.3 Mobility measurements

Most emulsion systems that have been previously studied have either been polydisperse or have had a surfactant present as a stabiliser. A liquid droplet with close–packed surfactant layers at the interface would be expected to behave like a solid particle which conventional electrophoretic theory describes [21]. In the case of the PDMS emulsions studied here there is no added surfactant. The emulsions are stabilised by a small fraction of functionalised linear PDMS. Hence, there should be a truly fluid interface rather than the 'solid–like' interface associated with surfactant–stabilised droplets. This is confirmed by the measured interfacial tension of the PDMS and water, which is of the order of 20 mN m^{-1} (section 3.4.2, figure 3.12). The droplets are expected to be deformable, i.e. internal flow will bear an influence on their motion in an applied electric field. Theory suggests that the

electrophoretic mobility for droplets compared to particles of the same potential and value of κa will be affected.

The presence of a small amount of cross-linker (MTES) within the PDMS phase causes a marked increase in the viscosity (refer to section 3.4.2, figure 3.11) of the dispersed silicone oil. The droplets made with 10% MTES will be about 2.5 times as viscous as those made with 0% MTES. The diameter of the droplets will be fairly similar (refer to section 3.4.1) with only approximately 5% difference at the most (typical diameter 0% MTES = 1000 nm; 10% MTES = 950 nm). Hence, there should be an observable difference in the mobility of these two systems.

Figure 4.14 shows the averaged data points measured using PALS taken in a series of five separate experiments using different samples. These were all dispersed in $1x10^{-3}$ mol dm^{-3} KCl as background electrolyte. Standard deviations were less than 8%.

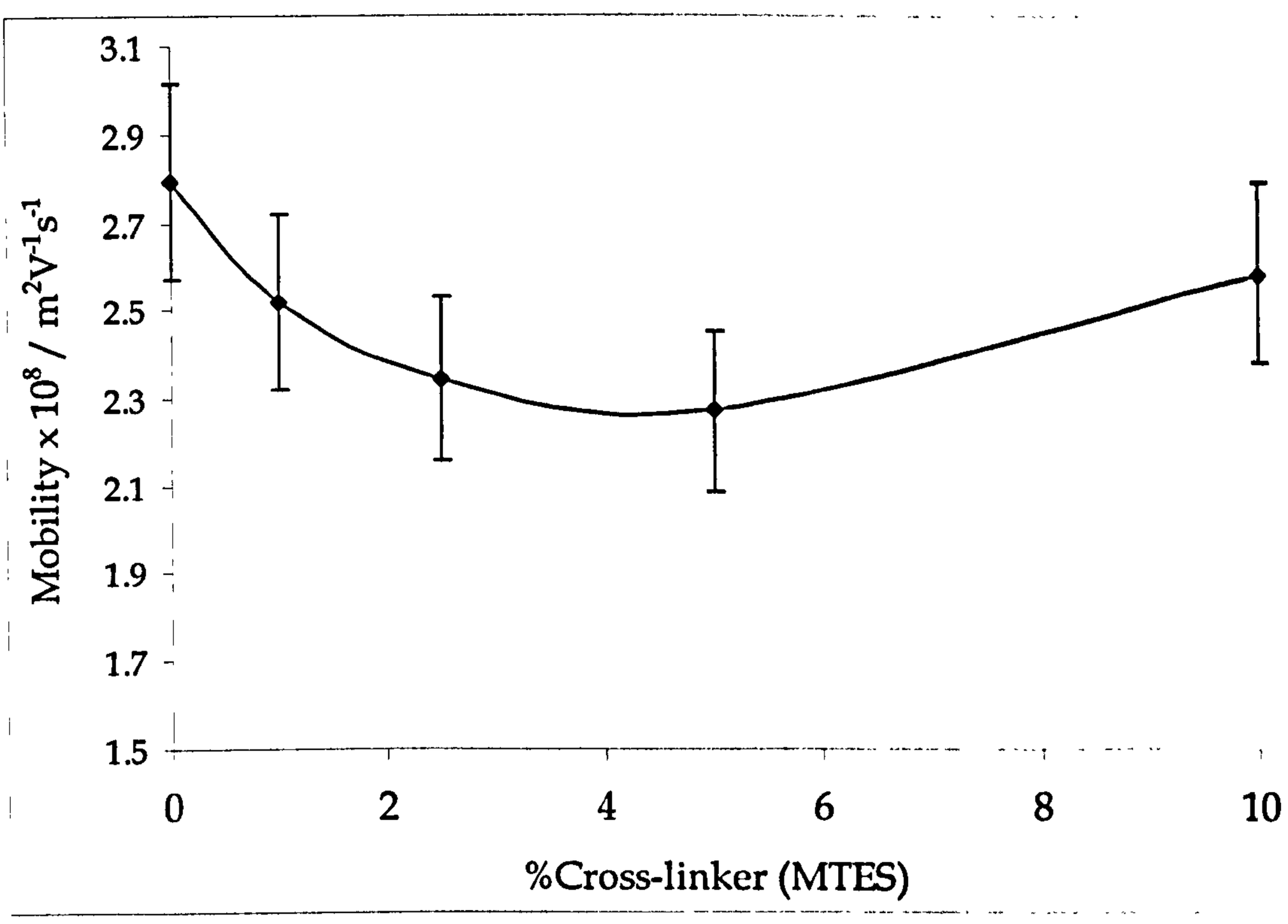

Figure 4.14: Effect of cross-linker on droplet electrophoretic mobility

As can be seen in figure 4.14 the mobility is greatest for the lowest viscosity sample (0% MTES) and decreases to a minimum at around 4 % MTES before it starts to rise again as the cross–linker concentration increases.

Figure 4.15 shows the averaged droplet size of the PDMS emulsions at equivalent cross–linker concentrations to those in figure 4.14.

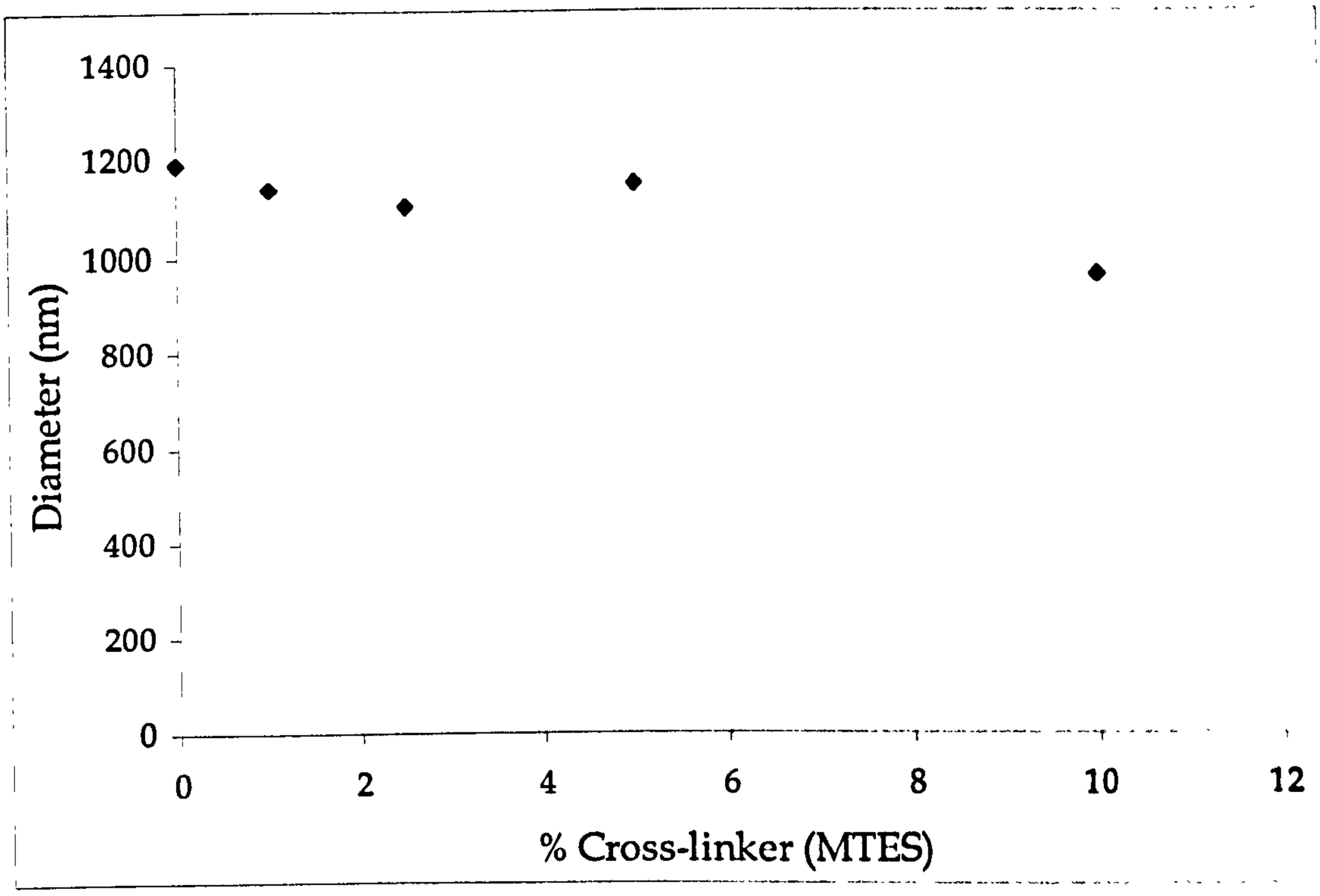

Figure 4.15: The averaged size of the emulsion droplets for electrophoresis

In figure 4.15 the average droplet size over the range of emulsions studied does not vary significantly over the range 0 to 5 % MTES. However, the 10% MTES emulsions were noticeably smaller in most instances. This will undoubtedly have some effect on the mobility data as mobility is inherently dependant upon κa.

Figure 4.16 shows the effect of electrolyte on the electrophoretic mobility of a PDMS emulsion with no added cross–linker, which also corresponds to the data shown in figure 4.6. The droplets still have a

significant amount of surface charge, even when the concentration of KCl exceeds the CCC (determined in section 4.2.1).

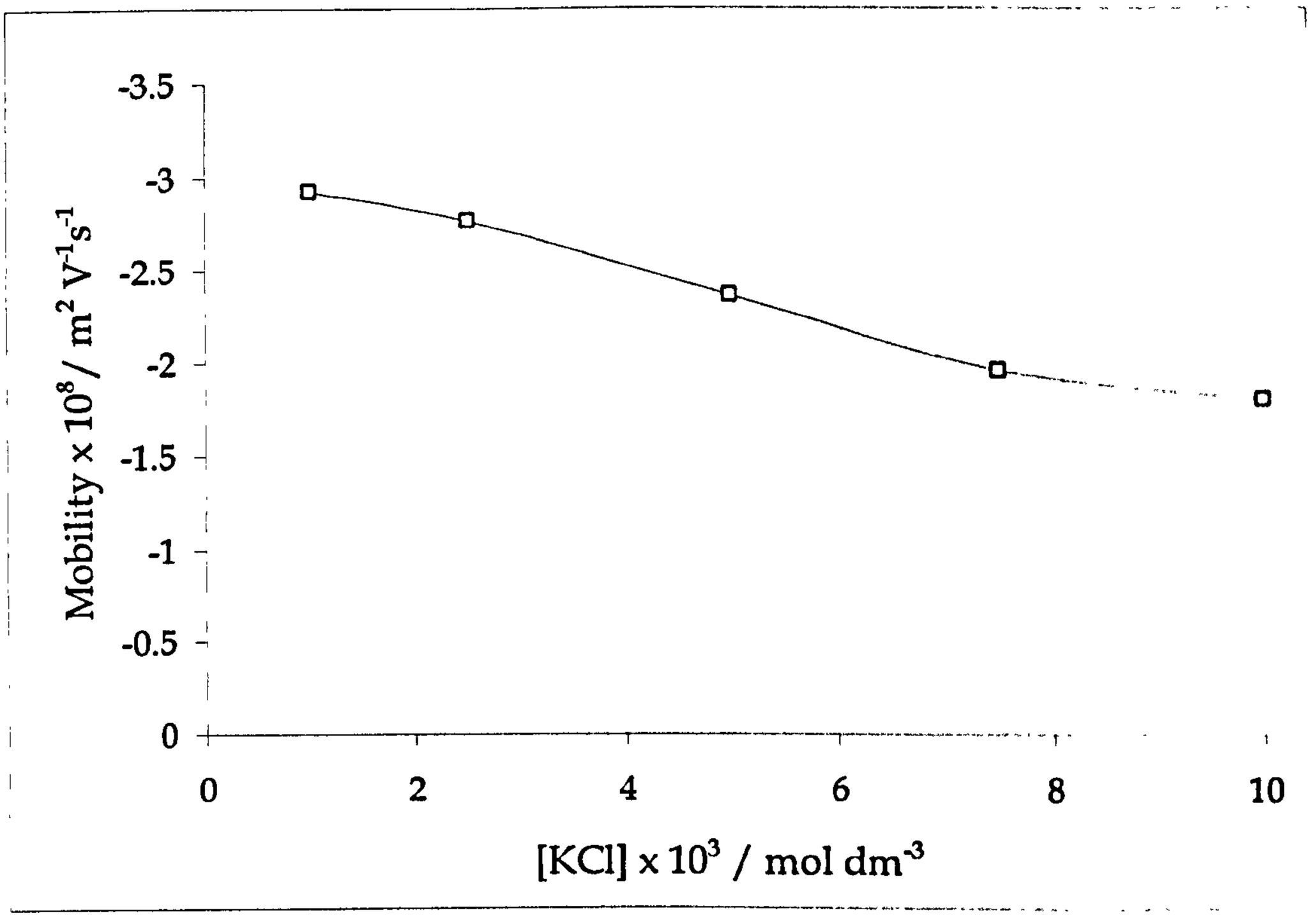

Figure 4.16: The effect of KCl on the electrophoretic mobility of a PDMS droplet

Figure 4.17 shows the effect of pH on droplet electrophoretic mobility for PDMS emulsions with different concentrations of cross-linker and corresponds to the data shown in figures 4.9, 4.10 and 4.11. It shows that the electrophoretic mobility of the emulsions only starts to significantly decrease below a pH of 5. Previous results on the stability of PDMS emulsions at low pH values showed that the higher concentrations of cross-linker in the emulsion caused the droplets to be more stable at low pH (refer to section 4.2.2).

The dashed line in figure 4.17 indicates zero mobility and where the fitted curves cross this line is the isoelectric point of that particular emulsion (pH_{iep}, where the droplet has no net charge).

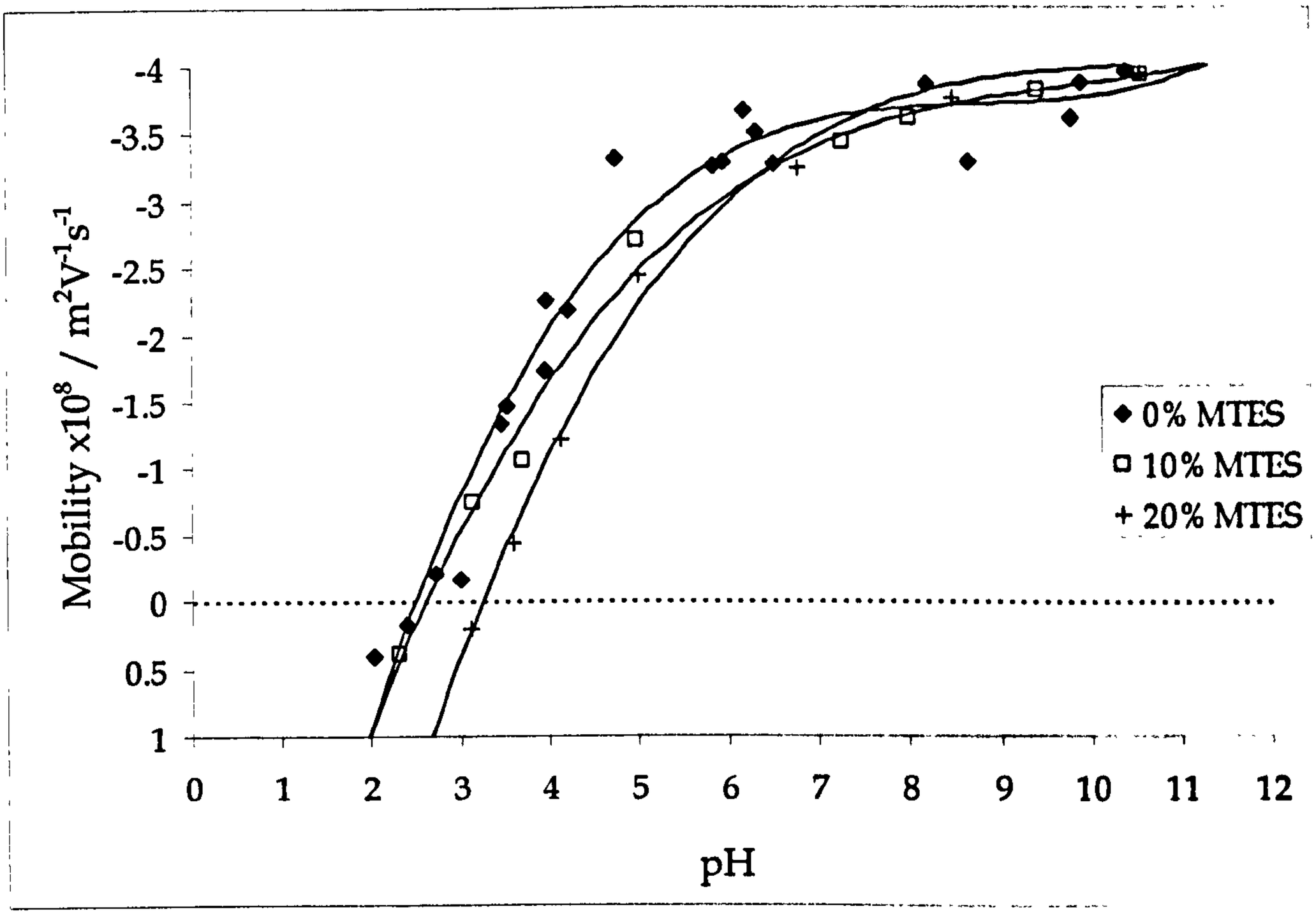

Figure 4.17: The effect of cross–linker on electrophoretic mobility with pH

The isoelectric point for various droplets increases with higher cross–linker concentration. Below a pH of 4 all emulsions are unstable (refer to section 4.2.2) so mobility data at pH values below this have to be considered approximate as the size distribution of the emulsion will change. The isoelectric points of PDMS emulsions are comparable with that of silica [22] (pH_{iep} = 2–3).

4.3.4 Calculation of zeta–potentials

Zeta–potentials (ζ) have been calculated using the methods of O'Brien and White and Booth [13,15] from the electrophoretic mobility data. Figure 4.18 compares how these two approaches affect the data from figure 4.14.

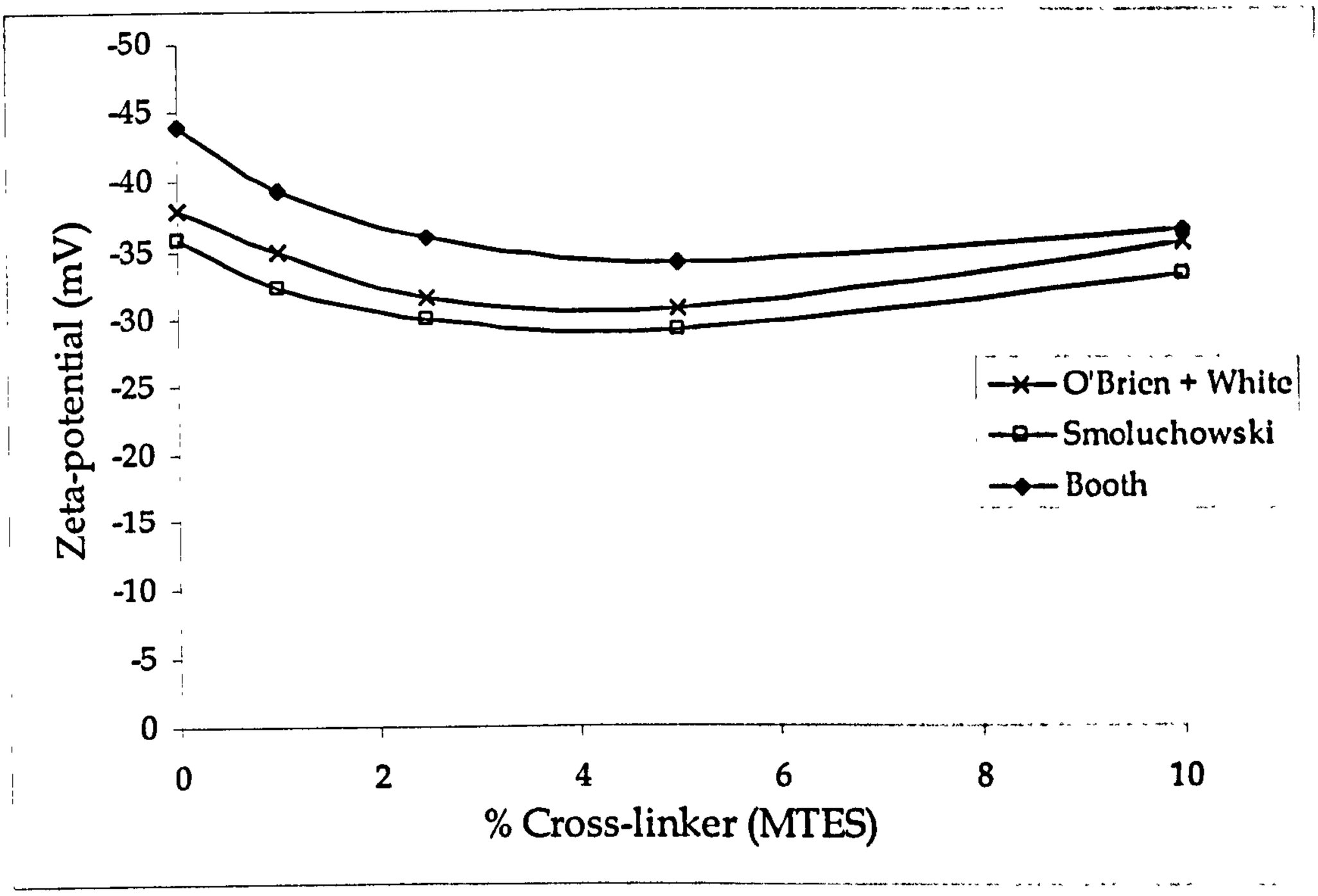

Figure 4.18: Zeta–potentials of cross–linked PDMS droplets

The values of the calculated zeta–potentials tend to converge somewhat as the droplets become increasingly viscous. At low viscosity the values differ the most, the theory accounting for the internal droplet viscosity (Booth) giving a much higher potential than the case for the solid particle (O'Brien). The change in κa as the drop size decreases is compensated for by the O'Brien treatment only.

Similar calculations lead to values for the zeta–potential at different electrolyte concentrations and pH.

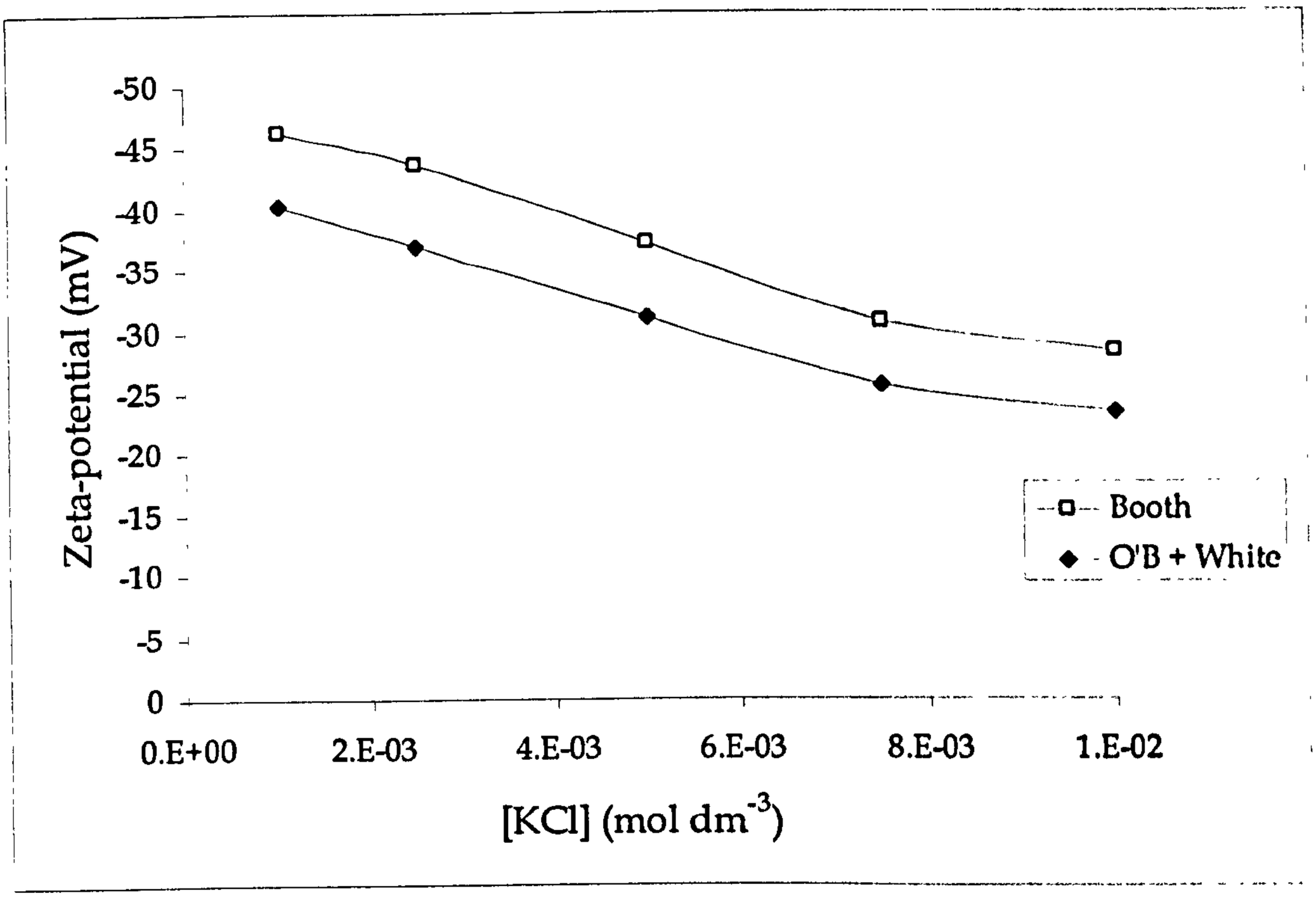

Figure 4.19: The effect of electrolyte on the ζ–potential of a PDMS emulsion

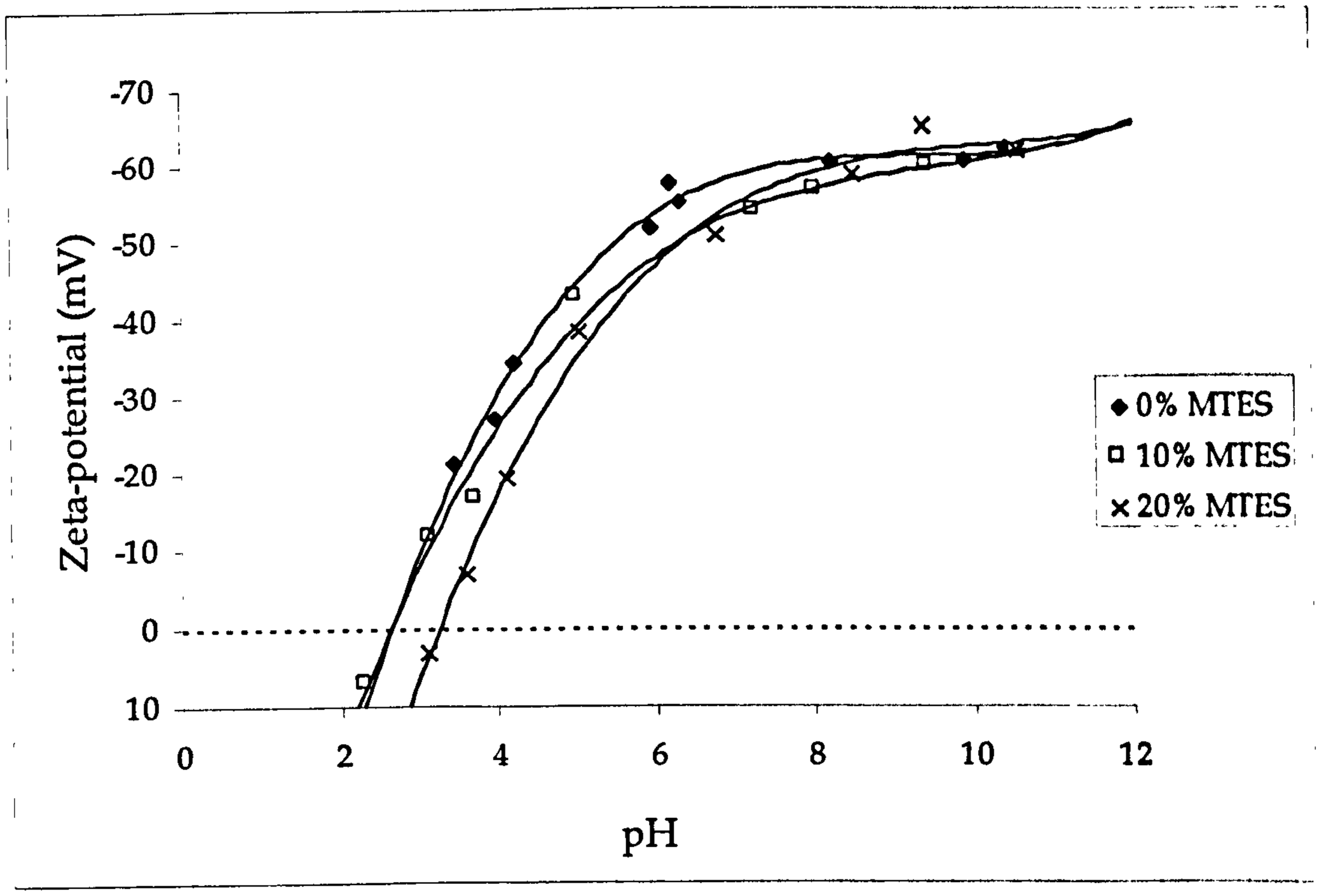

Figure 4.20: The effect of pH on the ζ–potential of cross–linked PDMS emulsions

It can be seen from figure 4.19 that the zeta–potential decreases with increasing electrolyte concentration. However, above 5×10^{-3} mol dm^{-3} (the CCC value) there is still an appreciable potential of about -30 mV on the surface of the droplet.

Likewise, from figure 4.20, below pH 4 there is still an appreciable potential on the surface of the droplets, although not as high as at the CCC. It is apparent from figure 4.20 that the PDMS droplets with no added cross–linker have the highest charge but the least stability at low pH. Higher concentrations of cross–linker in the droplet leads to a lower surface potential but concurrently greater stability. This could be due to the presence of a cross–linked gel network in the droplet, causing greater stability against coalescence.

4.4 DLVO Pair Potentials

4.4.1 Calculations from experimental data

DLVO pair potentials (refer to section 2.3.4) were calculated using the sum of the electrostatic and van der Waals interactions by the "Interparticle Potential Calculation Program" [23]. Total pair potentials calculated using zeta–potential data and an estimated Hamaker constant (refer to section 2.3.2) show large primary maxima due to a dominance of the electrostatic repulsive term over the van der Waals attractive term. Table 4.1 gives the calculated maximum potentials, in units of kT, for the data presented in figures 4.16 and 4.18 for two PDMS droplets. The maxima have been calculated using the zeta–potentials derived by both the Booth and the O'Brien and White methods. The estimated Hamaker constant for D_4 from optical data [24] was 4.96×10^{-20} J. The corresponding net Hamaker constant for two droplets

consisting of D_4 PDMS approaching (A_{12}) in water was calculated as being 0.35×10^{-20} J (refer to section 2.3.2).

Calculation Method	KCl concentration (mol dm^{-3})				
	1×10^{-3}	2.5×10^{-3}	5×10^{-3}	7.5×10^{-3}	1×10^{-3}
O'B+White (kT)	510	410	265	175	145
Booth (kT)	670	590	395	245	240

Table 4.1: Pair potential repulsive maxima

As the O'Brien and White zeta–potential is lower than the Booth calculated potential the repulsive maxima are less. The maxima for D_4 emulsions at KCl concentrations well above the CCC are relatively large compared to the thermal energy (kT) for an unstable system. At 145 kT, there exists a very large barrier to close approach by two droplets.

Table 4.2 gives the repulsive maxima, in units of kT, of the pair potential for the PDMS emulsions with pH. This has been calculated using ζ–potentials derived by the O'Brien and White theory only, which is accurate for droplets with high internal viscosity.

Max potential at pH	Cross–linker (MTES) in emulsion (%)		
	0	10	20
10.5 (kT)	935	1160	811
5 9 (kT)	730	535	285
3.8 (kT)	155	65	60
3.1 (kT)	85	25	3

Table 4.2: Experimental pair potentials for PDMS emulsions with pH

For a 20% MTES emulsion at pH 3.1 the barrier to coagulation is approximately of the order of 3 kT. This would not be sufficient to keep the dispersion stable over a long period of time.

4.4.2 Theoretical pair potential calculations

Theoretical pair potentials have been calculated for a PDMS emulsion in order to assess the influence of the measured zeta–potential at an electrolyte concentration just above the critical coalescence point (at [KCl] of 7.5×10^{-3} mol dm^{-3}). Experimental data suggested that the zeta–potential at this concentration (of electrolyte) is -26 mV. Pair potentials have been calculated for lower potentials at -20 mV, -15 mV and -10 mV in figure 4.21.

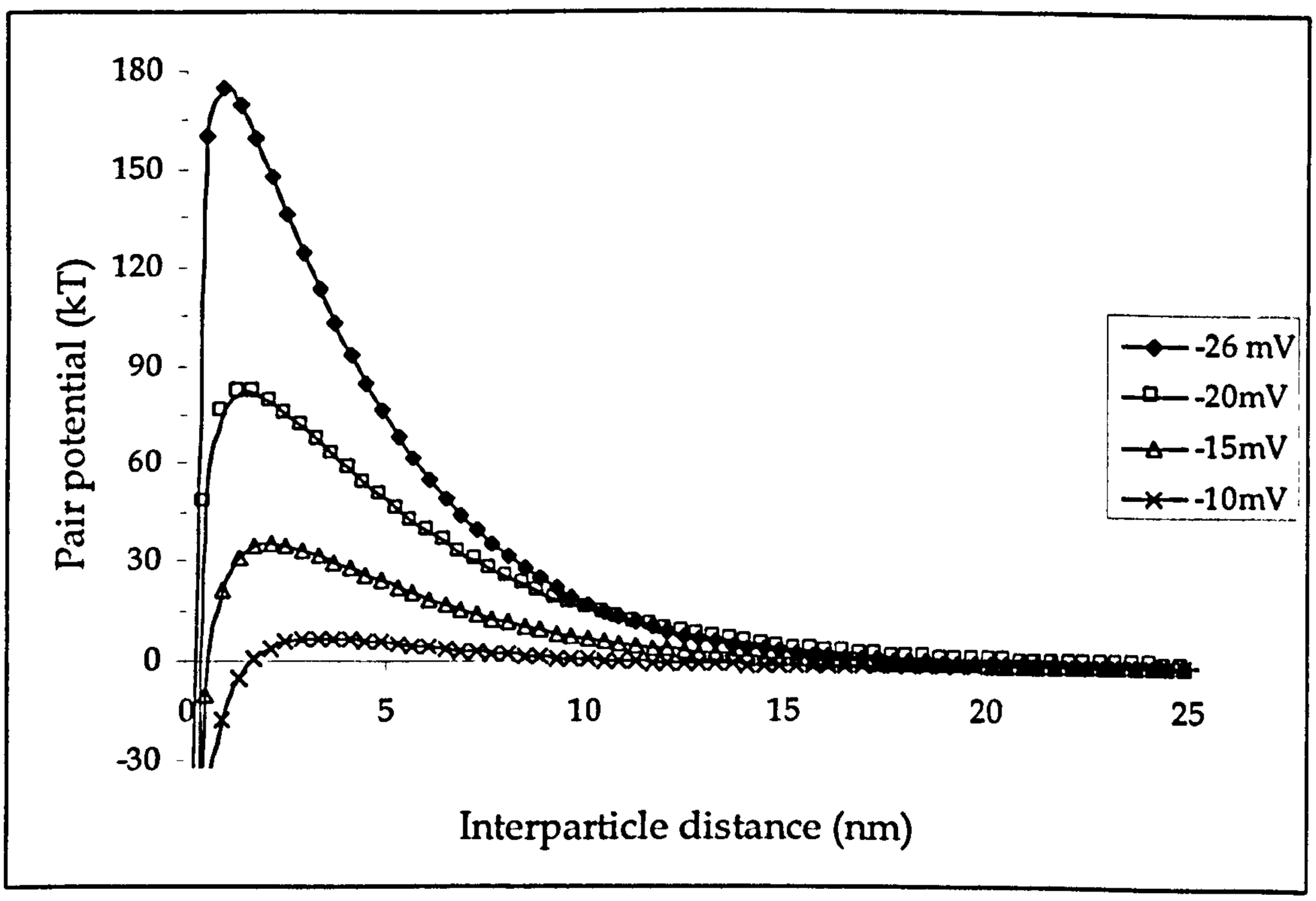

Figure 4.21: Theoretical pair potential curves for different ζ–potentials for PDMS droplets

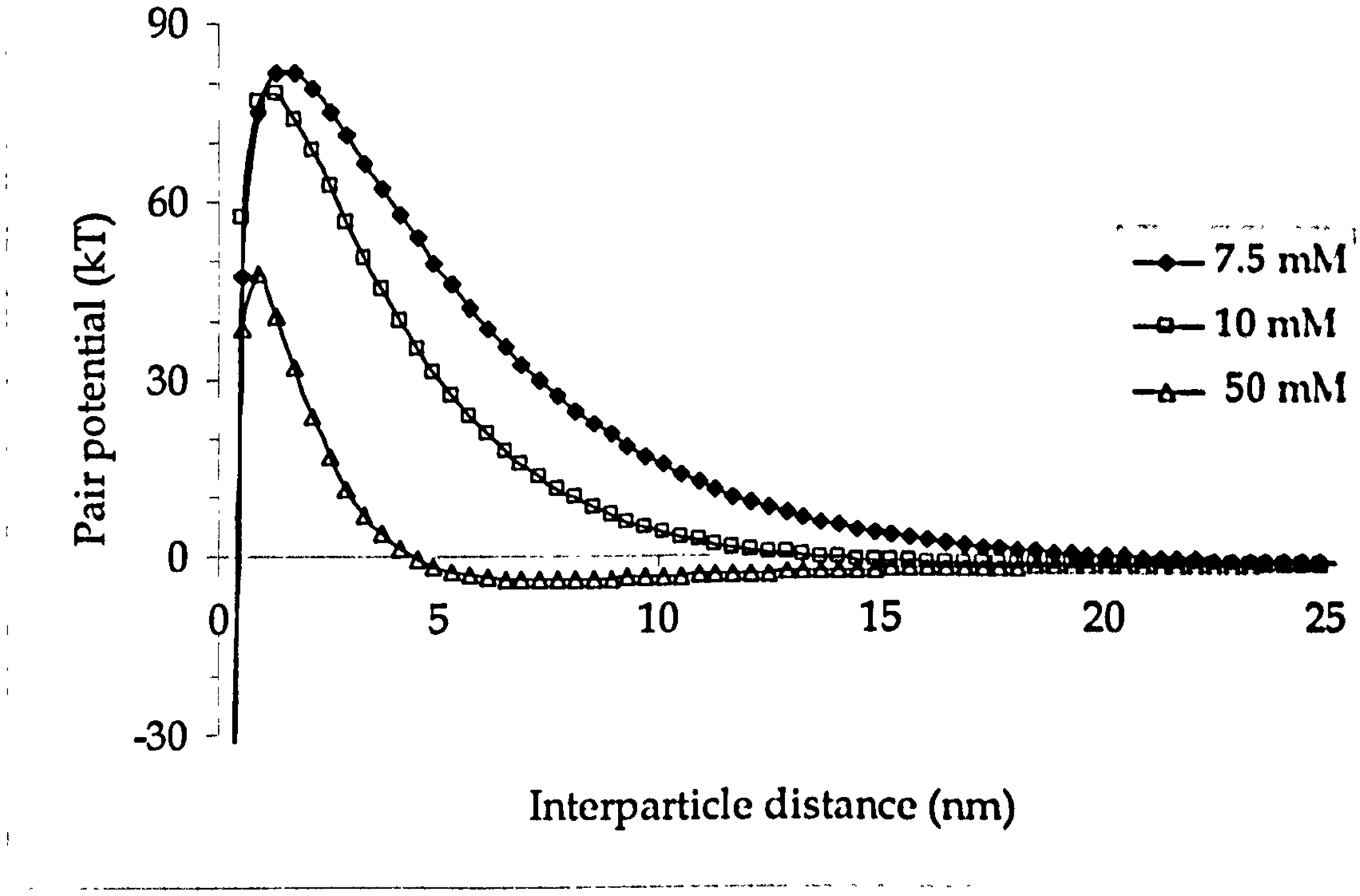

Figure 4.22: Theoretical pair potential curves for different electrolyte concentrations for PDMS droplets of constant zeta–potential

From figure 4.21 it is apparent that a zeta–potential of -26 mV causes a massive energy barrier to coagulation of ~180 kT. The required zeta–potential for a low energy barrier is -10 mV or less, coagulation and hence coalescence should follow for this system.

Calculations have also been made for a PDMS emulsion with a constant zeta–potential but increasing the electrolyte concentration. The pair potentials resulting from the calculation of the emulsion of a given zeta–potential of -20 mV at 7.5×10^{-3}, 1×10^{-2}, and 5×10^{-2} mol dm^{-3} KCl are shown in figure 4.22. Again there is a large maximum at a concentration just above the CCC. At a concentration of one order of magnitude greater than the CCC there is still an appreciable maximum of the order of 50 kT.

4.4.3 Possibilities for deviations from DLVO theory

The DLVO calculations above in section 4.4.1 predict that the emulsions should be stable at electrolyte concentrations above the measured CCC. There are two areas where an error could occur. One is with the measured experimental data and the other is the DLVO calculation. The only possible source of error caused by experimental methods is that the electrophoretic mobility of the emulsion at electrolyte above the CCC may be erroneous due to a change in the droplet size distribution (onset of coagulation and coalescence by thin film thinning).

More likely is an under–estimation of the Hamaker constant (A_{12}) for the system of two PDMS droplets interacting across an aqueous continuous medium. The Hamaker constant has been assessed for D_4, ignoring the linear fraction of higher molecular weight PDMS. It is also therefore, an estimation for emulsions containing high concentrations of cross–linker.

Also not considered here were van der Waals force retardation and screening. As these tend to an over–estimation rather than an under–estimation of the van der Waals force these can also be discounted.

More probable is that there is a considerable hydrophobic interaction which plays an important role in determining the stability of the PDMS emulsions. Droplet distortion, i.e. a flattening of the surace curvature, as two droplets approach can also be responsible for an increased van der Waals attraction at close interdroplet distances.

4.5 References

1. Tadros, Th.F. and Vincent, B., *in* "Encyclopaedia of Emulsion Technology" (P. Beecher, Ed.), Vol. 1, Chap. 3. Marcel Dekker, New York, 1983.

2. Long, J.A., Osmond, D.W.J. and Vincent, B. *Journal of Colloid and Interface Science* **42**, 545 (1973).

3. Sherman, P., *in* "Emulsion Science" (P. Sherman, Ed.), Chap. 3. Academic Press, London, 1968.

4. Parsegian, V. A., Rand, R. P., Fuller, N. L. and Rau, D. C. *Methods in Enzymology* **127**, 400 (1986).

5. Bibette, J., Morse, D.C., Witten, T.A. and Weitz, D.A. *Physical Review Letters* **69**, 2439 (1992).

6. Prouty, M.S., Schecter, A.N. and Parsegian, V.A. *Journal of Molecular Biology* **184**, 517 (1985).

7. Vink, H *European Polymer Journal* **7**, 1411 (1900).

8. Alexandrowicz, J. *Journal of Polymer Science* **40**, 113 (1959).

9. Adams, L.H. *Journal of the American Chemical Society* **37**, 1181 (1915).

10. von Smoluchowski, M. *Zeitschrift fur Physikalische Chemie* **92**, 129 (1918).

11. Henry, D.C. *Procedures of the Royal Society, Series A* **133**, 106 (1931).

12. Ohshima, H., Healy, T.W. and White, L.R. *Journal of the Chemical Society-Faraday Transactions II* **79**, 1613 (1983).

13. O'Brien, R.W. and White, L.R. *Journal of the Chemistry Society-Faraday Transactions II* **74**, 1607 (1978).

14. Ohshima, H. *Advances in Colloid and Interface Science* **62**, 189 (1995).

15. Booth, F. *Journal of Chemical Physics* **19**, 1331 (1951).

16. Levine, S. and O'Brien, R.W. *Journal of Colloid and Interface Science* **43**, 616 (1973).

17. Baygents, J.C. and Saville, D.A. *Journal of the Chemical Society-Faraday Transactions* **87**, 1883 (1991).

18. Miller, J.F., Schatzel, K. and Vincent, B. *Journal of Colloid and Interface Science* **143**, 532 (1991).

19. Petrarch Systems Silanes & Silicones Catalogue, "Silicon Compounds: Register and Review", ABCR GmbH & Co, Karlsruhe, 1987.

20. "CRC Handbook of Chemistry & Physics" (Lide, D.R, Ed.), 75th Edition, CRC Press, London, 1994

21. Hunter, R.J., "Zeta Potential in Colloid Science.", Academic Press, London, 1981.

22. Parks, G. A. *Chemical Reviews* **65**, 177 (1965).

23. Developed by Eastman, J., Bristol University, 1997

24. Clever, H.L. and Taylor, M.L. *Journal of Chemical and Engineering Data* **16**, 91 (1971).

Chapter 5: Swelling of Silicone Microgels by Solvents

5.1 Introduction

Large, 'monodisperse' PDMS droplets (i.e. > 1 μm in diameter) cannot be synthesised (refer to section 3.4.1, figure 3.7 and plate 3.1b) by the conventional method as described in section 3.2.2. One method to produce larger droplets would be to solubilise a second, water–immiscible, solvent with the PDMS droplets.

The swelling of colloidal particles dispersed in water with organic solvents or other low molecular weight species plays an important role in several processes such as emulsion polymerisation, drug delivery or phase–transfer catalysis.

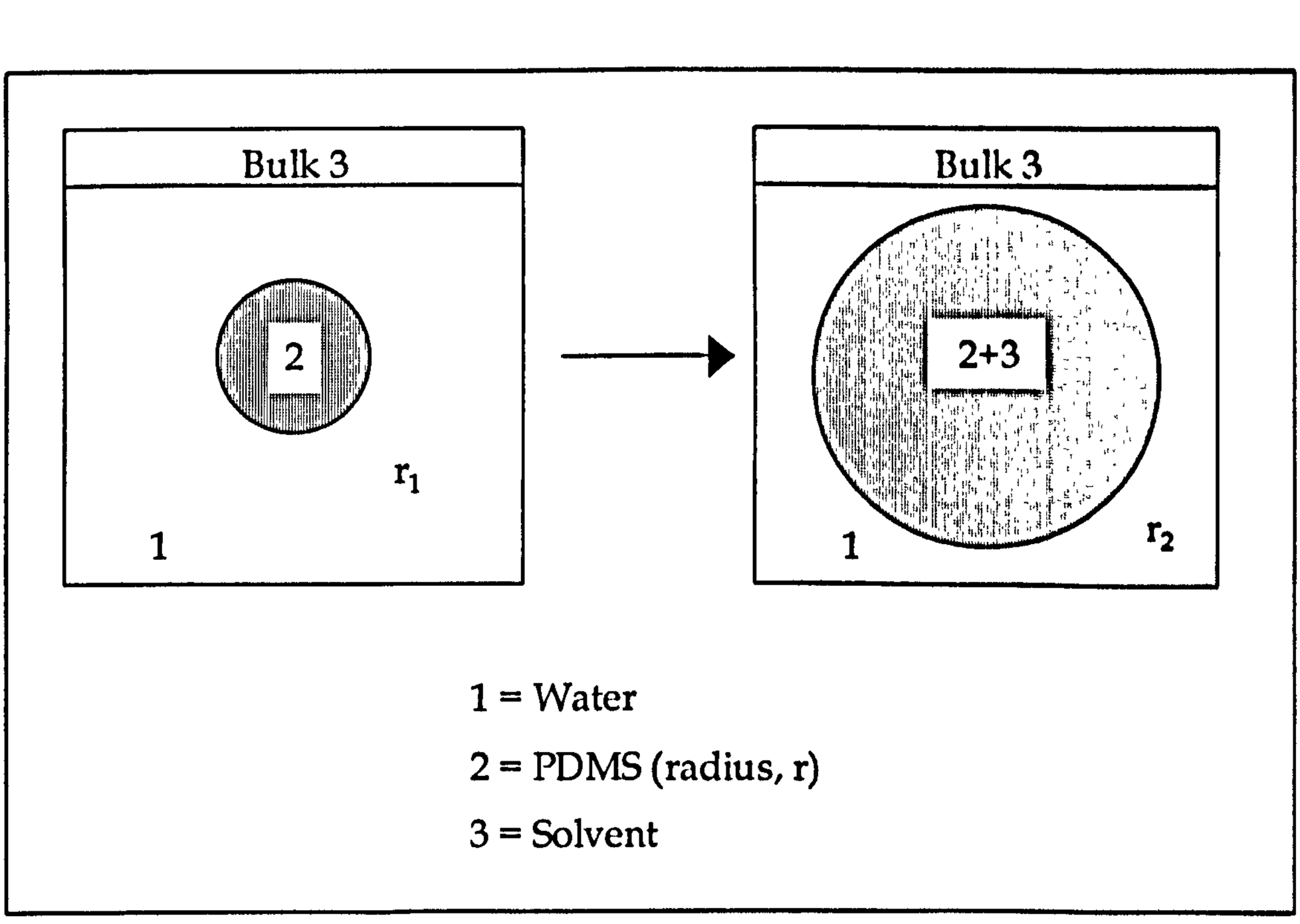

Figure 5.1: Schematic picture of PDMS droplets swelling by hydrocarbon

Figure 5.1 shows a generalised scheme of the swelling process. Solvent (phase 3) is drawn into the droplet (phase 2) from a bulk phase (phase 1) by an osmotic gradient and the droplet expands from an initial radius r_1 to a swollen radius r_2.

The control and stabilisation of the swelling of colloidal particles is of great importance in polymerisation [1]. Studies have been made of the preparation and stabilisation of emulsions of vinyl monomers for suspension polymerisation [2] by an 'activated swelling' method. 'Successive seeded' emulsion polymerisation involving the swelling of a primary polymer particle by monomer [3,4] also utilises an osmotic swelling of colloidal systems.

The first approach to understanding the thermodynamics of the swelling process was made by Morton, Kaizerman and Altier [5]. The swelling of colloidal particles by organic solvents will stop when local thermodynamic equilibrium is reached [3]. Swelling is normally considered to be an equilibrium process leading to a thermodynamically stable state. This refers to the local equilibrium of individual particles and does not reflect the unchanged situation of the overall metastable state of colloidal dispersions.

Equilibrium will be reached when the chemical potential of the solvent molecules inside the droplet (μ_3^2) is equal to the chemical potential of the those in the bulk phase (μ_3^1).

$$\mu_3^{\,2} = \mu_3^{\,1} \qquad 5.1$$

There are three contributions that apply to the chemical potential of the solvent inside the droplet (μ_3^2). The first is the free energy of mixing with PDMS (phase 2) in the droplet. The second is the elastic straining contribution due to a gel–like structure in droplets. Lastly there is an increase in the interfacial free energy as a droplet expands due to the increasing surface area.

5.1.1 Osmotic Swelling of O/W Emulsions

Ostwald ripening may be observed in emulsion droplets of solvents that are relatively soluble in water [6]. If a small amount of a highly water–insoluble second oil (compound 2) is added to a droplet of the more water–soluble oil (compound 1), the stability towards Ostwald ripening is greatly increased [2,5,7]. The transfer of partially water–soluble oil molecules out of the droplet containing a second highly insoluble, oil is greatly reduced, because any such transfer increases the osmotic pressure inside the droplet. Provided compound 2 does not itself transfer out of the droplet into the aqueous phase to any degree, equilibrium will be maintained inside the droplet.

At equilibrium, the increased interfacial area balances the osmotic swelling pressure of the solvent in the PDMS droplet. Morton, Kaizerman and Altier [5] considered a swollen particle in equilibrium with free solvent and described the molar free energy of the solvent ($\Delta\bar{G}_3$) together with the osmotic contribution ($\Delta\bar{G}_{m3}$) and the interfacial free energy contribution ($\Delta\bar{G}_{i3}$). This result is the 'MKA' equation:

$$RT\left(\ln(1-\phi_2)+(1-\frac{1}{DP})\phi_2+\phi_2^2\chi+\frac{2V_3\gamma}{rRT}\right)=\Delta\bar{G}_3 \qquad 5.2$$

where ϕ_2 is the volume fraction of compound 2 in the droplet, DP is the number–average degree of polymerisation of compound 2 (a liquid polymer in the case of a PDMS droplet), γ is the interfacial tension of the swollen particle to water, V_3 is the molar volume of the solvent and χ is the Flory–Huggins interaction parameter. The left–hand side of equation 5.2 is the standard expression of the Flory–Huggins theory [7] of polymer/solvent solutions together with a term describing the interfacial free energy due to swelling between the colloidal particle and water.

The increase of the interfacial energy due to swelling is expressed as $\gamma dA = 8\pi r\, dr\gamma$ with A as the swollen droplet surface area. The volume increase

can be expressed either as $4\pi r^2 dr$ or $dn_3 \times M_3/\rho_3$ where n_3 is the number of solvent molecules imbibed by the droplet, M_3 is the molecular weight of the solvent, and ρ_3 is the solvent density. Since M_3/ρ_3 is equal to the molar volume of solvent and $8\pi r\, dr\gamma = 2V_3(\gamma/r)$ it follows that $\Delta\bar{G}_{t3}=2V_3(\gamma/rRT)$. The radius of a swollen droplet is thus predicted for a given value of ϕ_2, χ, V_3 and γ. Equation 5.2 is depicted as a graph of the free energy of the solvent inside a swelling droplet in figure 5.2, for a PDMS droplet swelling by n-heptane (χ = 0.49 [8]). The swelling is denoted by the ratio of the volume of the swollen droplet ($V_{swollen}$) to the initial droplet volume (V_o).

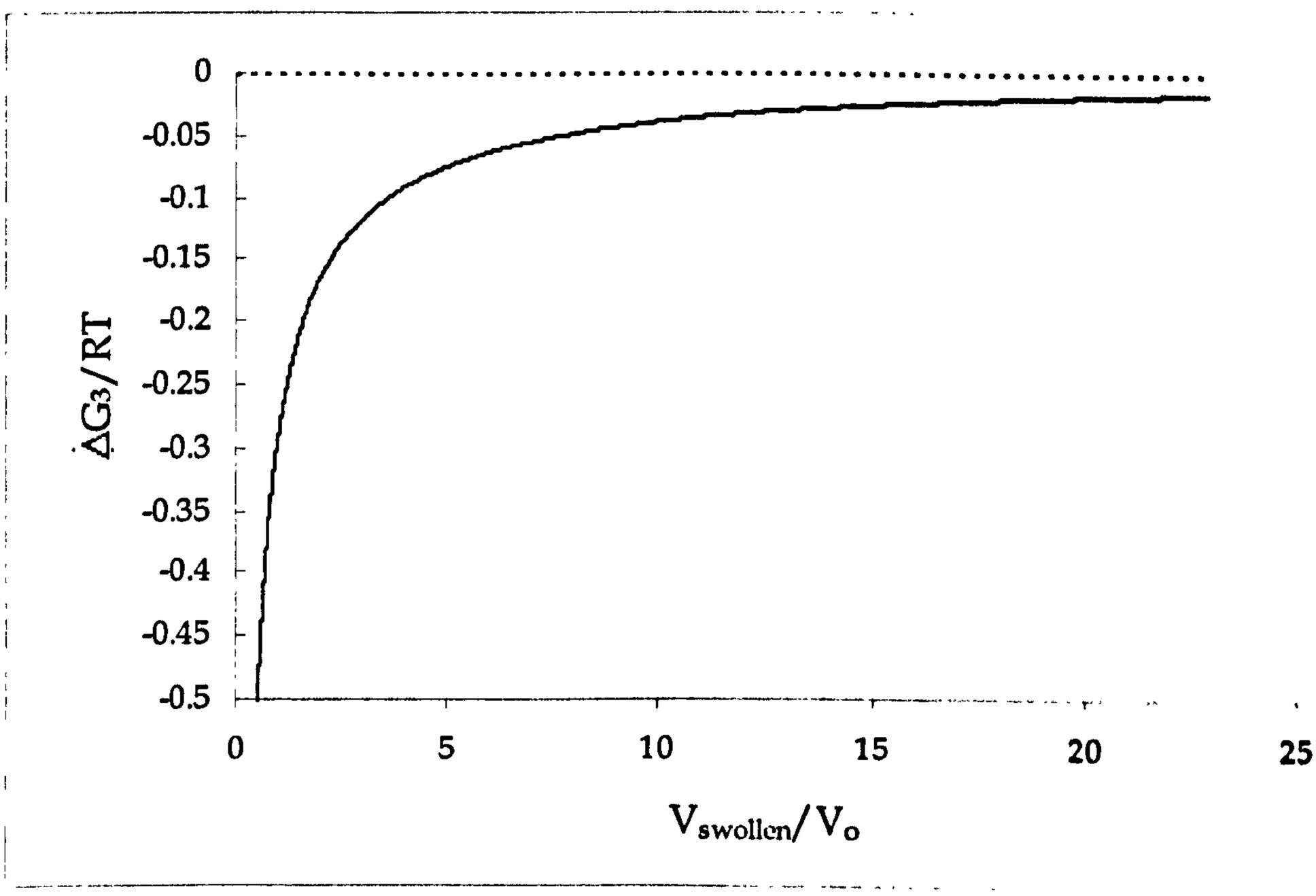

Figure 5.2: The partial free molar energy of solvent in a swelling droplet

$\Delta\bar{G}_3$ does not reach zero in figure 5.2. Equation 5.2 predicts swelling *ad finitum* for a pure, liquid drop swelling with solvent. Eventually the droplet will no longer be stable with respect to coalescence. This is because the charge density will drop as the area per molecule increases for any absorbed stabilising molecules (surfactant, polymer, *in–situ* PDMS etc.).

5.1.2 Osmotic swelling of cross–linked PDMS droplets

The considerations in section 5.1.1 are for liquid droplets consisting of oligomeric molecules of well–defined molecular weight. The situation changes on addition of cross–linking monomer into the polymer. Although the droplets are still fluid in nature at low cross–linker concentrations, at higher concentrations they become increasingly gel–like (refer to section 3.4.2, figure 3.11).

In these cases the major limiting factor to osmotically driven swelling is the effect of restraining elastic energy inside the droplets. Due to the tight gel network, which stores elastic energy when expanded, the maximum size attainable will be reduced. The swelling of cross–linked gel networks has been considered, among others, by Flory [7] and Stauff [9]. With cross–linked polymer in a PDMS droplet an additional term, ϕ^*_2, is required to describe the volume fraction of cross–linked PDMS ($1/DP \approx 0$) in the droplet. In PDMS droplets with low cross–linker concentration there will still be an appreciable amount of free, oligomeric PDMS (volume fraction, ϕ_2).

As a gel network is swollen by absorption of solvent the chains between cross–linking sites assume elongated conformations and an elastic straining force develops in opposition to the swelling process. As swelling proceeds the osmotic driving force decreases, but the elastic force increases. Therefore a state of swelling equilibrium between these two forces is reached. The elastic straining force can be interpreted as a de–swelling pressure acting on the swollen gel. This pressure is sufficient to increase the chemical potential of the solvent in the gel until it equals that of the solvent outside. The chemical potential is given by (for $(\phi_2 + \phi^*_2) << 0$):

$$\frac{\mu_3^a - \mu_3^b}{RT} = \ln(1-\phi_2) + \varphi_2^* + \chi\phi_2^2 + 2V_3\left(\frac{x}{V_o}\right)\left(\phi_2^{*1/3} - \frac{\phi_2^*}{2}\right) + \frac{2V_3\gamma}{rRT} \qquad 5.3$$

Where V_o is the initial volume of the unswollen droplet and x is the number of moles of cross–links in the droplet.

5.2 Swelling of PDMS Emulsions By Solvent: Experimental

PDMS emulsions, (at an initial monomer concentration of 0.01 v/v), containing different concentrations of cross–linking monomer (MTES), were mixed with various water–immiscible organic solvents. The emulsions used were either dialysed or undialysed. The experiments were performed 18 hours after initiation of polymerisation. Typically 20 mL of PDMS emulsion was mixed with 0.2 mL of solvent. The solvents used in the swelling experiments included n–heptane, n–octane, n–dodecane, cyclohexane, n–octanol, toluene, styrene, 1,1,1–trichloroethane, DMDES, PDMS (mol. wt. 550 g mol^{-1}) and PDMS (mol. wt. 28000 g mol^{-1}). To ensure efficient mixing throughout the experiments, the sealed vials were placed on a rotary tumbler. At regular intervals the average droplet size and polydispersity were measured using PCS (refer to section 3.3). Certain samples, which required dilution prior to measurement, were diluted by water saturated with the relevant swelling solvent. Problems arose when emulsions swollen by certain molecules (styrene and toluene) appeared to de–swell on dilution which made accurate measurement of the droplet size difficult.

Both dialysed and undialysed emulsions were swollen for up to 3 weeks. As a control experiment the size and polydispersity of equivalent tumbled emulsions, without additional oil, were also monitored throughout the experiment.

Black and white photographs of the swollen emulsions were taken using the Nikon 'Optiphot' optical microscope with a Nikon FX–35 camera and a × 40 long focal distance lens, two of which are shown in plate 5.1.

5.3 Swelling of PDMS Emulsions By Solvent: Results

5.3.1 Swelling by n-heptane

Figure 5.3 shows the droplet sizes of undialysed cross-linked PDMS emulsions swollen by n-heptane (refer also to plate 5.1a).

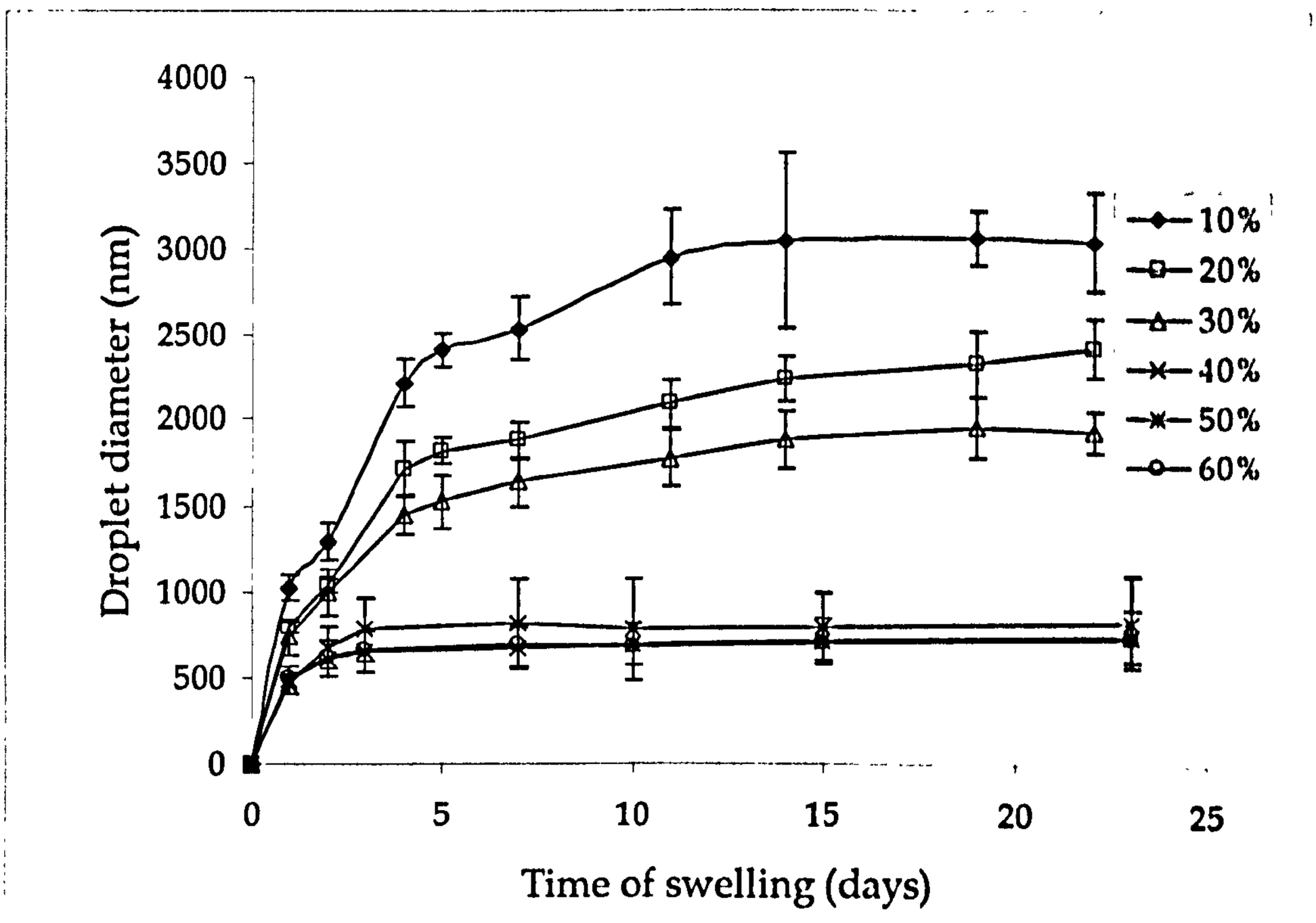

Figure 5.3: Size of PDMS emulsion droplets swollen by n-heptane as a function of swelling time for various concentrations of cross-linker

Figure 5.3 shows an apparent tripling of the initial average droplet diameter of the 10% MTES PDMS emulsion. The increasingly gel-like behaviour of the higher cross-linked emulsions is demonstrated by the restricted swelling apparent for the 40%, 50% and 60% v/v MTES in DMDES

droplets. These do not swell as much as droplets containing lower concentrations of cross-linker. This observation suggests that the presence of an elastic gel network limits the swelling. The polydispersities of the lower % MTES emulsions stayed consistently below 10%. The emulsions are not coalescing or undergoing Ostwald ripening.

A plot of the increase in volume (from the starting volume, V_o) shows how much n-heptane the swollen droplets apparently consist of.

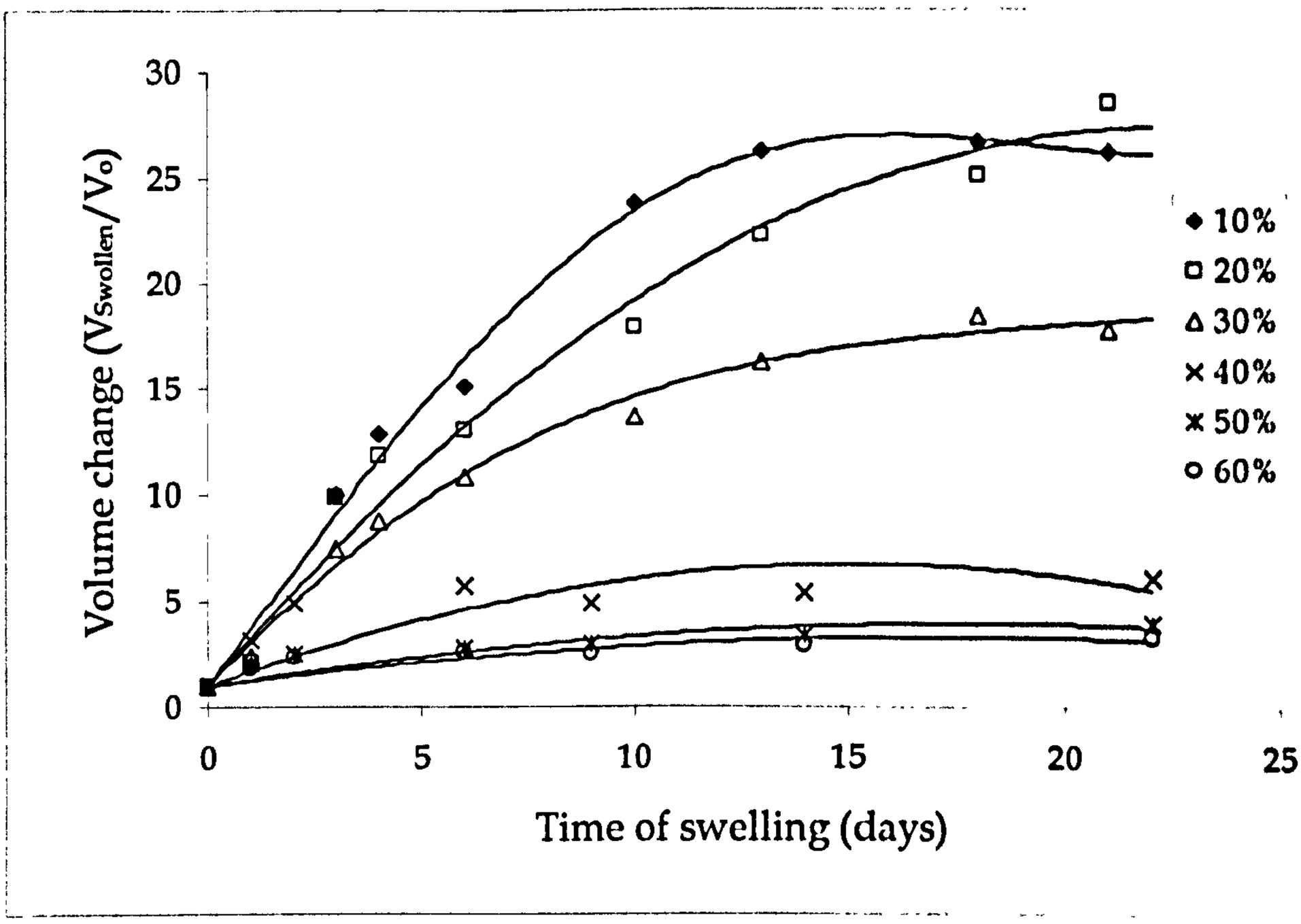

Figure 5.4: Increase in volume of n-heptane in swollen PDMS emulsion drops as a function of swelling time for various concentrations of cross-linker

The volume of the most swollen droplet is almost 30 times greater than the starting volume. This suggests that the droplet is 97% by volume n-heptane in composition. Even the more highly cross-linked emulsions more than doubled their size.

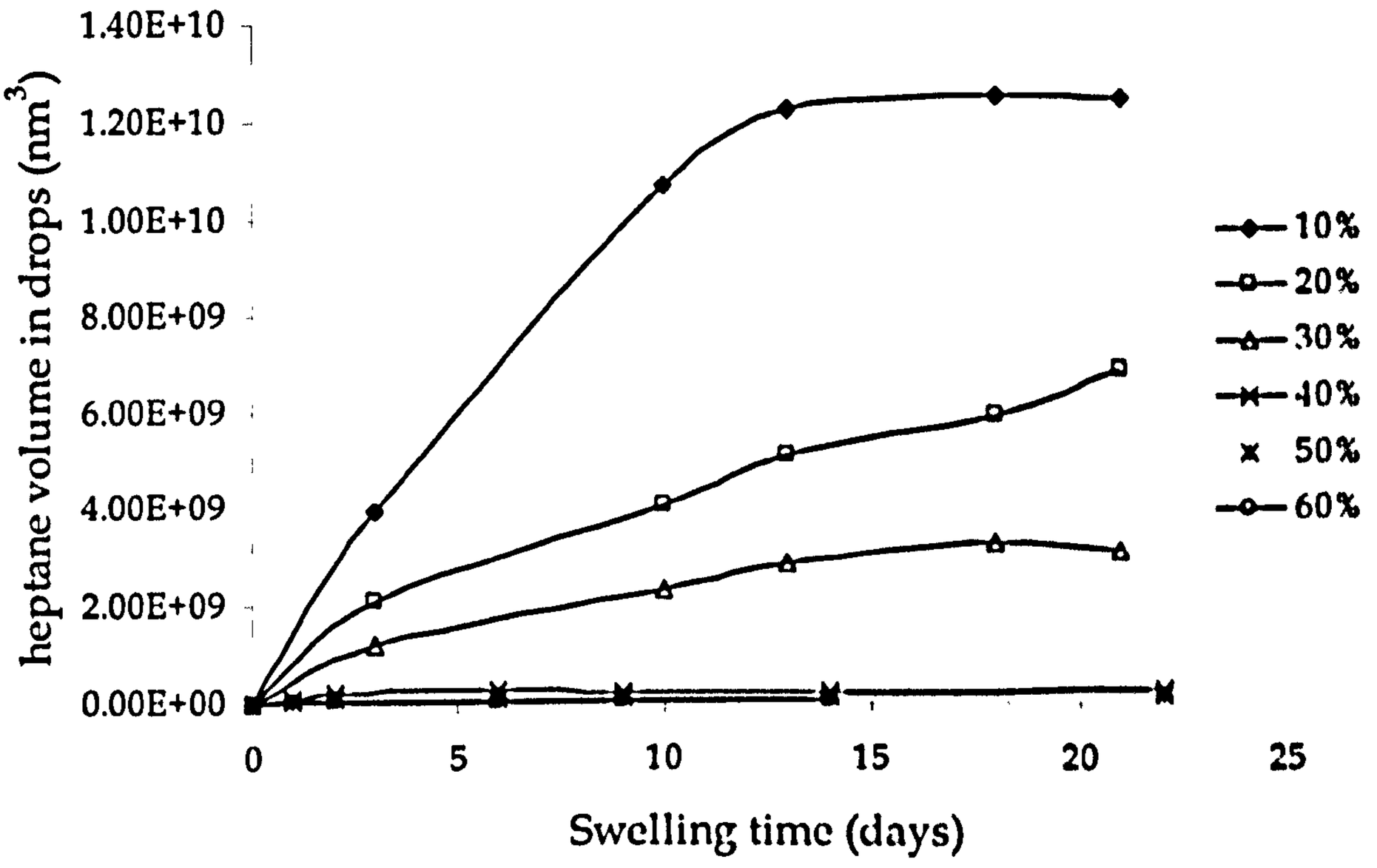

Figure 5.5: Actual volume of n–heptane in swollen PDMS droplets as a function of swelling time for various concentrations of cross–linker

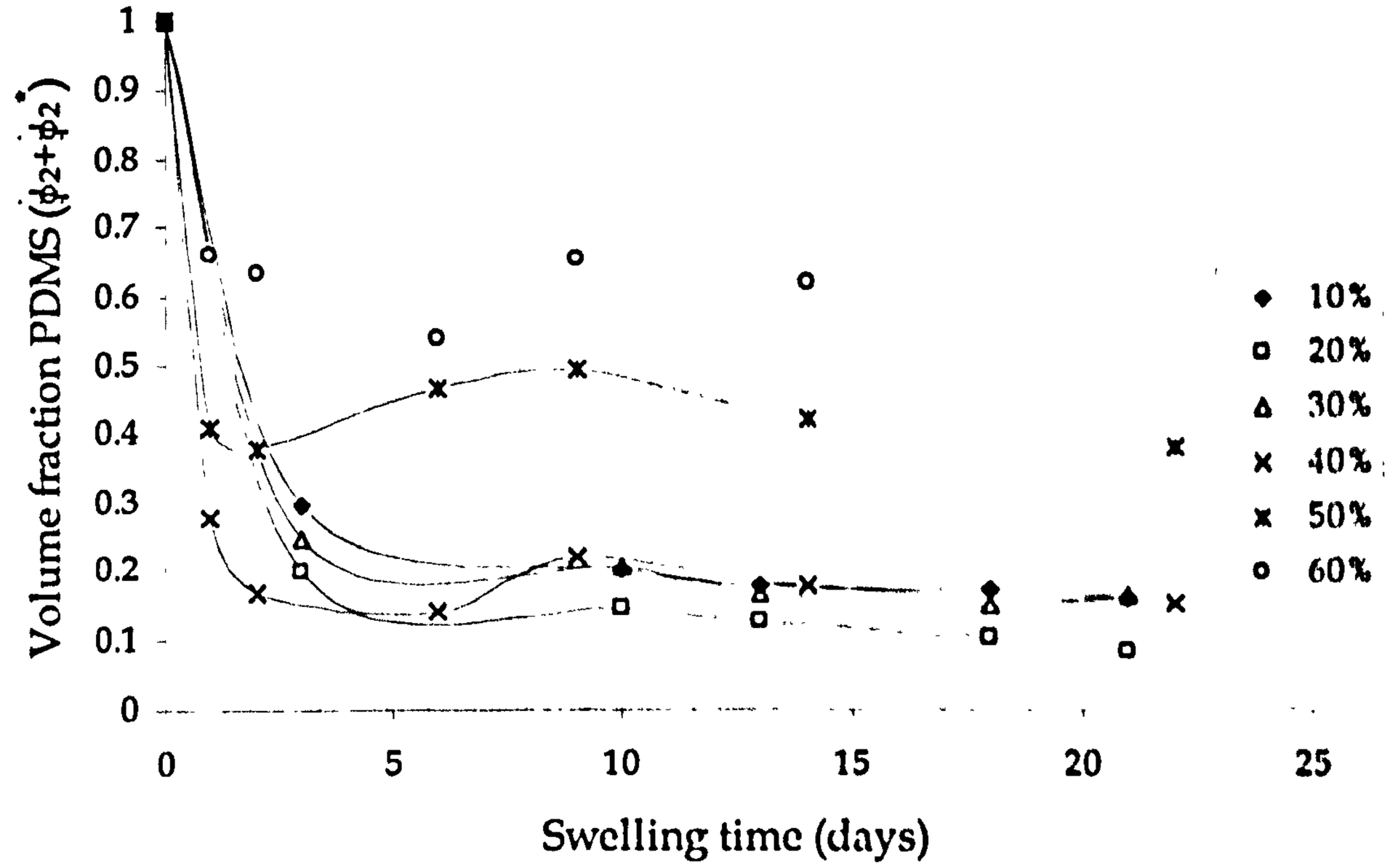

Figure 5.6: The volume fraction of PDMS in n–heptane swollen PDMS droplets as a function of swelling time for various concentrations of cross–linker

Using the data shown in graph 3.9 of section 3.4.1 for the growth of the undialysed emulsion droplets as a control experiment it is possible to calculate the volume of n–heptane imbibed by each PDMS droplet, and hence, the exact volume fraction of PDMS in the swollen droplets. The assumption is made that the droplets continue to swell with PDMS concurrently as well as by n–heptane to the same extent as in the control experiment.

Figure 5.5 shows the actual quantity of n–heptane absorbed into each droplet. It is clear that the lower the concentration of cross–linker in the PDMS the greater the amount of solvent that can be absorbed.

Figure 5.6 shows the volume fraction of PDMS as the droplets swell. Regardless of cross–linker concentration the swelling initially results in an immediate decrease in ϕ_2. The rate of decrease of ϕ_2 slows as swelling proceeds to a limiting value typically between 0.1 and 0.2 for all cross–linker concentrations below 40 % v/v MTES. Only at concentrations greater than 40% v/v MTES does there appear to be an effect of the concentration of cross–linker on the equilibrium value of ϕ_2.

Figures 5.3 to 5.6 show swelling data for PDMS emulsions continuously mixed with an excess of n–heptane using a rotary mixer. Emulsion swelling occurs by diffusion, therefore the need for agitation of the mixture should not be necessary. Figure 5.7 is a plot over a period of time for a 'standing' PDMS emulsion (with no cross–linker) with excess n–heptane. In this system diffusion is the only possible mechanism of swelling of the droplets, as there is no mechanical agitation.

The measured polydispersity of the solvent–swollen droplets was below 10% for all measurements made up to about 22 hours. The polydispersity after 22 hours was very high, (1857 ± 522 nm), and the intensity of the scattered light was very low as well. This can be attributed to the fact that the droplets cream rapidly, or coalesce with the excess n–heptane–water interface. The rate of creaming is enhanced by the increase in the density difference with water and the increase in size of the PDMS droplets swollen by n–heptane (refer to section 2.2.1 on emulsion creaming). As a result the

number density of droplets in the sample cell was insufficient for meaningful light scattering data to be recorded. This creaming is eliminated when the emulsions are tumbled on the rotary mixer. Hence, all swelling experiments were performed using the rotary tumbler to eliminate any creaming instability.

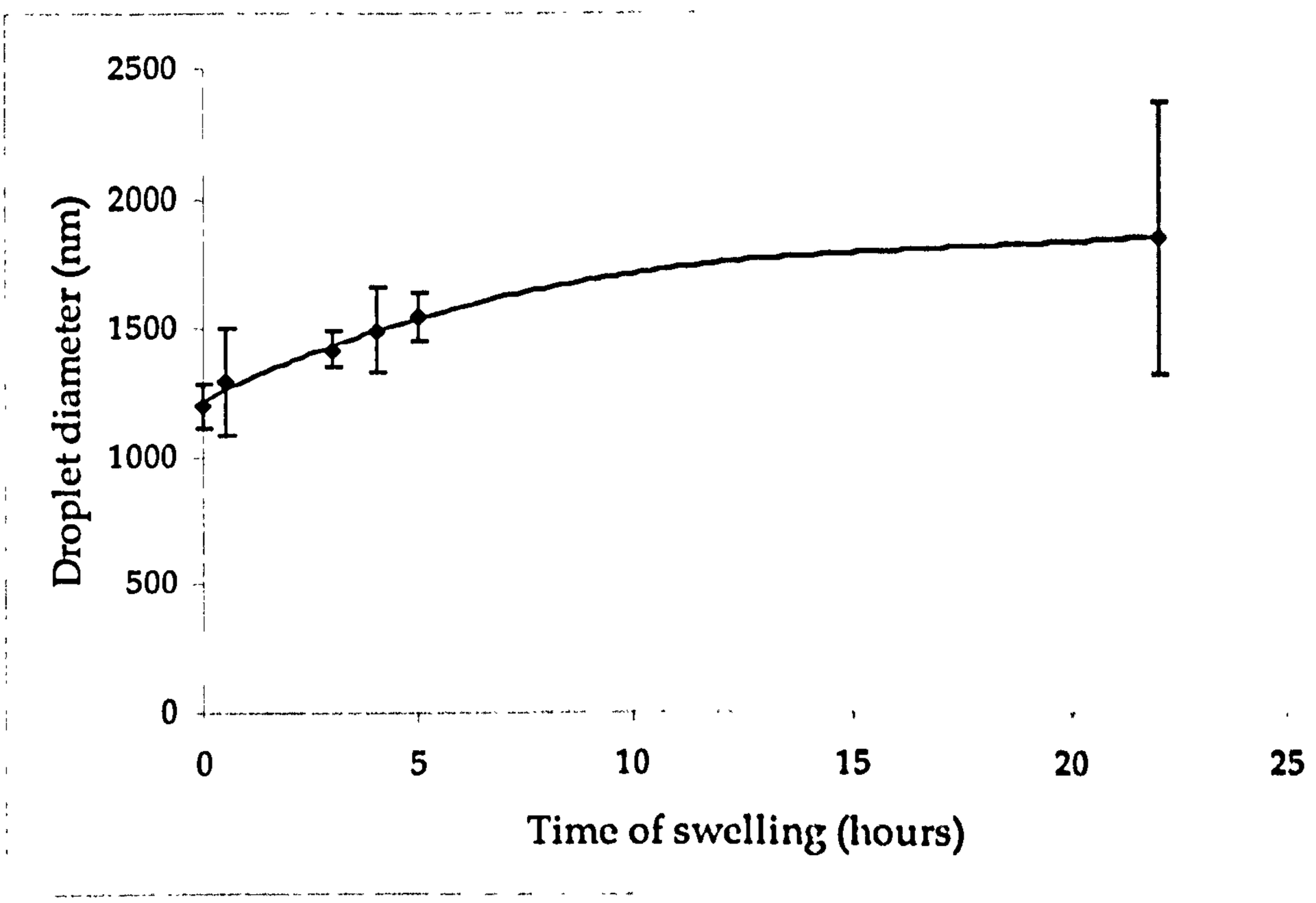

Figure 5.7: Size of PDMS droplets swollen by n-heptane as a function of swelling time by 'standing' diffusion

(a)

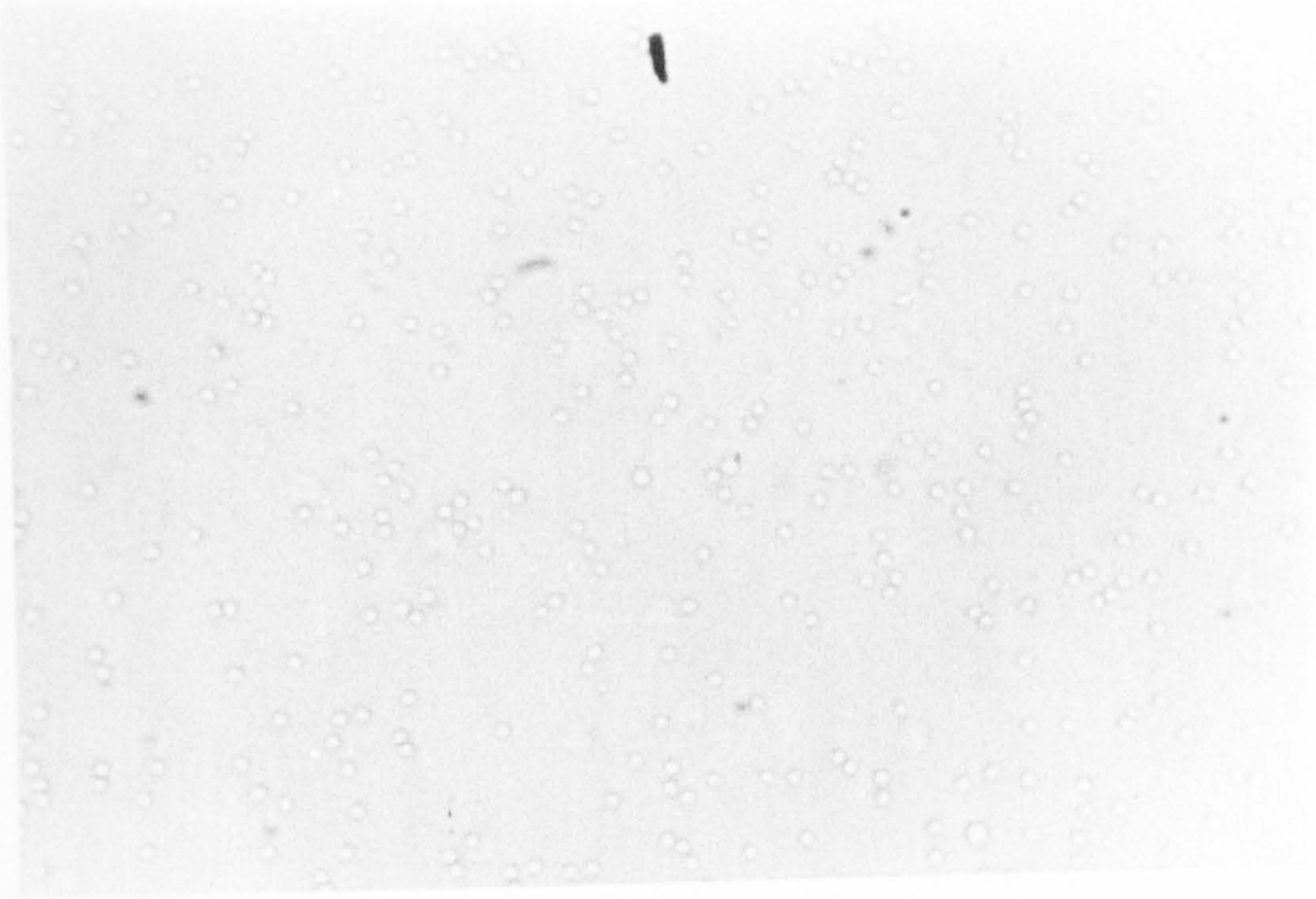

(b)

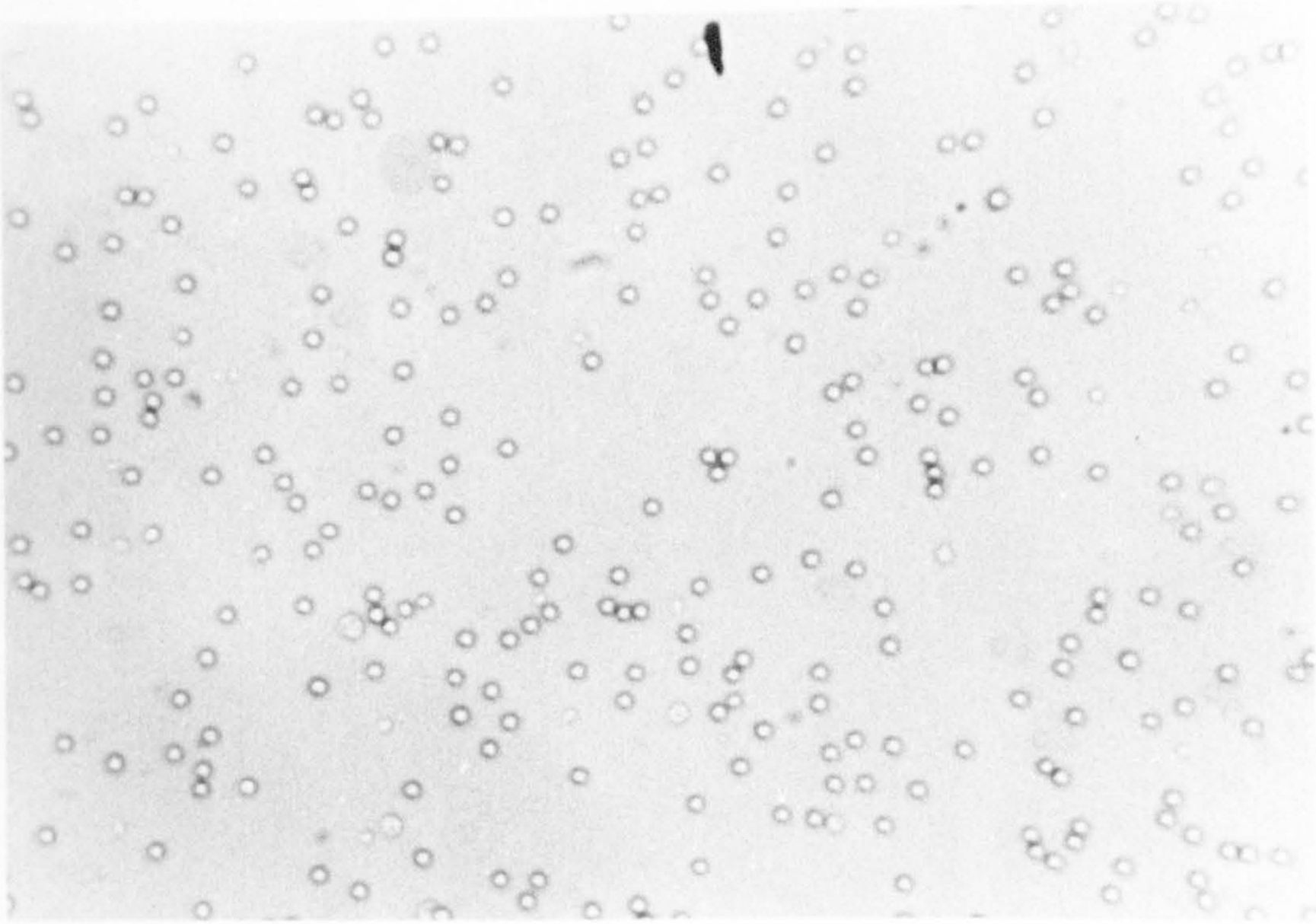

Plate 5.1 (a): 0.01 v/v PDMS + n–heptane emulsion (diameter = 2220 ± 190 nm)

(b): 0.04 v/v PDMS + toluene emulsion (diameter = 2440 ± 580 nm)

5.3.2 Swelling by other solvents

Increasing the amount of swelling solvent added to the PDMS emulsion enhances both the rate and the extent of swelling. The swelling is dependent on the solubility in the aqueous phase and the rate of diffusion into the droplets. The higher the solvent concentration, up to the saturation point in water, the quicker it will repartition into the droplets. Some solvents are more soluble in water than others, some are better solvents for PDMS than others. By examining the swelling rates from a range of solvents the effects of solvent type can be seen.

Other solvents used for swelling of PDMS emulsions included n–octane, cyclohexane, 1,1,1–trichloroethane, toluene, styrene, n–octanol, n–dodecane, dimethyldiethoxysilane and PDMS. An example of a PDMS emulsion swollen by toluene is shown in plate 5.1 (b). The droplets are much larger but remain 'monodisperse' in appearance. The toluene–swollen droplets are larger than the equivalent n–heptane swollen droplets in plate 5.1 (a) suggesting that toluene is a better swelling solvent.

Some solvents proved better at swelling the droplets than others. The solvents that produced data most similar to n–heptane were n–octane and cyclohexane. The data from these swelling experiments is shown in figures 5.8 and 5.9. Data from swelling by DMDES (i.e. adding more starting monomer after initial synthesis of droplets had occurred) and styrene is shown in figures 5.10 and 5.11. Finally data showing the total PDMS volume fraction of droplets swollen by n–octanol and n–octane is shown in figures 5.12 and 5.13.

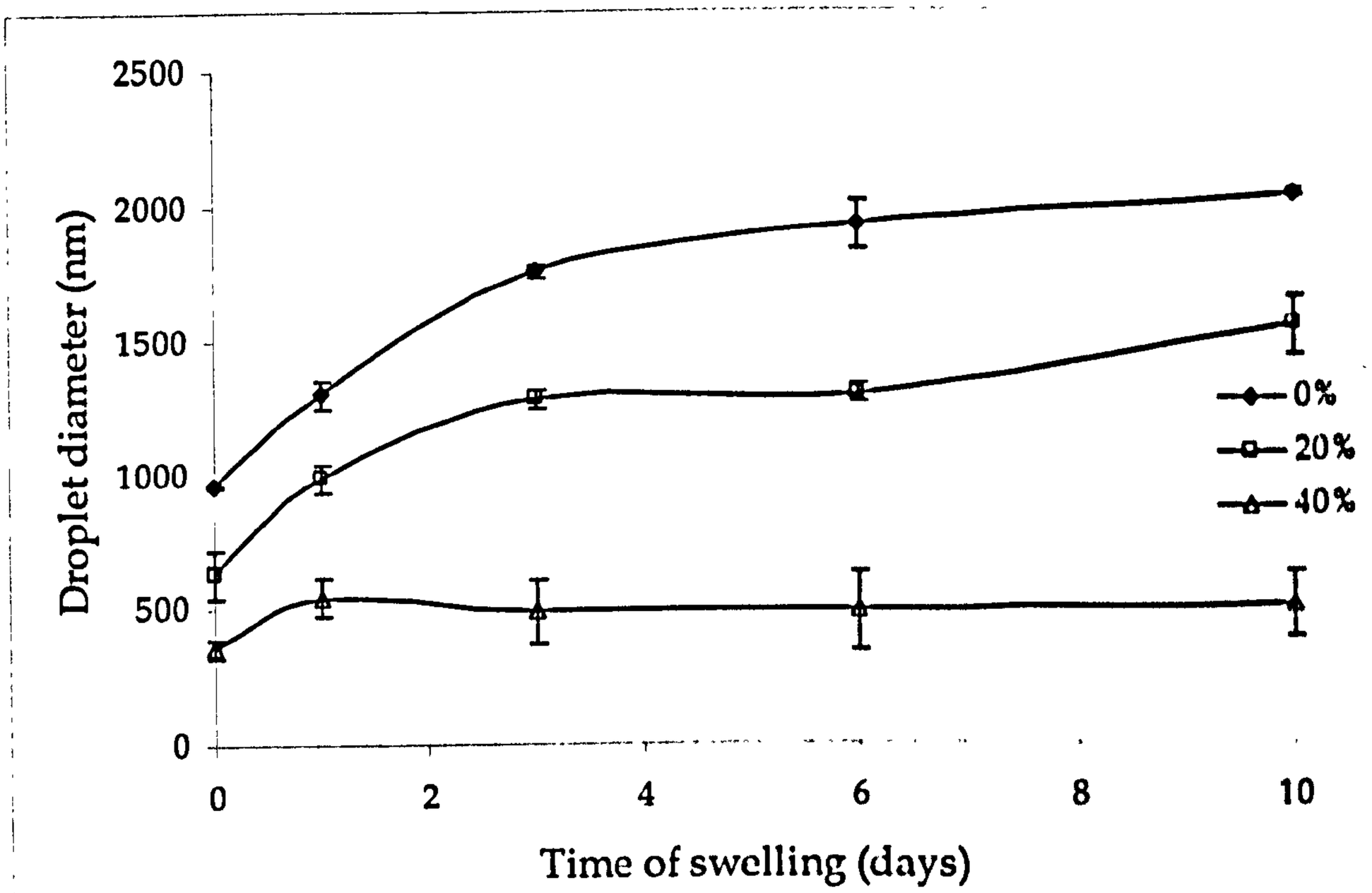

Figure 5.8: Size of PDMS droplets swollen by n-octane as a function of swelling time for various concentrations of cross-linker

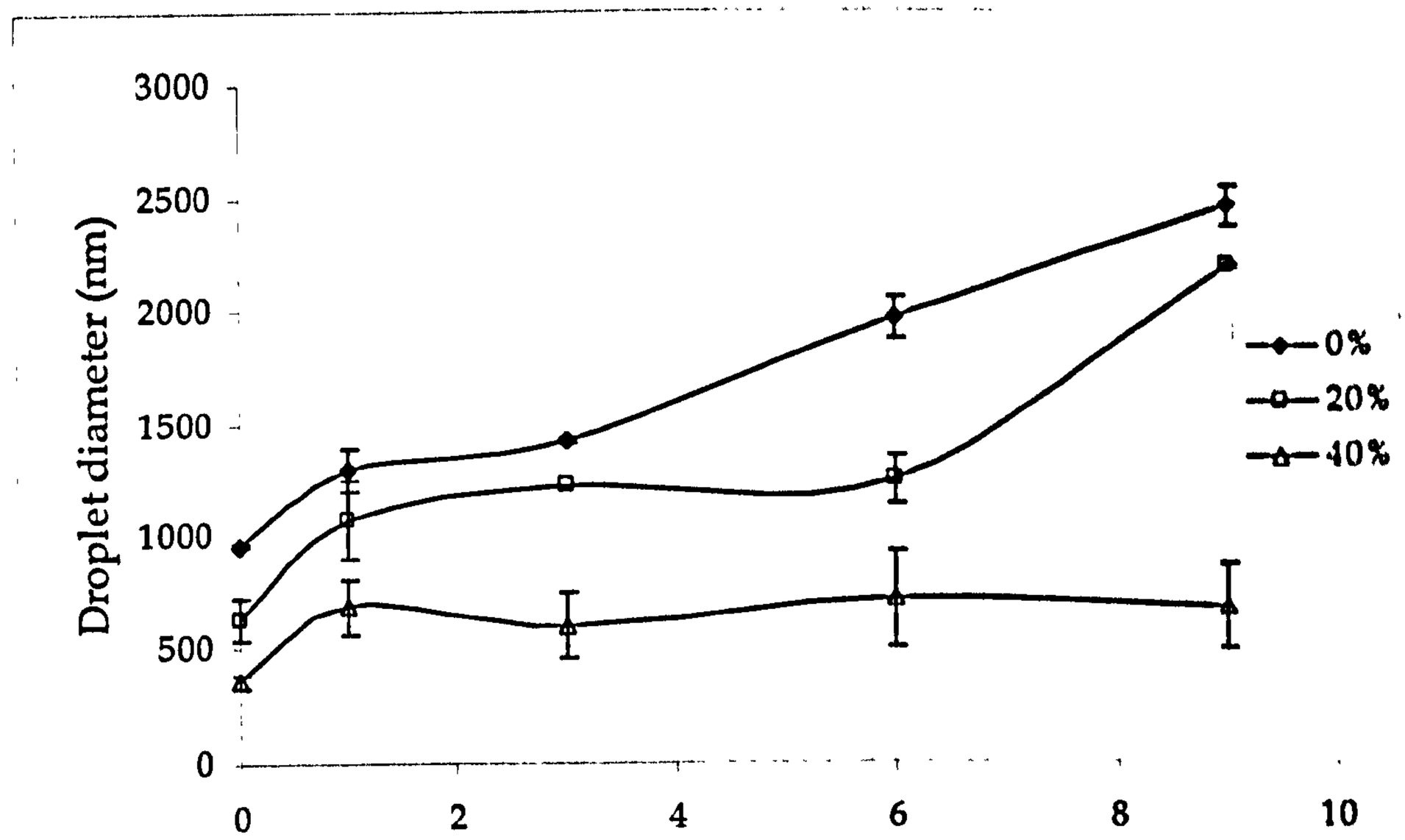

Figure 5.9: Size of PDMS droplets swollen by cyclohexane as a function of swelling time for various concentrations of cross-linker

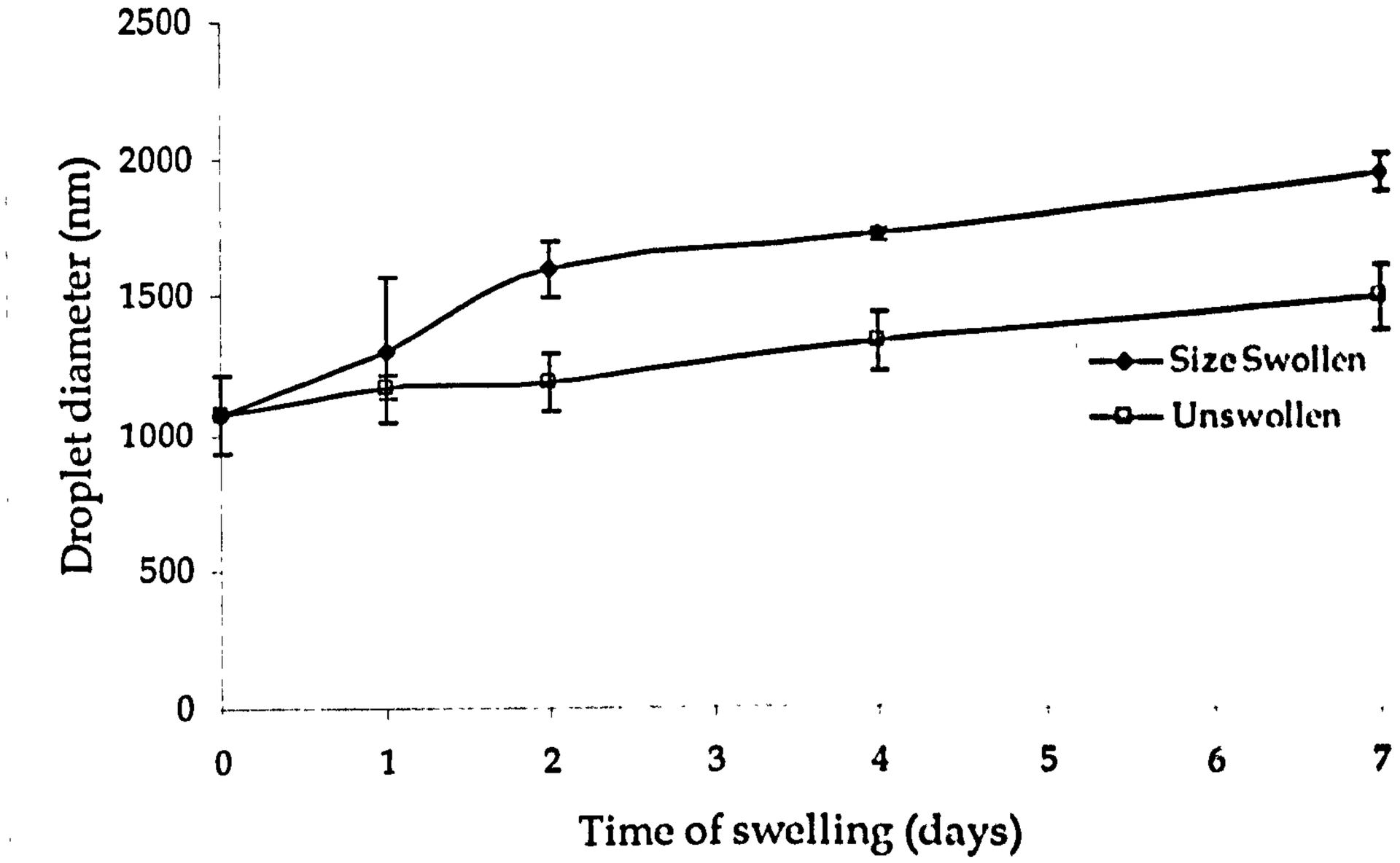

Figure 5.10: Size of PDMS droplets swollen by dimethyldiethoxysilane as a function of swelling time for various concentrations of cross-linker

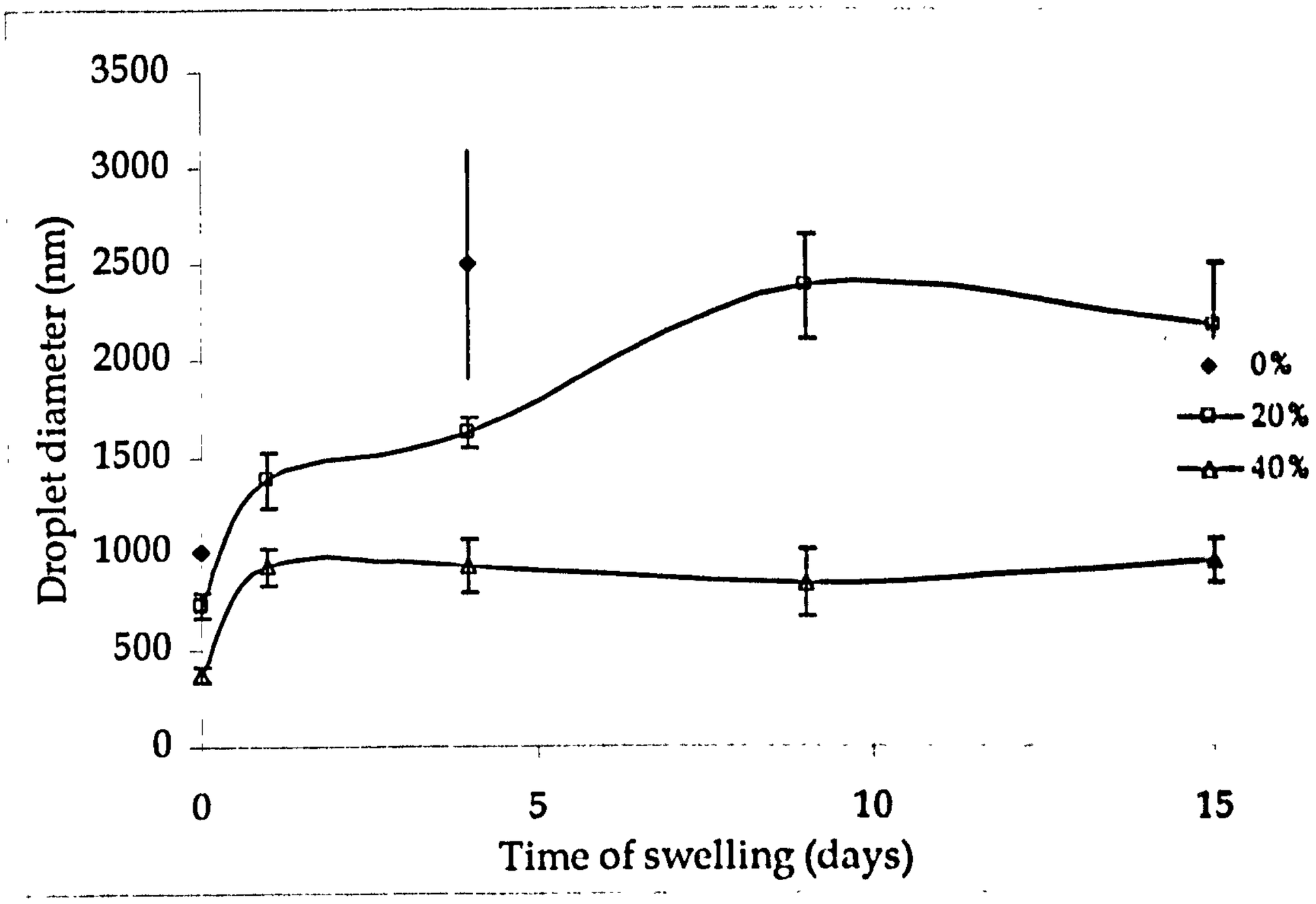

Figure 5.11: Size of PDMS droplets swollen by styrene as a function of swelling time for various concentrations of cross-linker

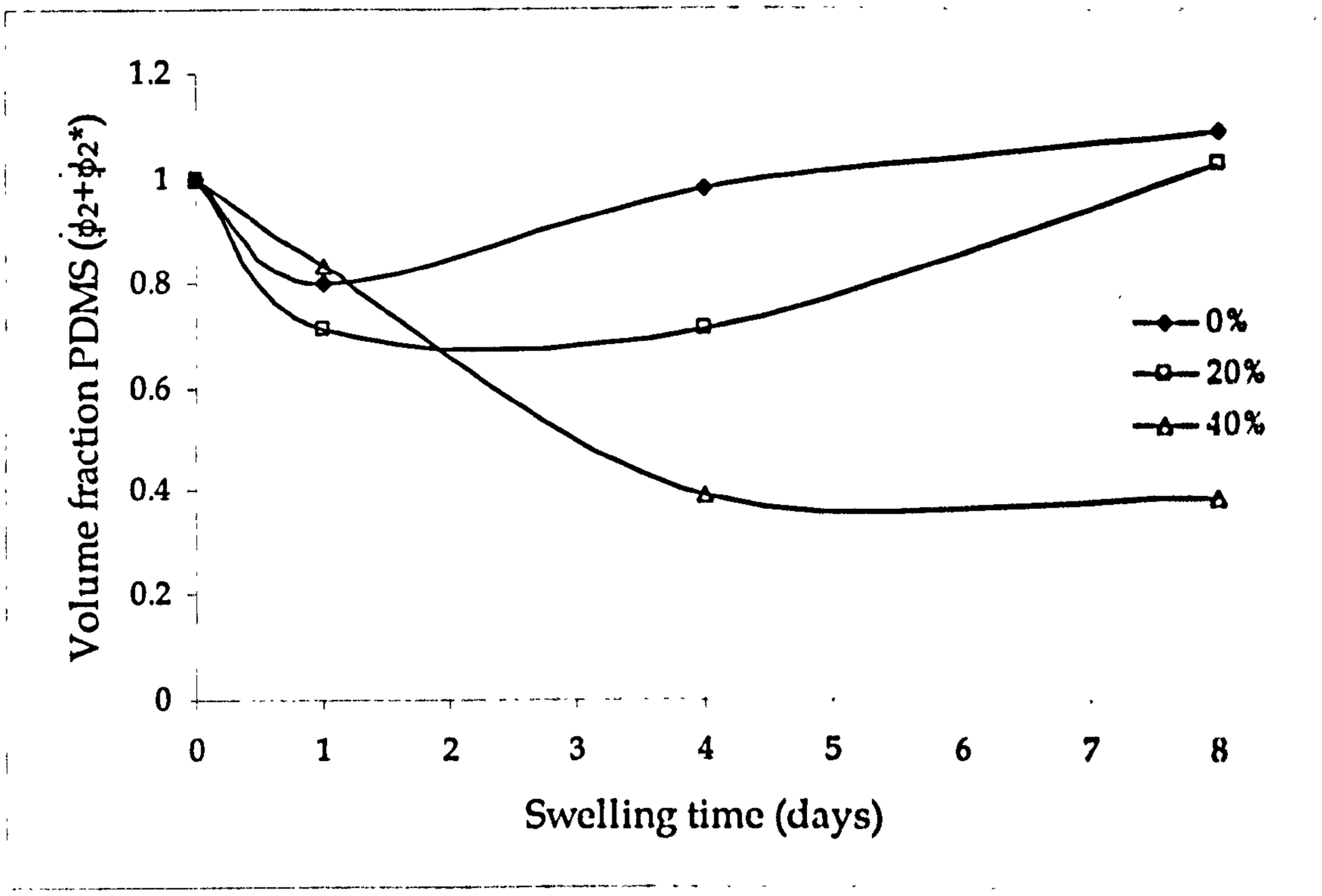

Figure 5.12: Volume fraction of PDMS in n–octanol swollen droplets as a function of swelling time for various concentrations of cross–linker

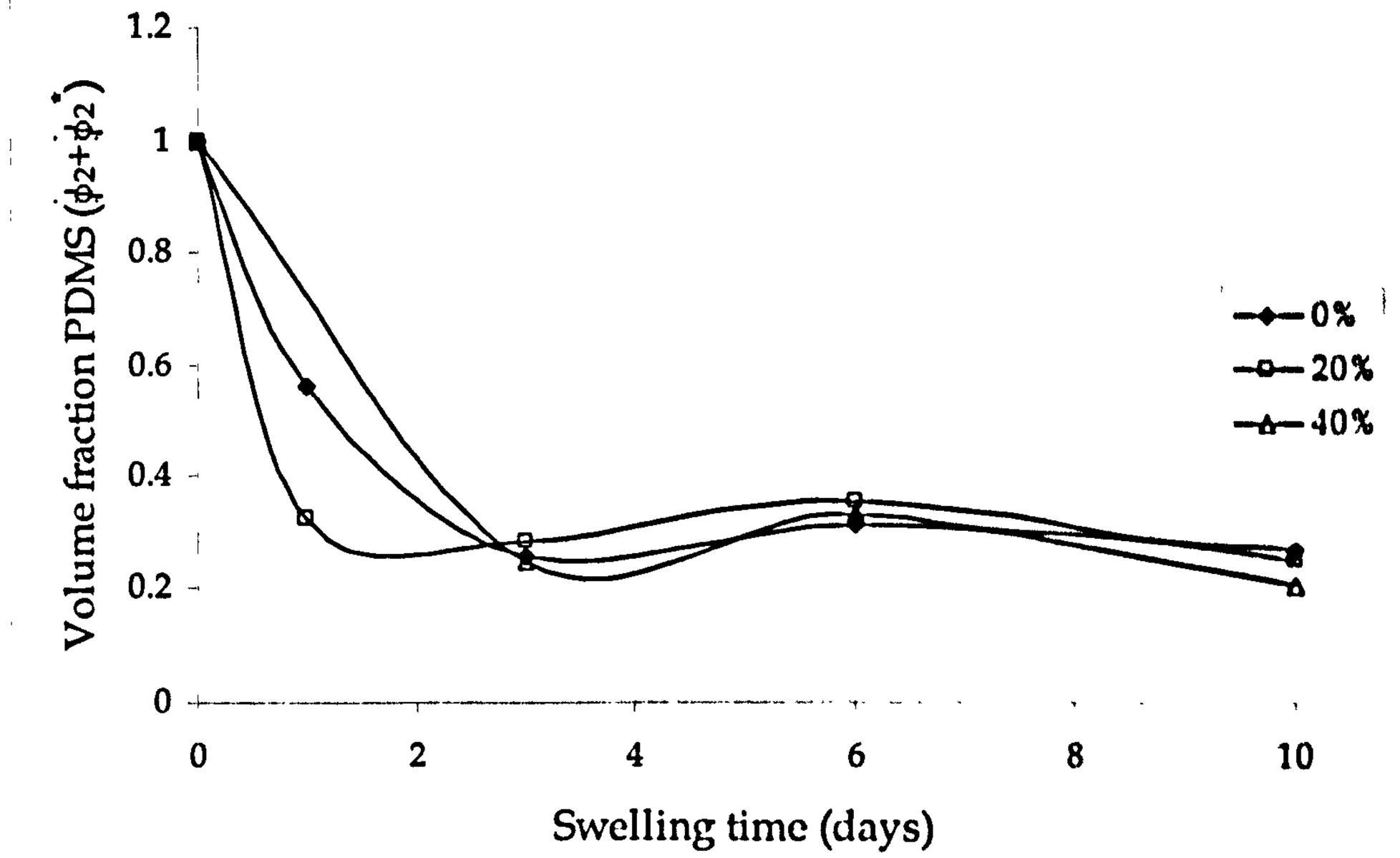

Figure 5.13: Volume fraction of PDMS in n–octane swollen emulsion droplets as a function of swelling time for various concentrations of cross–linker

The data shown in figures 5.8 and 5.9 is similar to that shown for n–heptane in figure 5.3. A substantial increase in droplet size is observed due to the solvent entering the droplets by osmotic diffusion. Droplets of lower cross–linker concentration swell to larger volumes than comparable systems with increased concentrations of cross–linker.

Figure 5.10 shows the swelling data for undialysed PDMS droplets swollen by DMDES. The data show that the droplets continue to grow by absorbing PDMS from the aqueous medium. If new droplets were forming by on–going nucleation and growth mechanisms an increase in polydispersity would be expected. As this does not occur, any new nuclei of PDMS droplets forming must coagulate and absorb into the emulsion droplets before they have time to become stabilised (refer to section 1.3). Sequential addition of more monomer to an undialysed emulsion presents a useful method by which larger PDMS droplets could be produced.

Figure 5.11 shows swelling by styrene into PDMS emulsion droplets. This was an example of the swollen droplets being difficult to measure accurately using PCS. The swollen emulsion is milky white in appearance and the large droplets were visible under the optical microscope (refer to plate 5.1). Hence, samples for PCS measurements needed to be very dilute in order to prevent multiple scattering. Even though the samples were diluted by water saturated by the solvent some emulsion breakdown occurred. This occurrence was most prevalent in PDMS emulsions swollen by toluene, styrene and 1,1,1–trichloroethane and least in hydrocarbon–swollen PDMS emulsions. This observation may be rationalised due to the rate of swelling of being extremely rapid. This rapid swelling of the PDMS emulsion may result in instability due to insufficient surface charge density to ensure repulsion caused by the over–expanded surface.

Higher molecular weight non–polar and polar solvent molecules did not swell the PDMS emulsion droplets to such an extent as observed with small solvent molecules. The data shown in figure 5.12 is an example of this, in this case with n–octanol as a swelling solvent. The total volume fraction of

PDMS ($\phi_2 + \phi^*_2$) appears to increase above 1.0. This is due to the emulsion actually decreasing in average droplet size as compared to the unswollen emulsion. This challenges the assumption that there would still be a significant volume of PDMS absorbing into the droplets as the swelling experiment proceeded. It appears, in this instance, that less PDMS has absorbed in the experiment as compared with the control. It is possible that a portion of the PDMS has absorbed into the n–octanol bulk phase. Thus, estimates of the total PDMS volume fraction ($\phi_2 + \phi^*_2$), may be overestimates.

5.3.3 Discussion of swelling results

A qualitative order of the best solvents for swelling of PDMS emulsions can be produced from the experimental data, together with some solubilities in water (expressed as weight % in parentheses following the solvent name) [10,11]:

1,1,1–trichloroethane (0.13) > toluene (0.049) > styrene (0.03) > cyclohexane (0.013) > n–heptane (0.005) > n–octane (0.002) > DMDES > n–octanol (0.059) > n–dodecane > n–hexadecane > n–decanol > PDMS.

The main factor determining this order is the solubility of the solvent in water. The effect of the solubility of the solvent in PDMS is not as important. One exception is n–octanol. Here, the molecule may not have sufficient solvency with PDMS for swelling to occur. No data for the solubilities of the latter solvents could be found in the literature so it can be assumed that they are minimal (less than 0.001 wt. %).

Studies of the variation of the volume fraction of PDMS with swelling time suggests that an equilibrium concentration is reached inside a droplet, regardless of cross–linker concentration, up to 40 % v/v MTES (refer to figures 5.6 and 5.13). This suggests that the presence of any elastic straining energy in these droplets is minimal; ϕ^*_2 is insignificant as a contribution to the

overall polymer volume fraction. Accurate estimates of cross-linker density from these data cannot be made. At cross-linker concentrations above 40% v/v MTES there is much more restricted swelling. This can be attributed to the presence of an elastic gel network. The PDMS at these MTES concentrations becomes solid rather than liquid in nature. Particles are visible using electron microscopy [12]. The driving force for the swelling is assisted by the continued absorption of PDMS out of the aqueous phase, thus maintaining ϕ_2 at high levels. This keeps the osmotic gradient for solvent repartitioning high as well.

The assumption that PDMS continues to absorb into the droplets as they swell could also be erroneous. If PDMS is also absorbed into the bulk solvent then the chemical potential of the solvent (μ_3^1) is not equal to the true pure solvent chemical potential (μ_3°). This will also effect the final equilibrium position.

5.3.4 Electrophoretic mobility of swollen PDMS emulsions

From the data that are shown in sections 5.3.1 and 5.3.2 it may be concluded that the emulsions can take up large quantities of organic solvent from solution and remain stable when an equilibrium size is reached. The stability is maintained by charge stabilisation. Either the surface charge density of the droplets stays the same as the surface area expands, or the charge on the droplets decreases, but remains sufficiently large to prevent two droplets coming into close proximity. The problem could be resolved using electrophoretic mobility measurements of the swollen droplets, which may reveal how the droplets remain stabilised.

Figure 5.14 shows the zeta-potentials calculated using the method developed by O'Brien and White [13] from experimental electrophoretic mobility data measured on the PALS apparatus. The PDMS emulsions

measured were dialysed prior to swelling. They had no added cross-linker and were swollen by n-heptane over a period of 2 days. Droplet sizes were measured as previously described using PCS.

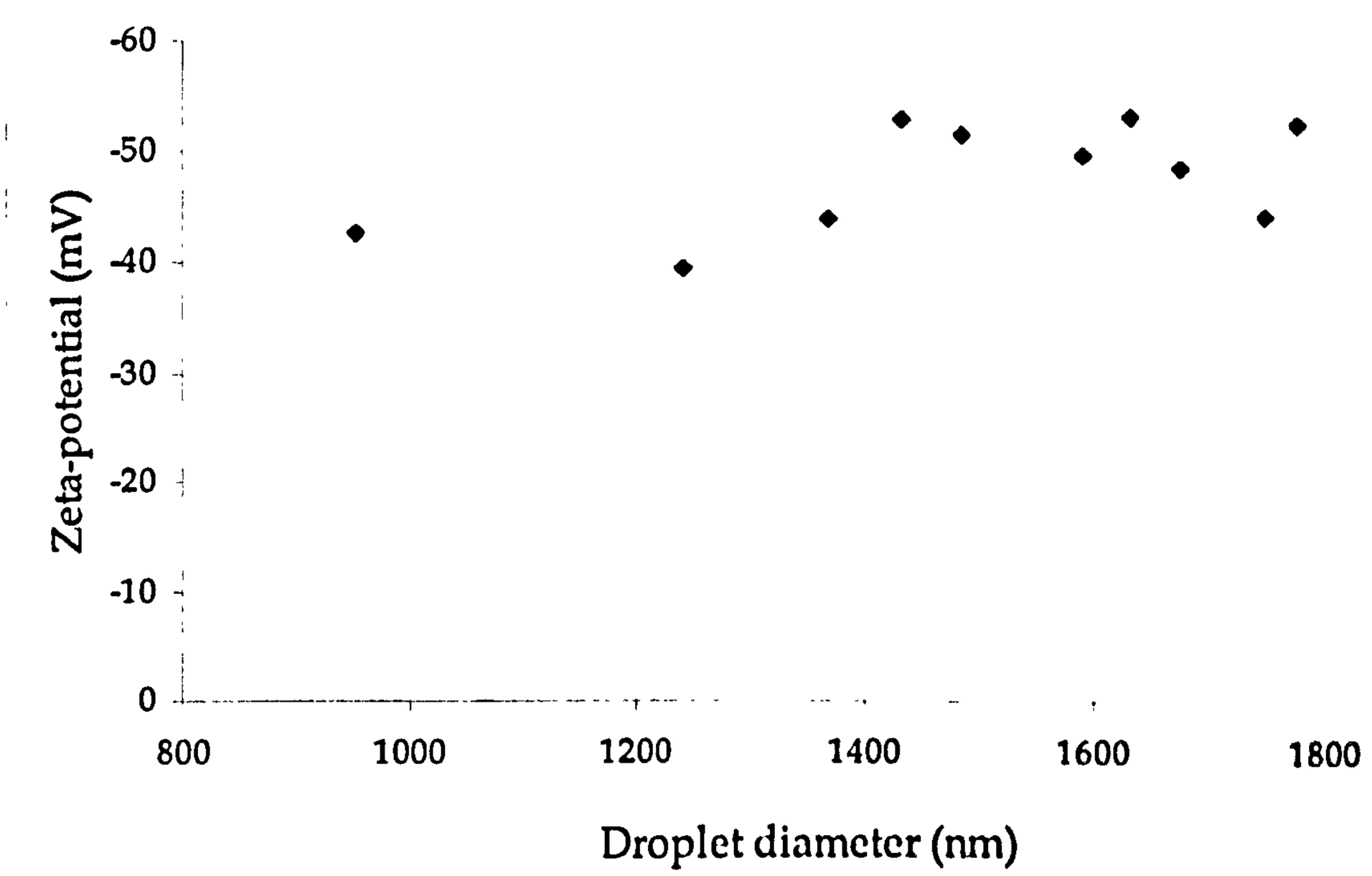

Figure 5.14: Zeta-potential of PDMS emulsions swollen by n-heptane

The zeta-potentials of the swollen droplets remain fairly constant between -40 and -55 mV. The surface charge density is not affected by the increase in surface area. It would appear that new charged oligomers absorb at the droplet/water interface in order to replenish the depletion of surface charge caused by the expansion. Thus the droplets are able to expand to large volumes and remain stable.

5.4 Introduction of Organic Dye Molecules into PDMS Emulsions

Sudan yellow, a water insoluble azo-dye, dissolves readily in most organic solvents and is also soluble in the separated PDMS phase. Hence, when introduced into a PDMS/water emulsion it should partition into the PDMS phase. It has previously been shown to absorb into latex particles [14].

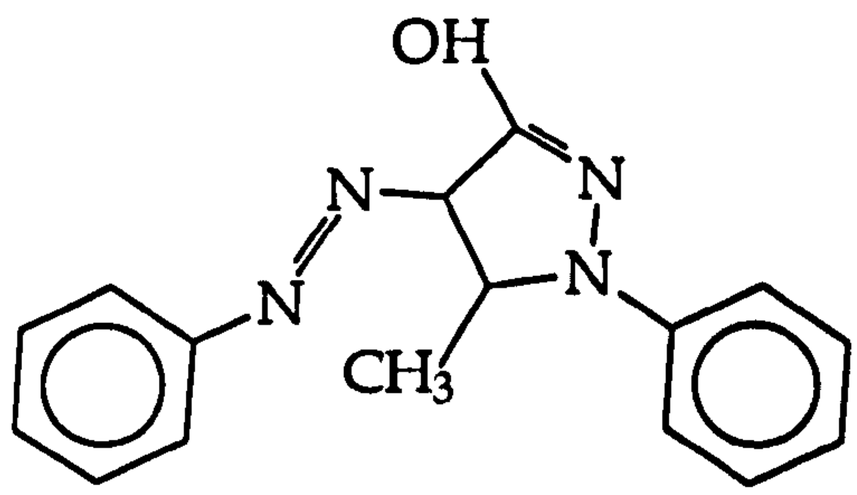

Figure 5.15: Chemical structure of Sudan yellow dye

Three methods were tried in order to incorporate the dye into the emulsion droplet. Sudan yellow, dissolved in either diethyl ether, n-heptane or toluene was added very slowly drop–wise to a PDMS emulsion in a stirred, round-bottom flask over a 24–hour period. Colour changes in the emulsion were noted. After complete addition of the dye containing solvent, the solvent was removed by opening the flask to air and allowing it to evaporate.

The second method involved using DMDES monomer containing dissolved dye. An attempt was made to synthesise the emulsion using monomer dyed with Sudan yellow and also to grow the emulsion as in the swelling experiments using the dyed monomer. After addition of the dyed monomer the emulsion was then dialysed.

These two methods were unsuccessful in achieving the desired result, namely a stable dyed PDMS emulsion. The emulsion appeared to be coloured

but following dialysis the emulsion was always broken and no dye remained dispersed.

For the final method the solubility of Sudan yellow in ethanol-water mixtures at concentrations greater than 0.4 v/v ethanol was utilised. At high ethanol content PDMS is also soluble [12], but if the ethanol content is lowered, the PDMS precipitates out of solution in droplets or as separate particles, if there is a high concentration of cross-linker. Therefore, systems of 50%, 20%, 10% and 0% MTES in 0.01 v/v DMDES in 80%, 60% and 40% ethanol in water concentrations were prepared. After 18 hours the samples were dialysed against pure water, thus lowering the concentration of ethanol in each of the samples. After 48 hours of dialysis the samples were then centrifuged to determine whether the sediment or the cream contained dye.

Depending on the concentration of cross-linker in the PDMS, it was found that the dye was contained in either the sedimented or the creamed layer. Thus, it can be inferred that the emulsions had become successfully dyed.

5.5 References

1. Horák, D. *Acta Polymer* **47**, 20 (1996).

2. Ugelstad, J. and Mork, P.C. *Advances in Colloid and Interface Science* **13**, 101 (1980).

3. Antonietti, M., Kaspar, H. and Tauer, K. *Langmuir* **12**, 6211 (1996).

4. Okubo, M. and Nakagawa, T. *Colloid and Polymer Science* **270**, 853 (1992).

5. Morton, M., Kaizerman, S. and Altier, M.W. *Journal of Colloid Science* **9**, 300 (1954).

6. Kabalnov, A. S. and Shchukin, E. D. *Advances in Colloid and Interface Science* **38**, 69 (1992).

7. Flory, P.J., "Principles of Polymer Chemistry.", Cornall University Press, Ithaca, New York, 1953.

8. "Polymer Handbook" (Brandrup, J. and Immergut, E.H., Ed.), Third Edition, John Wiley, New York, 1989

9. Stauff, J., "Kolloidchemie.", Springer Verlag, Berlin, 1960.

10. "Lange's Handbook of Chemistry" (Dean, J.A., Ed.), Mc Graw - Hill, 1985

11. "Solubilities of Inorganic and Organic Compounds" (Stephen, H. and Stephen, T., Ed.), Pergammon Press, Oxford, 1963

12. Wegener, M., M.Sc. thesis, University of Bristol (1993).

13. O'Brien, R.W. and White, L.R. *Journal of the Chemistry Society-Faraday Transactions II* **74**, 1607 (1978).

14. Waterson, J., Ph.D. Thesis, University of Bristol (1989).

Chapter 6: Conclusions and Further Work

6.1 Conclusions

PDMS ('silicone oil') in water emulsions, with controllable properties, may be synthesised by varying the starting monomeric reaction mixture. The size, density and viscosity of the emulsion droplets can be altered by addition of a trifunctionally active, cross–linking monomer, MTES, to the major difunctional monomer, DMDES. Analysis of the PDMS phase produced, following the polymerisation shows that, for cross–linker concentrations of less than 12 % v/v, the PDMS is less dense than the aqueous medium and the emulsion creams. At cross–linker concentrations above this the emulsion sediments. Simultaneously, the PDMS becomes increasingly more viscous. This is as a direct result of the cross–links increasing the molecular weight of the polymer. The PDMS produced from DMDES alone has density and viscosity values very close to those of D_4 (octamethylcyclotetrasiloxane), which is the major constituent of the PDMS phase.

The surface and PDMS/water interfacial tension of the PDMS phase agree closely with literature values. The addition of cross–linker appears to have no effect on the surface energy of the PDMS. The high interfacial tension values suggest a pure oil/water interface without any absorbed surfactant being present. The PDMS droplet interface should, therefore, be non–rigid.

Increasing the cross–linker concentration lowers the freezing and melting temperatures. This is due to the PDMS being increasingly cross–linked, thus giving the silicone molecules higher molecular weight.

Increasing the cross–linker concentration inside the droplets results in smaller droplets forming. Typically a 1 % v/v DMDES in 1 % v/v aqueous ammonia reaction mixture will produce 'monodisperse' droplets of average diameter 1 μm 24 hours after mixing the reactants. A minimum in the droplet

size occurs at cross–linker concentrations between 40 % and 60 % v/v monomer, at which stage the droplets become solid–like particles. At extremely high concentrations (greater than 90 % v/v) of cross–linker non–spherical crystalline silica–like particles are formed. The polydispersity of the droplets increases with increasing concentration of cross–linker. If the droplets are left undialysed they continue to grow in diameter and they typically reach maximum size after 2 weeks. Increasing the total starting monomer volume fraction results in larger droplets, but also tends to give more polydisperse size distributions.

PDMS emulsion droplets, at cross–linker concentrations of 0 %, 10 % and 20 % v/v MTES in DMDES monomer, with a concentration of KCl (a 1:1 electrolyte) greater than 5×10^{-3} mol dm^{-3} slowly coagulate over a 4 day period. Coagulation is faster at 7.5×10^{-3} mol dm^{-3}, where it occurs within 4 hours. The presence of cross–linker has no appreciable effect on the critical coagulation concentration (CCC). At pH values below 4 all the emulsions, regardless of cross–linker concentration coalesce. Droplets without cross–linker slowly coagulate below pH 4.5, whereas droplets containing 10 % and 20 % cross–linker tend to be stable at this pH.

Osmotic compression studied on the PDMS emulsions showed that a minimum osmotic pressure of around 0.17 atmosphere is required to coalesce the droplets. No floccs of droplets were observed at any stage in the stability experiments. This suggests that, in the regions of close approach the thin PDMS/water/PDMS film is unstable and always ruptures. In the absence of absorbed surfactant there is no Gibbs–Marangoni type stabilisation effect against film thinning.

From electrophoretic mobility measurements on the PDMS droplets the zeta–potentials were derived as a function of electrolyte concentration and pH. Calculations using the theory for liquid particles suggest higher potentials than the more conventional theories for solid spheres. The isoelectric points of the emulsion droplets lie in the same reported pH range as for colloidal silica. With higher concentrations of cross–linker inside the

droplets there is a slight increase in the value of the isoelectric point. Above the CCC and below pH 4 there is still a considerable potential at the droplet surface. Calculation of the interparticle pair potential from van der Waals attractive and electrostatic repulsive interactions reveal large primary maxima against coagulation and coalescence. Some possibilities for this deviation from DLVO theory can be attributed to droplet deformation and the possible presence of a large, unquantifiable attractive hydrophobic interaction.

PDMS droplets with variable concentrations of cross-linker swell osmotically with a range of good solvents. Restrictions due to cross-linking only become significant at cross-linker concentrations greater than 40 % v/v where the droplets are considered to be effectively gel-like solid particles. Below this concentration of cross-linker, if any cross-linked gel network exists in the droplet, there is no alteration in the equilibrium volume fraction of PDMS in the swollen emulsion droplet. In general, the higher the solubility of the swelling solvent in water, the better the swelling of the droplet. The PDMS droplets swollen with solvent can be up to 30 times as big as the original droplet's starting volume with the monodispersity and stability maintained. The swelling of PDMS droplets with DMDES is a method by which large and 'monodisperse' droplets can be formed.

Electrophoresis showed that the droplets increase their total surface charge, as their surface area expands, by absorbing more of the surface-active oligomers at the interface.

More complex, higher molecular weight molecules with very limited solubility in water can also be solubilised into the PDMS droplets, although the size distribution is altered and, in particular, the polydispersity of the size distribution is increased.

6.2 Suggestions For Further Work

6.2.1 Droplet coalescence at a planar oil/water interface

An observation was made, for a creamed layer of a 5 % v/v DMDES emulsion, which had been left standing for a month, that the droplets contained within the cream were large (~2.5 μm diameter) and 'monodisperse'. A separate, coalesced layer of PDMS existed above the cream layer. This suggests that there is a threshold size stability, which may be of importance in producing large, 'monodisperse' concentrated emulsion droplets.

` Experimental techniques exist whereby the lifetime of emulsion droplets at a planar oil/water interface may be examined [1,2]. In particular the droplet coalescence technique as used by Dickinson *et al* [1] is suitable for examining droplets in the micrometer size region. In general, the smaller the droplets then the longer the coalescence time. This could give credence to the above observation where a polydisperse cream became gradually more 'monodisperse' through coalescence of the large droplets.

The PDMS emulsions would be interesting systems to examine film-thinning and coalescence at a planar interface. A prototype glass coalescence apparatus was designed and built and droplet coalescence at the water/PDMS film was observed. Using optical microscopy incorporating the long working distance objective together with image analysis software available in this laboratory, following the droplet coalescence times at the interface should be possible. This would then be tied in with the stability results discussed in chapter 4.

6.2.2 Analysis of the PDMS by DSC

Thermometric determinations can reveal many interesting properties of materials. Differential scanning calorimetry (DSC) yields the enthalpies of transition for phase changes (e.g. the heat of fusion at the melting temperature). This could give information on the exact nature of the PDMS phase when cross–linker is incorporated, i.e. whether there exists gel–type networks inside the liquid droplets and at what concentration the transition from liquid to solid particles takes place.

6.2.3 Other possibilities for further work

There are numerous applications that can be found for a 'monodisperse' surfactant free emulsion. These include thin film studies of the PDMS/Water/PDMS interface, rheology of a concentrated emulsion and using the emulsions as a starting point for polymerisation to form high molecular weight PDMS. The PDMS emulsion is an ideal system to study further any hydrophobic interactions, for instance the effect of dissolved gas on emulsion stability [3].

6.3 References

1. Dickinson, E., Murray, B.S. and Stainsby, G. *Journal of the Chemical Society, Faraday Transactions I* **84**, 871 (1988).

2. Ivanov, I.B. and Kralchevsky, P.A. *Colloids and Surfaces A: Physicochemical and Engineering Aspects* **128**, 155 (1997).

3. Karaman, M. E., Ninham, B. W. and Pashley, R. M. *Journal of Physical Chemistry* **100**, 15503 (1996).